Journal of Controlled Release 381 (2025) 113549

Contents lists available at ScienceDirect

Journal of Controlled Release

journal homepage: www.elsevier.com/locate/jconrel

Supramolecular oral delivery technologies for polypeptide-based drugs

Jiawen Chen [a,b,c,d,1], Tianqi Liu [a,b,c,d,1], Mi Wang [a,b,c,d], Beibei Lu [a,b,c,d], De Bai [a,b,c,d], Jiaqi Shang [a,b,c,d], Yingjun Chen [e], Jiaheng Zhang [a,b,c,d,*]

[a] Sauvage Laboratory for Smart Materials, Harbin Institute of Technology, Shenzhen 518055, China
[b] School of Materials Science and Engineering, Harbin Institute of Technology, Shenzhen 518055, China
[c] State Key Laboratory of Advanced Welding and Joining and Research Centre of Printed Flexible Electronics, School of Materials Science and Engineering, Harbin Institute of Technology, Shenzhen 518055, China
[d] Shenzhen Shinehigh Innovation Technology Co., LTD., Shenzhen 518055, China
[e] Shenzhen JC innovation (Lazylab) Co., LTD., Shenzhen 518055, China

ARTICLE INFO

Keywords:
Supramolecule
Drug delivery system
Oral administration
Supramolecular interactions

ABSTRACT

Oral supramolecular drug delivery systems (SDDSs) have shown promising potential, along with a rapid increase in the development of polypeptide-based drugs. Biofriendly, biocompatible, and multistimulation-responsive SDDSs achieve their unique deliverability via noncovalent bonds, which can encapsulate drugs and release them at the target site along the oral tract. In this review, we analyze the oral tract from an anatomical perspective and explain the potential physical, microenvironmental, and systematic barriers, as well as the properties of drug delivery. After understanding the specific environment at different oral sites, the application of SDDSs to the mouth, stomach, small intestine, and cell targeting is summarized. Finally, this review summarizes the application of SDDSs for the successful delivery of drugs and describes how to overcome the barriers of SDDSs in drug delivery using a more biofriendly approach.

1. Introduction

Over the past 40 years, the global prevalence of overweight and obesity has nearly tripled, making it one of the most serious unmet public health challenges of the 21st century [1]. In 2015, overweight and obesity were estimated to affect two billion people worldwide [2], of which, 650 million were obese [3]. In 2016 alone, nearly 40 % of the adults in America were obese, according to the National Health and Nutrition Examination Surveys of the US Centers for Disease Control and Prevention [4]. Thus, overweight and obesity have become pandemics, affecting approximately 39 % of the world's population with a global prevalence rate of 12.5 % [5]. If this trend continues, it is estimated that more than one billion adults will become obese by 2030 [6]. The increasing proportion of obese individuals worldwide has resulted in huge expenditures. Currently, the cost of healthcare products and services for obesity is estimated to reach 2 trillion USD annually, which is

Abbreviations: 5-fluorouracil, 5-FU; Area under curve, AUC; Artificial duodenal fluid, ADF; Artificial gastric fluid, AGF; Artificial intestinal fluid, AIF; Berberine hydrochloride, BBH; Body mass index, BMI; Cyclic peptide, CPx; DDDEEKRWRWRWC-PEG, DRWP; Dexamethasone sodium phosphate, DEX; Dipeptidyl peptidase 4, DPP4; *Escherichia coli*, *E. coli*; Fluorine-assisted mucus surrogate, FAMS; Glucagon-like peptide-1 receptor, GLP-1R; Glucagon-like peptide-1, GLP-1; Glucose transporter 1, GLUT1; Hydrochloric acid, HCl; Hydroxypropyl methylcellulose, HPMC; Interleukin-22, IL-22; Matrix metalloproteinases, MMs; Melittin, MEL; Mesoporous silica nanoparticles, MSNs; Metal-organic framework, MOF; Nanoparticles, NPs; Nanosheets, NSs; Negative logarithm of the agonist concentration that produced 50 % of the maximum effect, pEC_{50}; Negative logarithm of the antagonist concentration that produces a twofold rightward shift in the agonist dose-response curve, pA2; Negative logarithm of the concentration of the inhibitor that produced 50 % inhibition, pIC_{50}; Negative logarithm of the dissociation constant, pK_d; Negative logarithm of the inhibition constant, pK_i; Not available, N. A.; Ovalbumin, OVA; Poly(e-caprolactone), PCL; Poly(N-isopropyl acrylamide), PNIPAm; Poly(vinylpyrrolidone), PVP; Reactive oxygen species, ROS; Rocket-inspired effervescent motors, RIEMs; Simulated gastric fluid, SGF; Simulated intestinal fluid, SIF; Simulated saliva fluid, SSF; *Staphylococcus aureus*, *S. aureus*; Supramolecular drug delivery systems, SDDS; Tacrolimus, TAC; Tofacitinib, TOFA; Tumor necrosis factor alpha, TNFα; Type 2 diabetes mellitus, T2DM; Ulcerative colitis, UC; β-cyclodextrin, β-CD.

* Corresponding author at: Sauvage Laboratory for Smart Materials, Harbin Institute of Technology, Shenzhen 518055, China.
E-mail address: zhangjiaheng@hit.edu.cn (J. Zhang).

[1] Jiawen Chen and Tianqi Liu contributed equally to this paper.

https://doi.org/10.1016/j.jconrel.2025.02.045
Received 18 September 2024; Received in revised form 11 January 2025; Accepted 18 February 2025
Available online 8 March 2025

2.8 % of the world's gross domestic product [2]. By 2060, predicted expenditure on obesity is expected to increase by 3.29 % of the world's GDP [7]. The World Health Organization has appealed to individuals to focus on obesity and published an acceleration plan for obesity prevention [8]. Body mass index (BMI) is commonly used to classify overweight (BMI: 25–30), obesity (BMI: 30–35), and severe obesity (BMI: ≥35) in adults [9]. Obesity is a pro-inflammatory state that can induce type 2 diabetes mellitus (T2DM) and oxidative stress, resulting in adverse cardiovascular function [10]. More than two-thirds of the deaths associated with high BMI, including overweight and obesity, are attributed to cardiovascular disease [10]. Obese individuals are at a higher risk of developing T2DM if their BMI is not controlled [11]. Therefore, restricting global obesity trends is a crucial and urgent mission that requires continued attention.

Supramolecular drug delivery systems (SDDSs) derived from supramolecular chemistry using noncovalent interactions to form drug formulations are a promising technology for the oral administration of polypeptide-based drugs [12,13]. Considering the specific environment of the human oral cavity and gastrointestinal tract, SDDSs are gaining importance owing to their abilities to adapt and respond to the gastrointestinal environment and achieve the targeted release of drugs at controlled sites and times. The mechanisms of SDDSs include host-guest interaction, self-assembly, protein-derived affinity interactions, metal coordination, and other noncovalent interactions including hydrogen bonding, van der Waals interaction, hydrophobic interaction, π-stacking, and electrostatic interaction [14,15]. Host-guest interaction arise from macrocycle host materials such as cyclodextrin and cucurbit [*n*]uril macrocycles [16–18], which are used in SDDSs to encapsulate drugs in intramolecular cavities. Self-assembly occurs in peptides under environmental stimuli, including pH, temperature, and ions. Self-assembly is controlled by chains of noncovalent interactions [19]. Protein-derived affinity interaction caused by the specific microenvironment in the human body, especially transport proteins, such as glucose transporter 1, participate in these interactions, [20,21]. The glucose-modified azocalix[4]arene was designed as a supramolecular transporter to deliver liproxstatin-1 to the ischemic site via glucose transporter 1 [22]. Metal-ligand coordination, using metal ions and chelating ligands to form a "capsule" to encapsulate polypeptide-based drugs, results in the controlled release of the drugs. For instance, Lys^{B29}-terpyridine modified insulin forms supramolecular networks with the metal ions Fe^{2+} or Eu^{3+} and exhibits a significant ability to control blood glucose with a higher maximum concentration in plasma than unmodified insulin [23]. Other studies using metal-ligand coordination to deliver peptides and proteins have also achieved progress in efficacy [24,25]. A series of supramolecular carriers have been developed in different forms, including vesicles (open and tupanvirus-like), micelles, and solid particles with spherical and tubular shapes, which are promising SDDSs for the oral delivery of peptide- and protein-based drugs [26]. The use of noncovalent interactions to manufacture SDDSs is widely in the drug delivery system design processes. These weak bonds are formed during the preparation steps and are broken down under the stimulation of a specific environment to achieve targeted delivery [27–33]. Because of stability, biotoxicity, and biocompatibility, halogen bonding SDDS was not been discussed. The mechanisms of oral administration of SDDSs are shown in Scheme 1.

The emergence and application of oral medicine in humans were first recorded at 1550 and 600 BCE, respectively. The concept of supramolecules was first proposed in 1937. With the development of molecular and biological research over the past few decades, the 1987 and 2016 Nobel Prizes in Chemistry were awarded to the field of supramolecular science. Supramolecular materials and mechanisms are increasingly being used for oral drugs, especially, for delivering polypeptide-based drugs to the gastrointestinal tract. The details of the development of supramolecular science are shown in Fig. 1.

Glucagon-like peptide-1 (GLP-1) is a hormone generated by pancreatic cells when blood sugar increases after food intake and can control the blood sugar to a normal level by stimulating the secretion of glucose-dependent insulin by binding to the GLP-1 receptor [49]. Habener et al. [50] identified the protein sequence in the 1980s by decoding anglerfish preproglucagon cDNA, and two glucagon-related peptides have attracted the attention of scientists. These glucagon-related peptides have been identified in various organisms, including rats [51], hamsters [52], pigs [53], bovines [54], and humans [55]. Recently, these glucagon-related peptides were classified and named as GLPs, GLP-1, and GLP-2 [52]. Truncated GLP-1 extracted from human and porcine guts can enhance insulin secretion in several animals [56–58]. In the last decade, the FDA has approved GLP-1 drugs to treat patients with T2DM [59–61]. GLP-1 shows the ability to induce weight loss through numerous beneficial mechanisms, including the promotion of insulin release [62], delay of gastric emptying [63], suppression of food intake [64,65], and dose-dependent increases in natriuresis and diuresis [66]. Data from numerous clinical cases have indicated that GLP-1 has a tremendous potential to treat patients who are overweight and obese. In the human gut environment, natural GLP-1, secreted from L-cells of the intestine, is cleaved and inactivated by dipeptidyl peptidase 4 (DPP4) within 2 min [67], which indicates a short plasma half-life. To

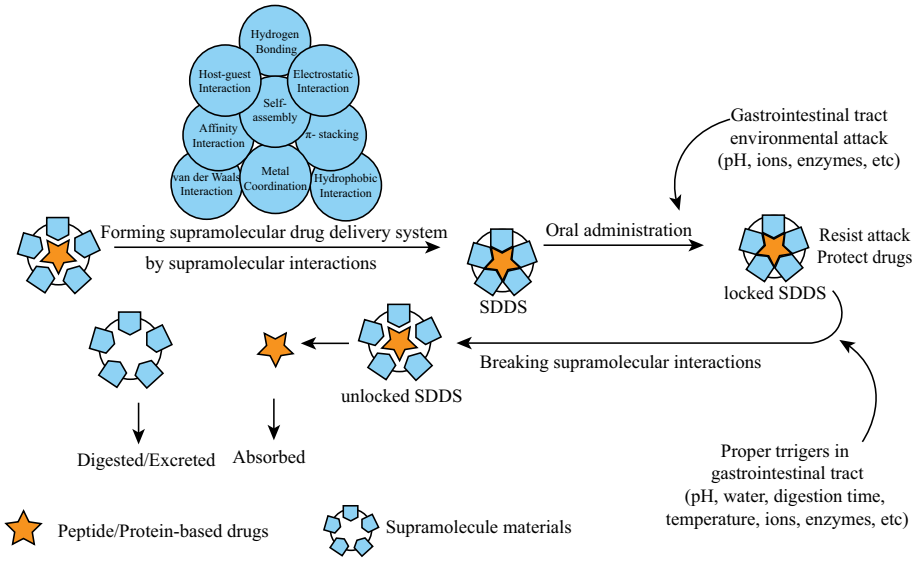

Scheme 1. Manufacture and application of supramolecular drug delivery system in the gastrointestinal tract by oral administration.

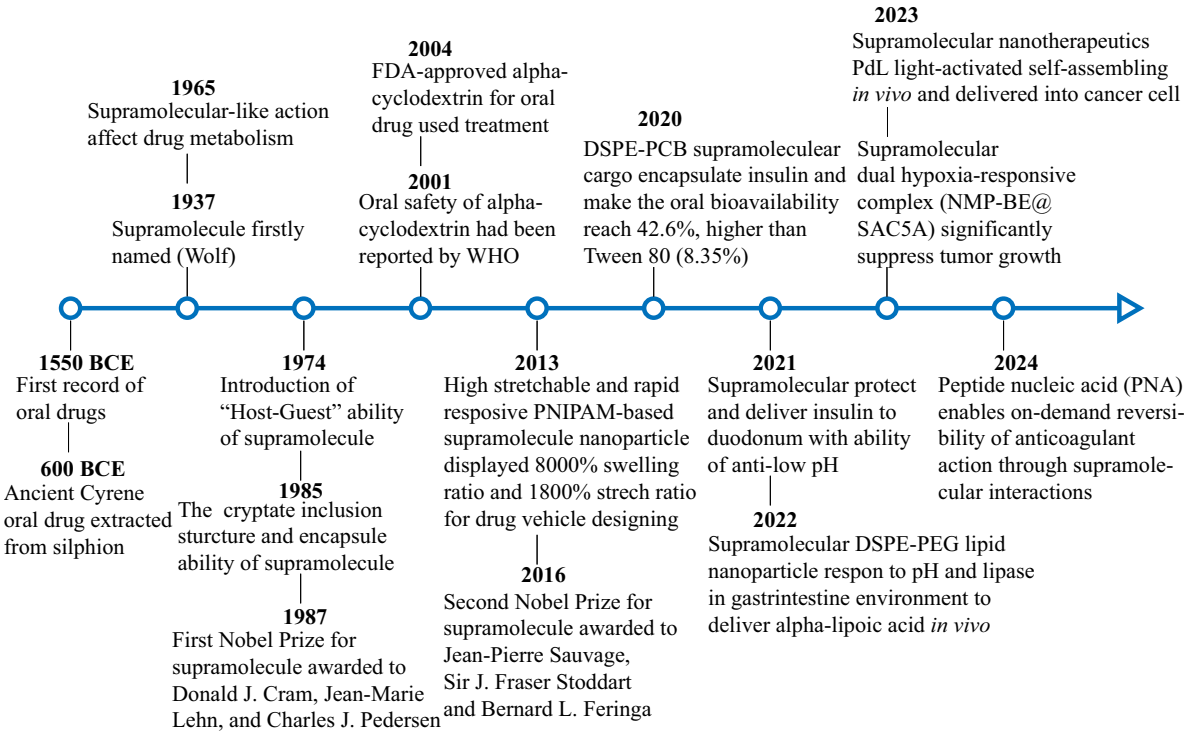

Fig. 1. The development of supramolecular drug delivery systems. 1500 BCE [34], 600 BCE [35], 1937 [36], 1965 [37], 1974 [12], 1985 [13], 1987 [38], 2001 [39],2004 [40], 2013 [41], 2016 [42], 2020 [43], 2021 [44], 2022 [45], 2023 [46,47], 2024 [48].

compensate for its short half-life, high doses of GLP-1 have been considered. However, high doses of GLP-1 can also induce nausea. Furthermore, administration by painful and impractical injection and barriers to oral administration, including the biochemical, mucus, and cellular barriers [34], also hinder the widespread application of GLP-1.

To overcome these problems, several strategies have been used to manufacture glucagon-like peptide-1 receptor (GLP-1R) agonists which are predominantly classified into two categories: peptides and small molecules. GLP-1R peptide agonists include exenatide [68,69], liraglutide [70], lixisenatide [71], semaglutide [72], dulaglutide [73], and tirzepatide (LY3298176) [74]. Small-molecule GLP-1R agonists include Compound 2 [75,76], orforglipron (LY3502970/OWL833) [77], danuglipron (PF-06882961) [64], PF-07081532 [78], TTP273 [79], Boc5 [80], and WB4–24 [81]. However, the chemical structures of RGT-075 and PF-07081532 have not been reported [82].

For the last two decades, GLP-1R agonists have been used to treat patients with T2DM by helping maintain their body weight at a healthy level. With the rapid development of GLP-1R agonists, the delivery of different polypeptide-based drugs has attracted the attention of researchers. However, new SDDSs for polypeptide-based drugs have not been developed.

In this review, we demonstrate the main delivery barriers present along the oral tract from the mouth to the small intestine, and we focus on cells according to the specific properties of polypeptide-based drugs, summarize their delivery strategies, and outline the supramolecular mechanisms involved. We also discuss the future directions of supramolecular drug delivery technologies.

2. Anatomy and barriers to drug delivery

2.1. Physical barriers

Physical barriers should be considered before the oral administration of the drug. They occur in the digestive tract, mainly in the gastrointestinal tract, as shown in Fig. 2a. Each barrier is derived from a specific biostructure of the human body, including the mouth, pharynx, esophagus, stomach, pylorus, and small, and large intestine. The design and manufacture of an appropriate SDDS must consider the physical barriers along the digestive tract.

2.1.1. Mouth

The mouth, the first place of contact for drugs during oral administration, has an inner volume of approximately 26–96 cm^3, as detected by magnetic resonance imaging scans [84,85]. Approximately 0.5–1.5 L of saliva would be produced every day [86]. The sublingual and buccal areas feature abundant salivary glands (Fig. 2b) [86], and secreted saliva plays an important role in cleaning the buccal environment, often resulting in drug clearance [87]. Numerous gustatory receptors are located in the tongue area. On sensing an unpleasant taste such as bitterness, drugs stimulate the gum and induce a risk of choking [88]; thus, a possible block of the uvula, and drug adhesion on the palate need to be considered.

2.1.2. Pharynx

The pharynx is an important part of the human body that connects the mouth and esophagus, ensuring food and drug intake through swallowing, as the bolus is swallowed via the route shown in Fig. 2c [89]. Considering that the physical structure of the pharynx can be a limitation for drug structure design, the dimensions of each part of the pharynx have been described by Inamoto et al. [90]. The shape and structural design of a drug should rely on a "reasonable worst-case scenario principle" to avoid undesired risks and adverse effects [91]. According to this principle, the following pharynx characteristics should be considered: the volume of the oropharyngeal cavity is 13.5 (standard deviation: 4.3) cm^3, the width of the pharynx is 35.5 (3.9) mm, and the length of the pharynx is 76.0 (6.7) mm [90]. Mouth throat simulation devices have also confirmed these data [92], such as the United States Pharmacopeia induction port [93], mouth-throat structural replica [94], and a conductive rubber mouth throat device designed by the Lovelace Respiratory Research Institute [95]. These size and shape limitations indicate that preparations should be designed to avoid the risk of accidentally aspirating or blocking the windpipe, resulting in coughing and

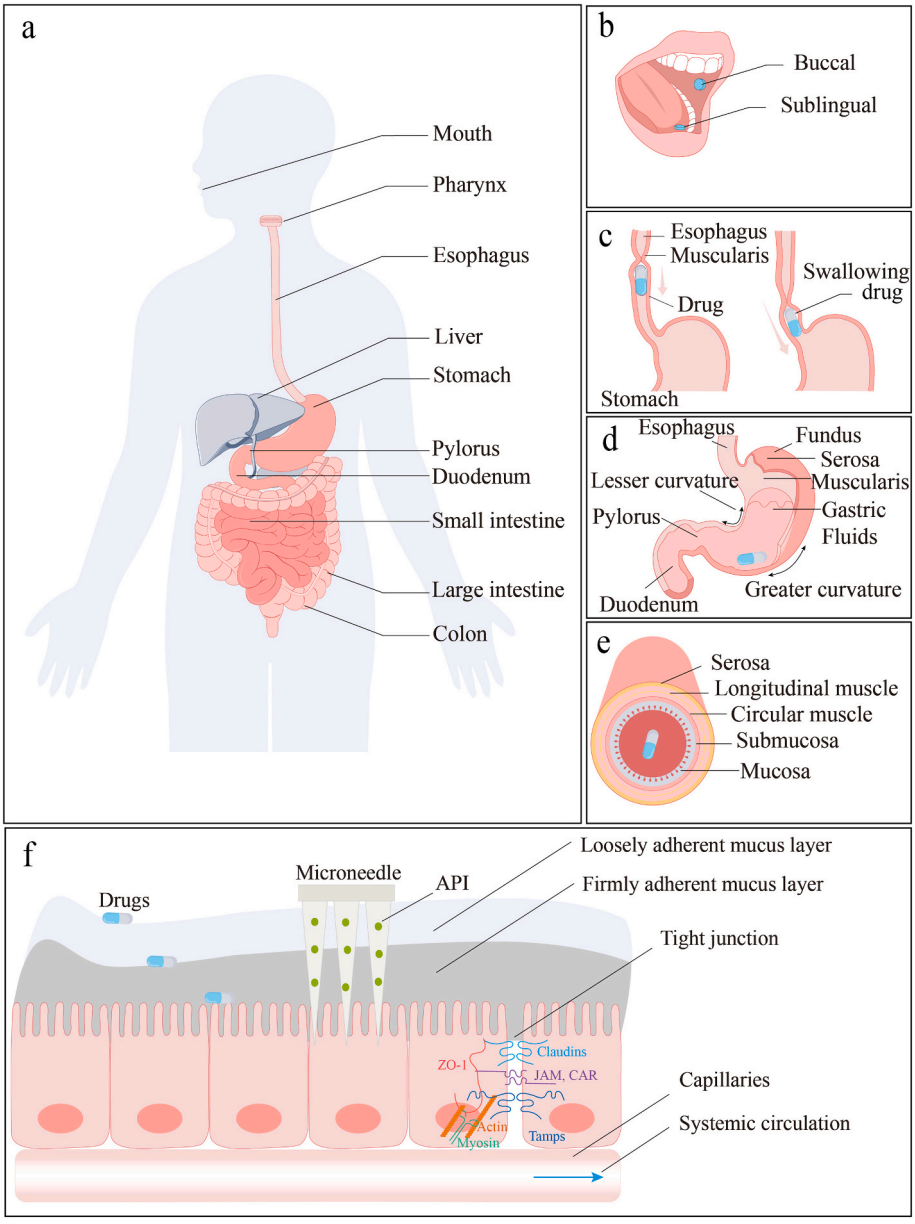

Fig. 2. Physical barriers to drug delivery in gastrointestinal tract. (a) Anatomy diagram of the oral digestive tract. (b-e) Drugs delivered in mouth,esophagus, stomach, and small intestine. (f) Drugs delivered through transcellular transport and tight junction. Adapted from Ref [34, 83] with permission.

choking.

2.1.3. *Esophagus*

The esophagus is similar to a vertical tube nearly 25-cm long and consists mainly of the upper esophageal sphincter, which moves drugs from the pharynx to the esophagus, and the lower esophageal sphincter, which continues to move drugs from the esophagus to the stomach. Physiologically, the esophagus secretes mucus to deliver a bolus smoothly [89].

2.1.4. *Stomach*

The stomach is a J-shaped organ connected to the esophagus and duodenum, whose inner wall is distributed with numerous rugae of the mucosa, and is divided into four parts: the cardia (linked to the esophagus), fundus (store gas or food), body (store and digest food), and pyloric part (linked to the duodenum), as shown in Fig. 2d. For oral drugs, the stomach has the following functions: mixing saliva, drugs, and gastric fluid to form chyme, acting as a container for drugs before they are forced into the duodenum and small intestine, secreting gastric fluid into the stomach chamber, and gastrin into the bloodstream [89]. Owing to the presence of HCl and pepsin in gastric fluid, polypeptide-based drugs are digested in the stomach. However, the folds and rugae structures of the inner wall of the stomach provide adhesion sites for drugs that prolong their retention time. Every 15–20 s, peristaltic waves occur in the stomach to move the drugs to the duodenum, a process known as gastric emptying. As drugs move forward, pyloric acid is the next digestion station in the stomach. The pylorus, with a diameter of 12.8 ± 7 mm [96], is a gradually narrowing structure connecting the main body of the stomach to the duodenum. Considering the unique biostructure of the pylorus, it is possible to develop drug delivery systems that can adapt to the physical structure of the pylorus to control drug release.

2.1.5. *Small intestine*

The small intestine, the main site of digestion and absorption, is divided into three parts: the duodenum (~25 cm), jejunum (~1 m), and ileum (~2 m), as shown in the left part of Fig. 2e. The duodenum is the

most important digestion site. Pancreatic fluid, secreted by the pancreas and bile secreted by hepatocytes are transported into the duodenum and mixed with drugs, which allows them to be continuously digested and absorbed. The human body secretes 1.2–1.5 L of pancreatic fluid per day, at pH 7–8, and contains a variety of salts and digestive enzymes. Furthermore, 0.8–1 L of bile is secreted at a similar pH and contains bile salts, cholesterol, lecithin, bile pigments, and various other ions. Fully mixed with small intestinal fluid (containing pancreatic fluid and bile), orally administered drugs are partially absorbed and moveinto the jejunum and ileum for further digestion and absorption [89]. The villi and submucosal folds result in irregularity of the mucosal surface, which increases the surface area of the small intestinal absorption area. Moreprecisely, the mucosal area has been measured to have a surface area of ~2.2 m^2 [97]. Among these barriers, the secreted mucus layer is an obvious hindrance to drug absorption owing to its hydrophobic properties and abundant mucus secretion, as shown in Fig. 2e [98]. The mucus layers are composed of two parts, a loosely adherent mucus layer, and a firmly adherent mucus layer. Mucus layers coat the gastrointestinal tract and form a 2 − mm thick physical barrier to reach the epithelial cell layer from the lumen [34]. The epithelial cell layer is the final barrier in the small intestine after the drug penetrates or is absorbed through the mucus layer, as shown in Fig. 2f, including absorptive, goblet, enteroendocrine, and paneth cells [89]. Drugs are delivered viaactive absorption by cells. However, drugs can also be delivered through tight junctions using substances that expand and penetrate the tight junctions, which may damage this barrier and lead to autoimmune disease, inflammatory bowel disease, bacterial infection, and interstitial osmotic imbalance [43].

As the main absorption area is the small intestine and fewer drugs target the colon (a part of the large intestine), here, we focused on the barriers before reaching the colon and in the small intestine. The physical structure and chemical environment of the gastrointestinal tract are the bases for the development of oral drug delivery systems. Microenvironmental barriers and polypeptide-based drug properties should also be considered.

2.2. Microenvironment barriers

Different digestive fluids form microenvironment barriers in specific regions involved in digestion, including the saliva, gastric fluid, and intestinal fluid. Digestive fluids comprise ofwater, ions, peptides, proteins, enzymes, cells, and other substances.

Digestion fluids include saliva and gastric and intestinal fluids. Saliva secreted from the salivary gland contains 99 % fluid [99], and the remaining components include a mixture of ions (Na^+, Mg^+, Ca^{2+}, Cl^-, HCO_3^-, etc.), proteins (glycoprotein, lipoprotein, mucin, histone, etc.), enzymes (amylase, lysozyme, etc.), and growth factors [100,101]. Gastric and intestinal fluids have been studied by scientists for numerous years, and their standard concentrations have been published (Table 1).

Table 1
Salt concentrations in the digestive fluid including simulated saliva fluid (SSF), simulated gastric fluid (SGF), and simulated intestinal fluid (SIF) determined according to INFOGEST 2.0 [102].

Salt	Concentration (mM)		
	SSF	SGF	SIF
KCl	15.1	6.9	6.8
KH_2PO_4	3.7	0.9	0.8
$NaHCO_3$	13.6	25	85
NaCl	–	47.2	38.4
$MgCl_2$	0.15	0.12	0.33
$(NH_4)CO_3$	0.06	0.5	–
$CaCl_2$	1.5	0.15	0.6

2.3. Systematic barriers

Systematic barriers to drug absorption in the oral gastrointestinal tract include gastric emptying time, gastrointestinal motility, and first-pass effect. Gastric emptying time and gastrointestinal motility are related to drug retention time. According to INFOGEST 2.0, these include the oral phase (30 min), gastric phase (2−3*h*), and intestinal phase (2–3 h) [102]. First-pass metabolism, which occurs in the liver and gastrointestinal tract, affects the concentration of polypeptide-based drugs in the serum, resulting in decreased bioavailability [103]. First-pass metabolism results in peak concentrations of active pharmaceutical ingredients occurring earlier than parenteral administration [104,105]. To resist first-pass metabolism, higher dosages of drugs should be taken orally; however, an excessive dose of drugs can damage the liver and kidney. Moreover, gastrointestinal intolerance can occur under this condition [106]. Systemic barriers must be considered before polypeptide-based drug design or formulation protection.

2.4. Drug properties and barriers

Drug properties include solubility, stability, bioactivity, efficacy, toxicity, biocompatibility, and transport mechanism. The solubility and stability of peptide- and protein-based drugs are associated with the manufacturing process andloading of the drug. Bioactivity and efficacy are considered the most important properties of drugs and are related to the usage and their therapeutic effects. Toxicity and biocompatibility are different, and toxicity aims to describe the damage from the drugs themselves to the body, whereas biocompatibility is used to describe the potential damage caused by the multiple materials used in drug formulation. The transport mechanism should be understood sufficiently to help develop an appropriate delivery system, such as knowing the precise delivery route of drugs in the epithelium layer, especially the transport proteins or routes on the cellular membrane, such as the GLP-1 receptor [107] or the tight junction pathway (Fig. 2f) [108].

3. Supramolecular oral drug delivery strategies and technologies

3.1. Oral supramolecular drug delivery system

The development of SDDSs through supramolecular interactions and deformation by triggers is summarized in Table 2. From the anatomical perspective, the targets of supramolecular drug delivery systems are the mouth, stomach, small intestine, and cells.

Oral transmucosal (sublingual and buccal) areas are important for oral drug administration because of the abundant capillaries distributed in these two main areas. Buccal SDDS is attracting attention, and its treatment area is shown in Fig. 2b. Xin et al. focused on the development of a peptide-polymer conjugate with adaptive properties that can prevent biofilm formation, which is a common challenge for maintaining the efficacy of buccal delivery systems. The selected peptide, comprising 13 amino acids (DDDEEKRWRWRWC, DRWP), was conjugated to poly (oxyethylene) (PEG) to form DRWP-PEG. The arginine and tryptophan residues of the peptide exhibit antibacterial properties due to their (de) protonation state [109]. Supramolecular interactions between arginine and tryptophan help the composite adsorb onto hydroxyapatite and lead to antibacterial ability. The supramolecular bond also demonstrated self-healing ability during buccal tissue treatment. Under the effect of ionic interactions and the abundant H − bonds formed by ureidopyrimidinone methacrylate, the coating layer containing the zwitterionic trimethylamine N-oxide and triclosan acrylate conjunction showed supramolecular self-healing ability, especially when incubated in the SSF for 2 h. The PTTU-10 % coating containing supramolecular bonds, showed rapid surface crack repair and restoration ability compared with its original state [110]. Patients with diabetes mellitus also experience the side effects that affect matrix metalloproteinases (MMs). To treat this

Table 2
Development of supramolecular drug delivery system platform via supramolecular interactions and release by triggers.

Supramolecular materials	Supramolecular interaction	Active pharmaceutical ingredients	Disease	Deformation triggers	Deliver site	Ref.
Polylysine/NH2-β-Cyclodextrin	Host-guest recognition	Allicin	Cancer	Electrostatic interaction	HepG2 cell	[121]
2-Hydroxypropyl-β-cyclodextrin	Host-guest recognition	Chloramphenicol, Ampicillin, Kanamycin, Gentamicin	Bacterial infection	H_2O, saliva	Mouth	[122]
Sulfonated azocalix[4] arene	Host-guest recognition	Hydroxychloroquine	Rheumatoid arthritis	Hypoxia	Inflammatory articular cavity	[123]
Sulfonated azocalix[4] arene	Host-guest recognition	Doxorubicin	Cancer	Hypoxia	Tumor	[124]
Glucose-modified azocalix[4]arene	Host-guest recognition	Liproxstatin-1	Ischemic stroke	Hypoxia	GLUT-1	[22]
Pillar[5]arene	Host-guest recognition	Guanidine pillar[5]arene	Bacterial infection	Self-assembly in H_2O	Lung, skin	[125]
Poly-cucurb[7]uril	Host-guest recognition/affinity-mediated/ion-dipole interaction	F-KLAK (cytotoxic peptide)	Cancer	Electrostatic interaction	Tumor	[126]
P11–4	Self-assembly	P11–4	Early caries	Ca^{2+}	Mouth	[127]
EAK-16	Self-assembly	Camptothecin	Cancer	pH or ion concentration	Tumor	[19]
RADA16-IKVAV	Self-assembly	Proregenerative cytokines	Injured spinal cord tissue	pH or ion concentration	Human neural stem cells	[128]
DNA-PNA	Hydrogen bonding	DNA-PNA	Brain injury or spinal cord	95 °C or "invader" oligonucleotide	Astroglial cells	[129]
PNA	Hydrogen bonding	Bivalent Direct Thrombin Inhibitor	Thrombotic events	Antidote	Circulatory system	[48]
Fmoc-FF	Charge-charge interaction	Fmoc-FF	Alzheimer's or Parkinson's disease	pH	Brain	[30]
Peptide-photosensitizer conjugates	π-stacking	PheoA	Cancer	Rising temperature	Tumor	[29]
HPMC	Hydrophobic interaction	Fenofibrate	Hyperlipidemia	Oral digestion environment	Oral	[130]
PNIPAm	Hydrophobic interaction	5-FU and DEX	Oral ulcers and early melanoma	37 °C	Oral	[131]
Magnetic-graphitic-nanocapsule	van der Waals interaction	Doxorubicin	Gastric disease	Gastric fluid	Stomach	[31]
Sulfated glycopeptide nanostructures	Affinity interaction	BMP-2	Bone diseases	Spine microenvironment	Spine	[132]
AuTPyP-Cu MOF	Metal coordination	Cu^{2+} and AuTPyP	Cancer	Low pH and ultrasound	Tumor	[133]

disease, a PEG/DNA gel was developed as a SDDS to deliver exosomes (to treat MMs). This hydrogel structure was stabilized by supramolecular interactions from Watson−Crick base pairings within the DNA. These interactions are likely to enhance the viscoelastic and self-healing characteristics of SDDS compared to those of other hydrogel systems. In addition, recovery of mandibular alveolar bone of diabetic mice was evaluated through the buccal area, and the results showed that the bone volume fraction reached 58.4 ± 7.4 % in the hydrogel loading exosomes compared to 16.5 ± 6.3 % in the diabetes mellitus group, indicating the promising regeneration capacity of the supramolecular hydrogel [111]. Supramolecular microneedles have also shown potential in the oral treatment of diabetes. Caffarel-Salvador et al. developed a SDDS for oral delivery using a polydimethylsiloxane model. The reduced pain potential indicated that buccal insulin delivery was preferred over injection [112]. Similar microneedle systems have been reported [113].

The sublingual SDDS are applied below the tongue, as shown in Fig. 2b. A type of sublingual tablet manufactured by self-assembling supramolecules to deliver vaccine peptide (OVAQ11) showed higher stability (45 °C, 1 week), higher antibody response (60-fold antibody concentration), and easier administration than conventional carrier vaccines (keyhole limpet hemocyanin) [114]. Another study has evaluated the same application area. The OVAQ11 peptide modified with PEG self-assembled into fibers with lengths of hundreds of nanometers and widths of 10–20 nm showed strong immunogenicity upon sublingual administration. Small-angle neutron scattering indicated that supramolecule PEG encapsulated Q11 and promoted mucosal delivery in the sublingual area [115]. Furthermore, this supramolecular material was manufactured as a vaccine against tract infections caused by uropathogenic *Escherichia coli* [116]. A minimal supramolecular nanovaccine fluorinated aromatic peptide containing a fluorinated aromatic peptide that enhances antigen binding and transmembrane capabilities has also been proposed. In mouse models, the vaccine exhibited considerable higher antibody titers than traditional adjuvants; specifically, four-fold higher than untreated aromatic peptides and 501-fold higher than the conventional aluminum adjuvants [117]. These advantages are from the supramolecular material fluorine, which enhances the transmembrane deliver ability of the drug delivery system owing to its lower surface energy and lipophobicity. This supramolecular material has also been investigated in another study [118].

Drug delivery systems loaded with ovalbumin (OVA) have been designed using supramolecular mechanisms [118–120]. Jia et al. used peptides as modules to achieve self-assembly, resulting in encapsulation of the OVA [118]. 4RDP(F5)-OVA demonstrated the most promising ability to achieve long-term immune memory to resist tumor challenge, which was recorded after 68 days of treatment, and its safety was confirmed [118]. Chung et al. showed that L-arginine-modified dextran nanohydrogels were formed through supramolecular interactions involving H − bonds and hydrophobic interactions, and by encapsulating OVA, the release of OVA was controlled by the dissolution of the formed supramolecular network points [120].

3.2. Supramolecular drug delivery system in the stomach

The gastrointestinal tract is the most important digestion area and the main absorbance area for drugs. They are mainly divided into the esophagus, stomach, small intestine, and colon. Considering the specific bioproperties of different gastrointestinal sites shown in Fig. 3a, oral drugs can be released by molecular materials stimulated by different digestion times, temperatures, gastric rugae, gastric emptying rates, and intestinal motility.

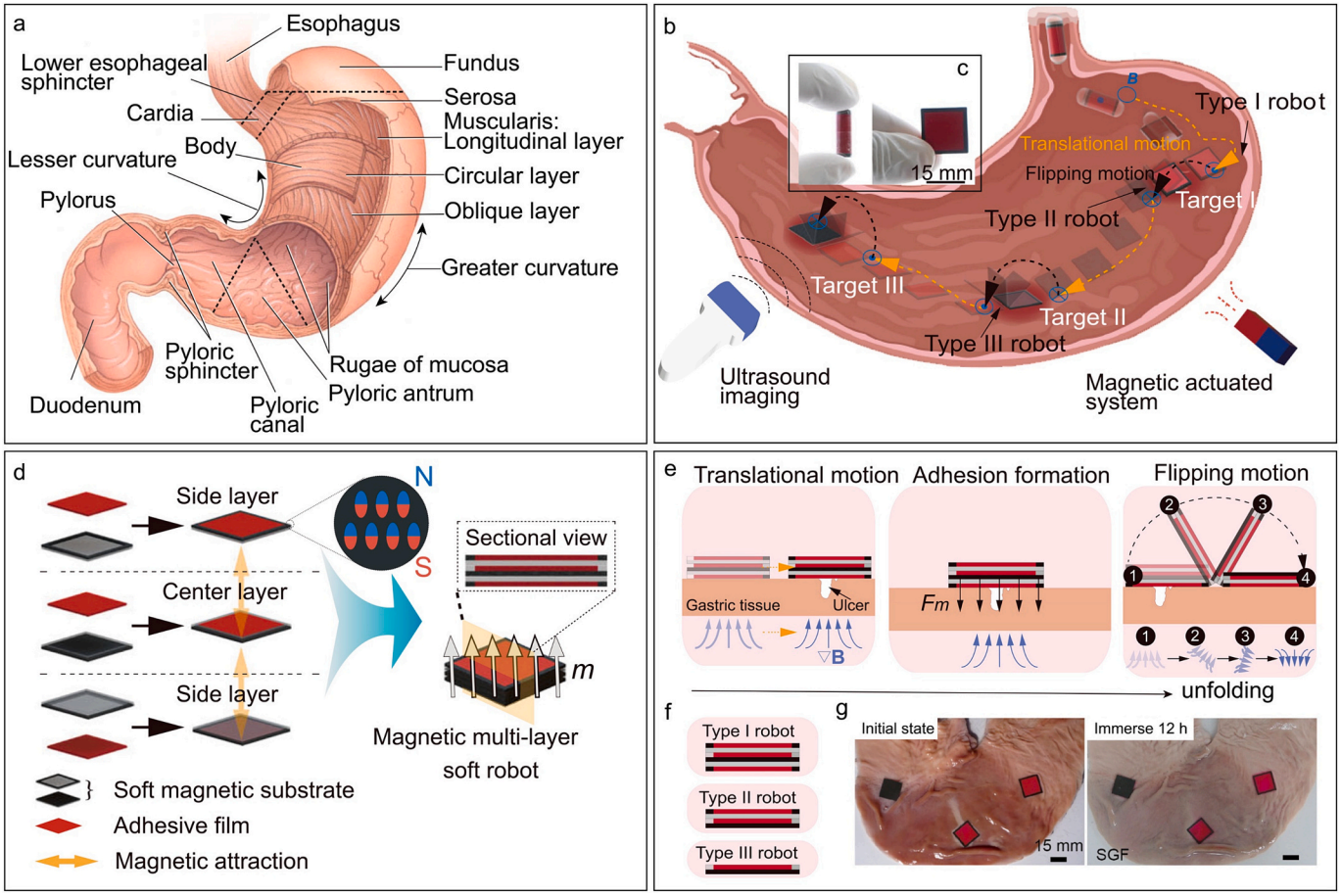

Fig. 3. Schematic diagram of stomach and developed SDDS in stomach. (a) scheme of the biostructure of stomach. (b-g) Schematics of a magnetic multi-layer soft robot and its application for on-demand multi-targeted adhesion. Reprinted and adapted from Ref [89, 134] with permission.

Time-dependent SDDSs have also been developed. These mainly comprise of three mechanisms: mucus adhesion, resistance to polyrus, and stomach swelling (Fig. 3a). Chen et al. used supramolecular materials such as cabopol, poloxamer, and hydroxypropylmethylcellulose to manufacture a mucoadhesive film and achieved nearly 12 h of gastric tissue and stomach retention; the process of delivery and retention in the stomach is shown in Fig. 3b–g [134]. Schematics of the magnetic soft robot are shown in Fig. 3b. The robot unfolded and adhered to the stomach mucosa using magnetic stimulation. First, the robot was in a released and encapsulated state, that is, it was a Type I robot. Second, multitarget adhesion was determined using a robot in the stomach, which was tracked by ultrasound imaging. The sizes of the robot layer and the capsule are shown in Fig. 3c. The side layer of the soft magnetic substrate features a magnetic frame and a nonmagnetic base, whereas the center layer is characterized by a nonmagnetic frame and a magnetic base (Fig. 3d). A schematic of the unfolding process of the Type I, II, and III robots is shown in Fig. 3e, based on the foldable structures of the robot shown in Fig. 3f. In Fig. 3g, the pattern on the left shows the initial state of the gastric tissue with the layers of the robot. The right pattern shows that the robot layer remained adhered to the tissue in the stomach after immersion in SGF for 12 h [134], which indicates the long-term adhesion of this SDDS in the stomach.

Swelling and stacking in the stomach may be useful strategies to prolong drug release. Jin et al. established a double network SDDS, where the first network swelled owing to the PAM network, and the second network continued to swell owing to the chitosan and sodium alginate. These two networks ensure SDDS retention in the stomach and prolonged drug release. This swollen SDDS is affected by gastric fluid owing to the breaking of weak supramolecular bonds (Fig. 4a) [136].

Carbopol has been used to design a drug carrier to delay the oral drug release time [137,138], which promotes the adhesion ability of the drug delivery system via the gastric route. Another time-dependent strategy was inspired by a biostructure adapted to the stomach structure. A starfish-like supramolecular drug carrier was designed and encapsulated and drug retention was achieved over a long period (weeks or months) in the pig stomach [139]. Supramolecular materials such as poly(e-caprolactone) (PCL) and Pluronic P407, act as drug-loaded carriers, Eudrigt L100–55 acts as an enteric linker, Plastoid B acts as an adhesive plasticizer, and PCL-polyurethane acts as an elastomer. After taking the drug orally, at a specific time, the drug “unfolded” due to digestion of the gastric fluid and adopted the shape of a starfish to adapt to the gastric cavity and adhere to the pylorus (pyloric diameter: 12.8 ± 7.0 mm [140]) to prolong the gastric retention of the drug [139]. Similar strategies have been applied in research on oral drug delivery systems [96,141,142]. Swelling SDDS can also be orally administered. The SDDS concentration reached 10-fold after contact with SGF for 50 min [136], whereas another study demonstrated a higher swelling rate of 100-fold in 10 min (Fig. 4b–d) [135]. Polyacrylic acid and polyvinyl alcohol formed a SDDS through supramolecular interactions, and the formation process and mechanism are demonstrated in Fig. 4b and Fig. 4c. As the absorbance time increased, the swelling ratio increased from 5 min to 60 min, as shown in Fig. 4d.

Wang et al. [143] found that montmorillonite nanosheets functionalized via carboxymethyl β-cyclodextrin were successfully synthesized and self-assembled into supramolecular networks of organoclay with hydrogen bonding junctions. Berberine hydrochloride (BBH) was loaded into the networks, and the antimicrobial properties of *Escherichia coli* (*E. coli*) and *Staphylococcus aureus* (*S. aureus*) were investigated. BBH

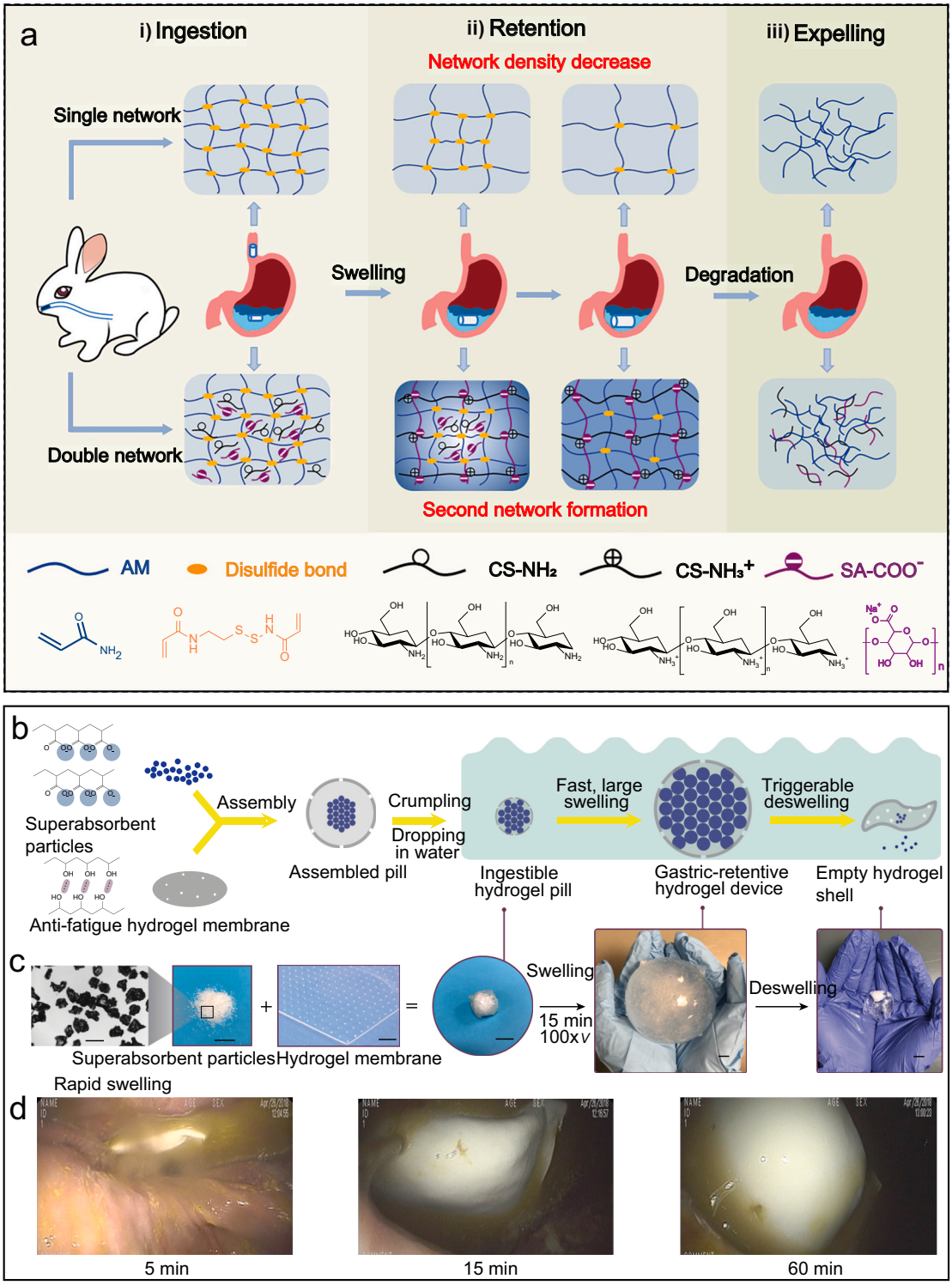

Fig. 4. (a) Design concept of swelling SDDSs. (b-d) Schematic representation and photographs illustrating the fabrication process and working mechanism of the hydrogel device. Scale bars represent 0.5 mm for the first image and 10 mm for subsequent images. Endoscopic images demonstrate the swelling behavior of the hydrogel device in a stomach of pig. Reprinted and adapted from Ref [135, 136] with permission.

demonstrated higher concentration-dependent antibacterial activity after the formation of D-networks. Time-dependent antimicrobial activity showed that the D-network dispersion system with 600 mg/ml BBH almost suppressed the growth of *E. coli*, whereas D-networks with 250 mg/ml BBH inhibited the growth of *S. aureus* by 97.81 % for more than 3 days. In summary, supramolecular organoclay networks may serve as promising antimicrobial delivery systems to facilitate the delivery of BBH to *E. coli* and *S. aureus*, thereby reducing the potential environmental risk of antibiotic abuse.

Temperature-responsive SDDSs are derived from temperature-responsive supramolecular molecules, and are classified into three main categories: high-temperature dissolution, sol-gel transparent supramolecules, and thermal shrinkage or expansion supramolecules. Babaee et al. [141] described an esophageal and gastric-resident drug

delivery system mainly composed of poly(ε-caprolactone or PCL), which opens as a flower-like shape after oral administration and allows long-term retention in the esophagus. In the presence of hot water (55 °C), the "arm" shrinks, leading to the unfolding of the SDDS, as shown in Fig. 5a-b. More precisely, the figures demonstrate the configuration of the device in various states: folded before deployment, fully deployed, lodged within the esophagus, and refolded following activation with hot water to facilitate its exit from the esophagus (Fig. 5b). Poloxamer 407, poly(2-(*N*-dimethylamino) ethyl methacrylate), PNIPAm, poly(oligo-ethylene glycol (meth)acrylates), poly(N-vinyl caprolactam)-based, poly ((meth)acrylate)-based, and poly(2-oxazolines) material are some temperature-responsive materials applied for oral drug delivery [144]. PNIPAm-based supramolecular materials have been used and designed with the structure of a blue-ring octopus [131], which collapses and releases the drug after stimulation at 37 °C from 20 °C. Protein-based materials also act as temperature-tracker switches. As shown in Fig. 5c, the microneedles within the patch, which were integrated with silk fibroin, PNIPAm, and F127 to form a composite hydrogel, exhibited a responsive drug delivery mechanism. Upon tissue penetration, these microneedles activated their injection behavior in response to the body's temperature, ensuring a swift drug release within a 2-h timeframe. Subsequently, they facilitated prolonged drug release to sustain the therapeutic impact over several days. A schematic of the temperature-response mechanism of the PNIPAm-based hydrogel is shown in Fig. 5d. Because of the increase in temperature, the viscosity of the silk-Fp hydrogel reached approximately 500 mPa·s at 37° °C from about dozens mPa·s (Fig. 5e). The release abilities of 5-FU and DEX as active pharmaceutical ingredients were tested, and the results indicated that the release speed was fast during the first 2 h and then controlled at a relatively low speed in 2–24 h (Fig. 5f and g, respectively).

Several studies have reported the use of a sol-to-gel transparency mechanism. Chen et al. [130] established a thermogelling film to orally deliver a nanoemulsion of fenofibrate with the supramolecular material hydroxypropyl methylcellulose (HPMC). The mechanism of SDDS is shown in Fig. 6a–c. Tween 80 was used to encapsulate the hydrophobic drug fenofibrate and HPMC to form an emulsion (Fig. 6b) via hydrophobic interaction between the methyl groups upon heating (Fig. 6c). Photographs of the oral films are shown in Fig. 6d and e. A film with a thickness of 111.8 μm was formed containing 0.4 g oil. The release capacity of this oral gel was recorded (Fig. 6f), indicating that the release ability of SDDS was controlled by erosion. Similarly, Wang et al. [146] manufactured temperature-responsive SDDS using methylcellulose/PEG/xylitol/Na_2HPO_4, and conversion from sol to transparent gel from approximately 25 °C to 37 °C was observed (Fig. 6g-k). As a generally regarded as safe supramolecular material, chitosan can form a thermogel with increased ionic strength, controlled release rate, and drug retention [147]. Chitosan also exhibits high mucoadhesion to mucins via electrostatic interactions [148]. Temperature-triggered self-assembly materials have attracted attention; monolinolein can form a Pn3m cubic phase (Q) at 38 °C from a less viscous lamellar phase (L) with la3d symmetry structure at 25 °C (Fig. 6g) [145]. By understanding the structural transformation of the SDDS, the release abilities of tofacitinib (TOFA) (Fig. 6h and i) and tacrolimus (TAC) (Fig. 6j and k) were studied. The results demonstrated that the controlled-release ability of SDDS after structural transformation resulted in the formation of a gel upon increasing the temperature to 38 °C.

pH-responsive SDDSs have been designed based on the pH of the human gastrointestinal tract. The mechanism of pH-responsive SDDS usually involves H^+ concentration, functional group status (-COOH and -NH_2), electrostatic interactions, structural transformation (peptides and proteins), and swelling or shrinking (pH-responsive polymers). Hu et al. [149] used DNA and acrylamide to form copolymers to encapsulate insulin. Within an acidic pH range of 1.2 to 6.0, a copolymer with a hydrogel-like state was created through crosslinking by A-motif duplexes arranged in parallel at pH from 1.2 to 3.0 and i-motif quadruplexes at pH from 4.0 to 6.0. Upon reaching physiological pH, the adenine and cytosine bases become deprotonated, leading to the dissociation of the copolymer into a solution. This process resulted in the separation of the A-motif and i-motif structures into their respective single-stranded forms, which were characterized by adenine-rich and cytosine-rich sequences. Orally administered insulin was controlled in the cross-linked networks in the stomach and duodenum and released from the supramolecular hydrogel owing to the elimination of reverse Hoogsteen and electrostatic interactions in the intestine (Fig. 7a). For the in vitro digestion test, the release ability of pH-responsive SDDS was determined in artificial gastric (pH 1.2), duodenal (pH 5.0), and intestinal (pH 7.2) fluids the results are shown in Fig. 7b-d. The pH sensitivity of SDDS allowed it to resist the pH of the fluid in the stomach and duodenum (nearly 0 % in 120 min) and release insulin in the intestine, confirming the controlled-release ability at specific sites (nearly 100 % in 60 min in the intestine). The ELISA results also indicated the controlled-release capacity of SDDS (Fig. 7e). The unique pH resistance of the A-motif and i-motif structures of SDDS is shown in Fig. 7f, and the combination of these two structures would help achieve promising pH resistance and release at the pointed site (intestine). Compared to subcutaneous injections of insulin, the SDDS showed interesting efficacy. More precisely, as shown in Fig. 7 g, no reduction in blood sugar was observed in unencapsulated insulin administered orally (30 IU/kg), whereas a 20 % decrease occurred after 2 h of subcutaneous injection of insulin (3 IU/kg). Insulin release was effectively managed for over 12 h using the insulin@DNA hydrogel administered orally. This SDDS led to a peak in the serum insulin level at 6 h post-administration, recording a level of 15.2 ± 4.2 μIU/kg. Changes in the structure of SDDS with pH were also demonstrated in another study. The self-assembling peptide (Fig. 7h) was combined with PEG to achieve pH-responsive capacity to control drug release owing to structural transformation (Fig. 7i). In an alkaline pH environment, SDDSs remain in the sol state (Fig. 7j), but after being placed in an acidic pH environment, they transforms into a gel state with a high storage modulus (G', Fig. 7k) [150].

A DNA-based hydrogel has been reported to promote controlled release, with FcRn showing a similar ability. Martins et al. [151] found that chitosan with a positive surface ζ potential coating (25 ± 0.5 mv) on the surface of FcRn-modified porous silicon particles could prolong the gastrointestinal retention time on the negatively charged mucin layer in the intestine. Hypromellose acetate succinate (HF) was designed as an enteric pH-responsive part due to its property of being soluble at alkaline pH and its tendency to precipitate in an acidic pH environment, the manufacture of the SDDS is shown in Fig. 7 l and m. The difference in the release capacity of the coated and uncoated SDDS is shown in Fig. 7n, indicating that the HF coating layer offers a low pH (1.2) resistance. The in vitro permeability of SDDS was effectively confirmed to be significant in Fig. 7o. Cell viability demonstrated that SDDS safety was ensured within a concentration range of 25–600 μg/ml (Fig. 7p). Martins et al. used this formulation to deliver GLP-1 agonists and achieved a controlled release of drugs. The same strategies were used in other studies [45,150,152,153].

Zhang et al. [154] developed micelles loaded with ginsenoside CK (APDCK) using a chitin-derived homing peptide (A54 peptide) to target hepatocellular carcinoma cells. This SDDS demonstrated a pH-responsive drug release ability and achieved sustained release via a non-Fickian diffusion mechanism. In vitro studies have demonstrated that micelles loaded with APDCK exhibit significantly higher toxicity to HepG2 and Huh-7 cells than CK alone. In addition, the increased cellular uptake of these micelles by the mentioned cells was validated through confocal laser scanning microscopy and flow cytometry analyses. Furthermore, western blotting analysis demonstrated that APDCK micelles promoted apoptosis in hepatocellular carcinoma cells by elevating caspase-3, caspase-9, and PARP proteins. Therefore, APDCK micelles can act as a platform for delivering hydrophobic drugs and enhancing drug targeting and anticancer activity.

Miller and Medina [155] developed a synthetic colonic mucus mimetic fluorine-assisted mucus surrogate (FAMS) that replicated the

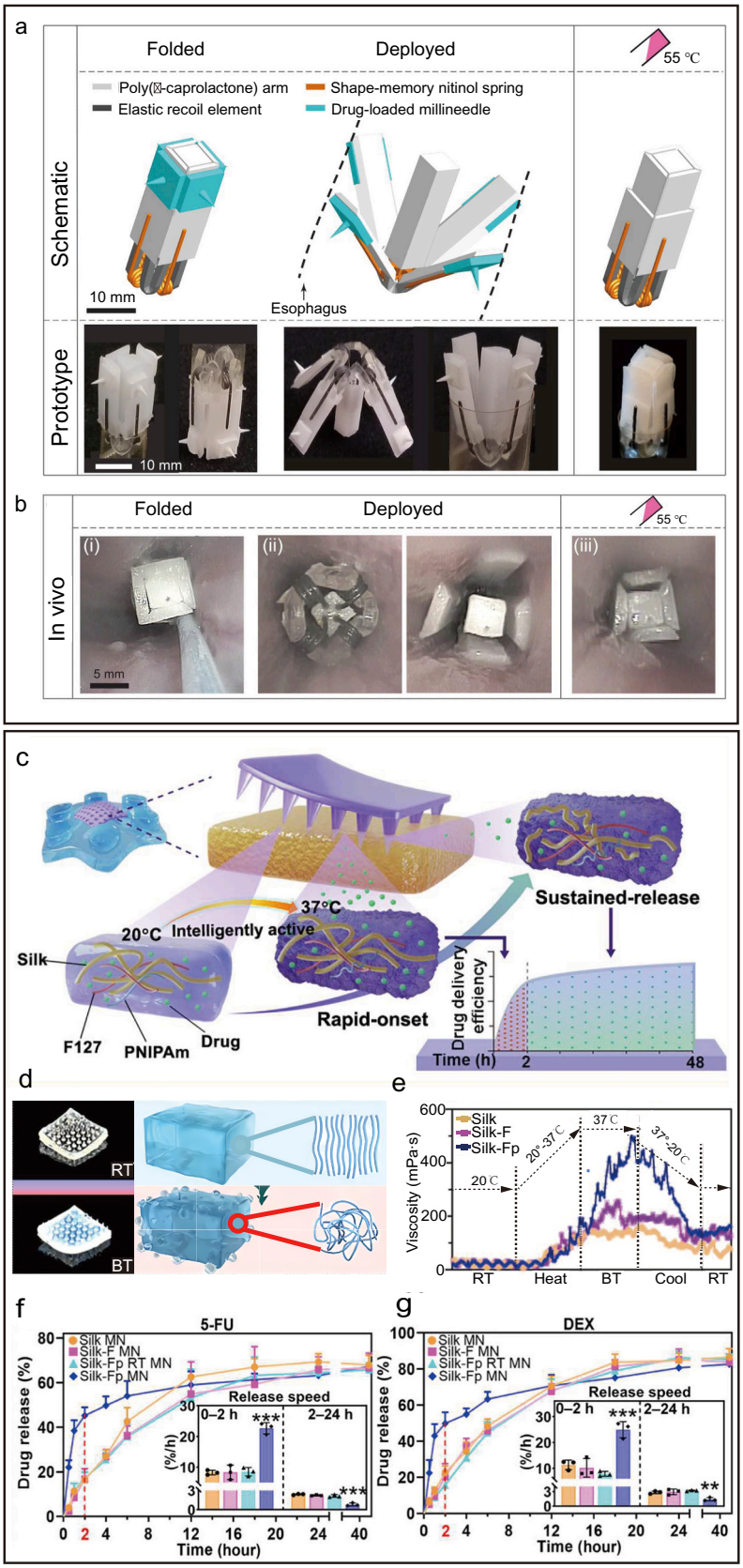

Fig. 5. Temperature-responsive SDDSs in oral administration. (a) Schematic and prototype images of the flower-like system. (b) Endoscopic in vivo images showing the prototype in a porcine esophagus under various configurations: (i) folded, (ii) deployed in both forward and reverse directions, and (iii) refolded after exposure to 100 ml of water at 55 °C. (c-g) Octopus-inspired SDDS. (c) scheme and controlled release ability of the SDDS. (d) Silk-Fp MN contracts as the temperature increases from 20 °C to 37 °C. e: Viscosity of samples across temperature variations. (f-g) Drug release profiles and average release rates (0–2 h and 0–24 h) for 5-fluorouracil (5-FU) or dexamethasone sodium phosphate (DEX). Reprinted and adapted from Ref [141] [131] with permission.

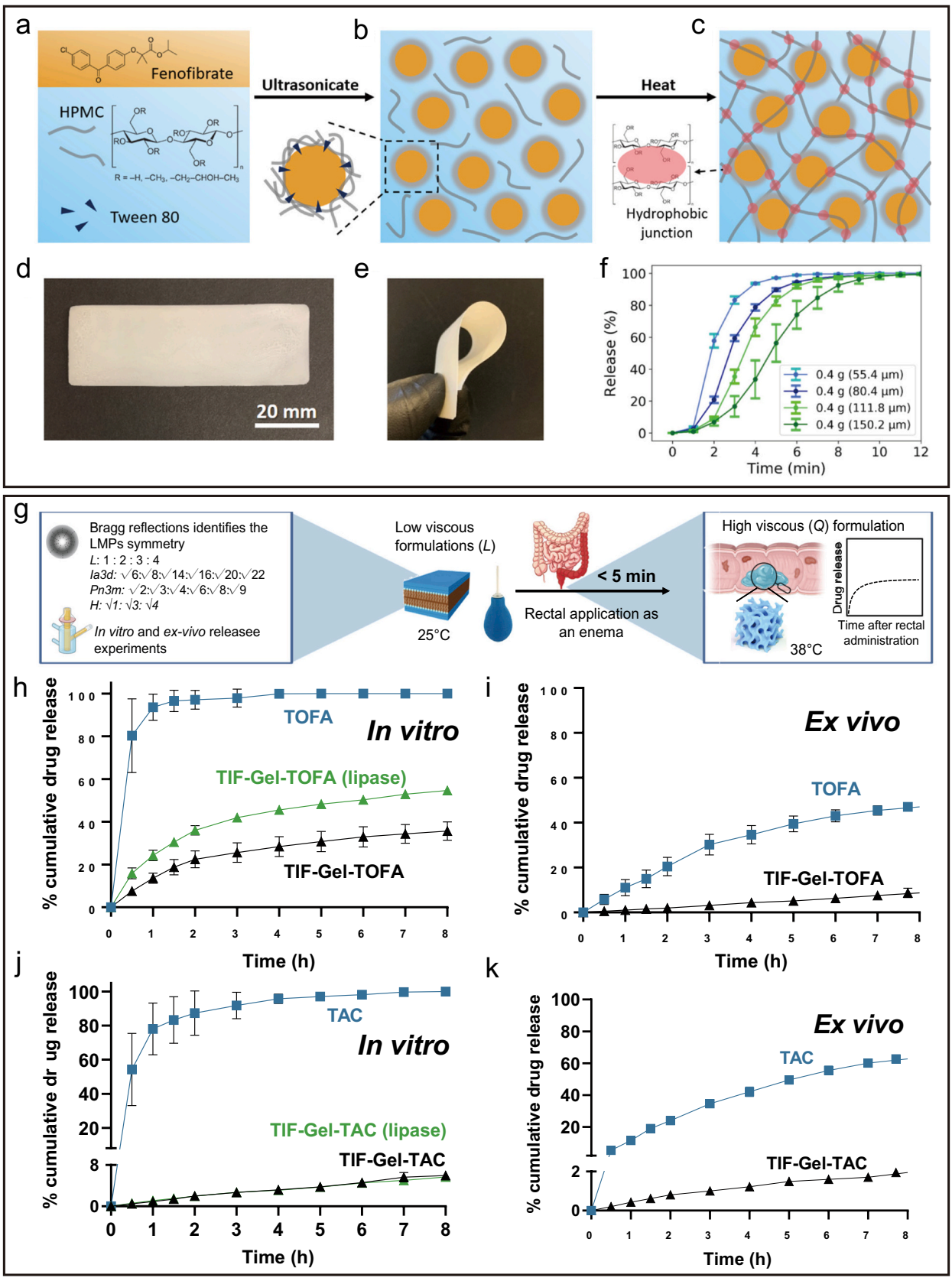

Fig. 6. Thermogelling SDDSs administrated orally. (a-f) Overview of the preparation of HPMC thermogel nanoemulsion. (a-c): Oral film manufacture process. (d-e) Images of oral film after drying. (f) Release profiles of 55.4 μm oral film [130]. (g-k) Temperature-triggered SDDS for the oral treatment of ulcerative colitis (UC). (g) A schematic depiction of gel formation. (h-i) In vitro and ex vivo release profiles of TOFA and TIF-Gel-TOFA. (j-k) In vitro and ex vivo release profiles of TAC, TIF-Gel-TAC [145]. Reprinted and adapted from Ref [130] [145] with permission.

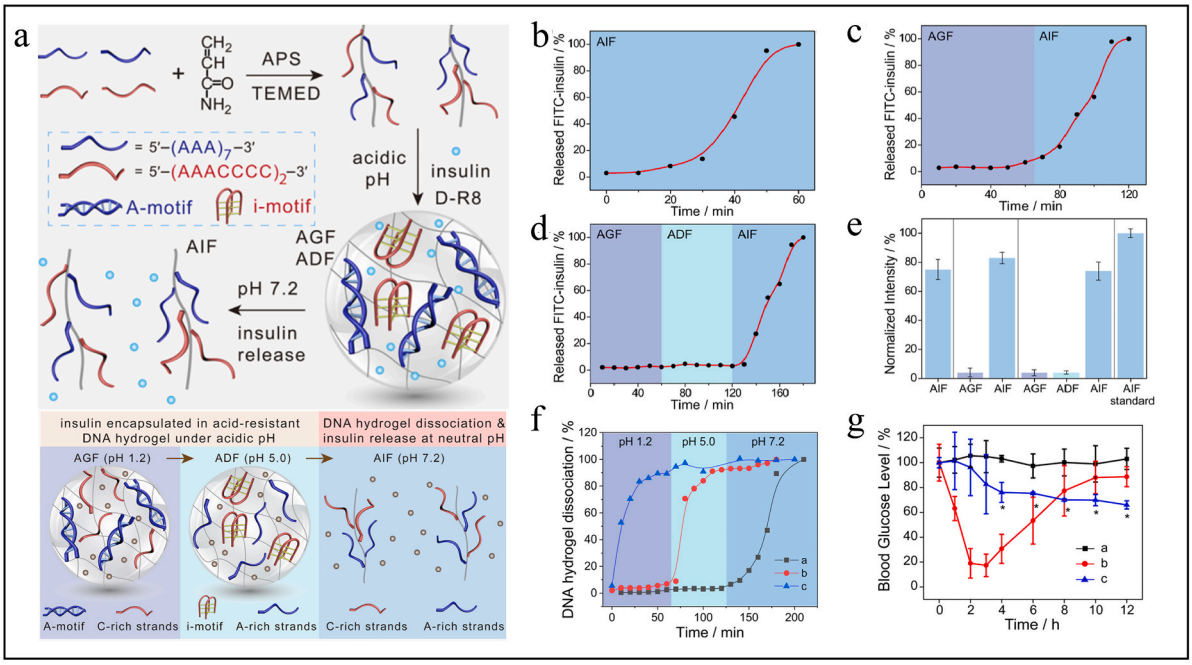

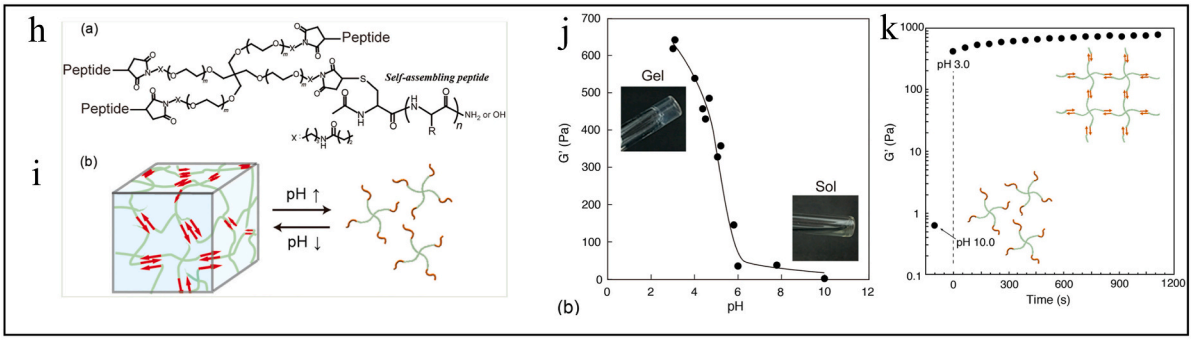

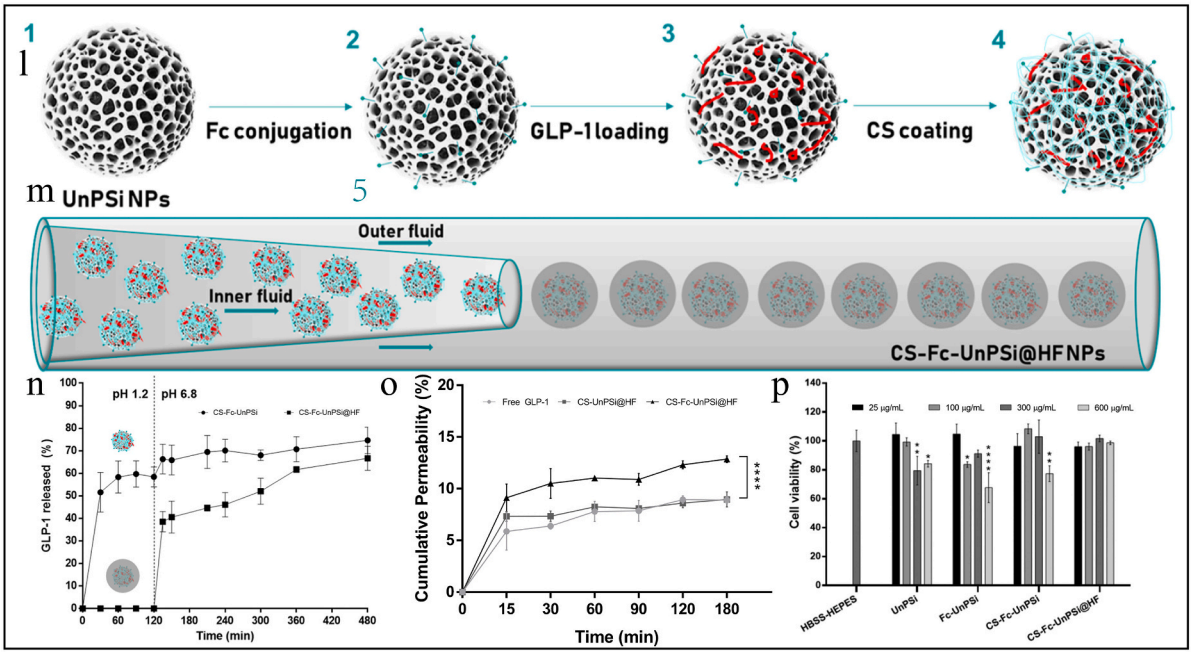

(caption on next page)

Fig. 7. pH-responsive SDDSs. (a-g) A-motif and i-motif synergy DNA hydrogel with pH-resposive ability for oral insulin delivery. (a) Schematic depiction of the preparation and release profiles of pH-responsive DNA hydrogel. (b-d) Release profile of FITC-insulin from DNA hydrogel in AIF, AGF, and ADF. (e) ELISA of insulin released from DNA hydrogel in different artificial digestive fluid. (f) Dissociation behaviors of DNA hydrogel cross-linked by both A-motif and i-motif (curve a), A-motif alone (curve b), and i-motif alone (curve c) at pH 1.2, 5.0, and 7.2. (g) Blood glucose levels versus time in diabetic mice after oral taken free insulin solution (curve a), subcutaneous injection (curve b), and insulin@DNA hydrogel (curve c) [149]. (h-k) Fast pH-responsive SDDS. (h) Chemical structure of the peptide−PEG polymers utilized as self-assembling blocks. (i) Schematic depiction of the pH-responsive hydrogel. (j) pH-dependence of G' values of the hydrogel. (k) time sweep profile of storage modulus of hydrogel in different pH from 10.0 to 3.0 [150]. (l-p) pH-responsive SDDS made by chitosan-modified FcRn-targeted porous silicon nanoparticles@hypromellose acetate succinate (HF). (l) the manufacturing process of CS-Fc-UnPSi@HF nanoparticles. (m) Coating process of CS-Fc-UnPSi@HF using glass capillary microfluidics. (n) GLP-1 release profiles from CS-Fc-UnPSi and CS-Fc- UnPSi@HF NPs. (o) In vitro GLP-1 permeability of GLP-1, CSUnPSi@HF, and CS-Fc-UnPSi@HF NPs loaded with GLP-1. (p) Cell viability values of different intestinal cells when exposed to the different NP formulations (UnPSi, Fc-UnPSi, CS-Fc-UnPSi, and CS-Fc-UnPSi@HF NPs) [151]. Reprinted and adapted from Ref [149] [150] [151] with permission.

structural, mechanical, and biochemical properties of human colonic mucus. FAMS forms a network of viscous fibers by self-assembling fluorinated amino acids at the liquid-liquid interface, which can bind to mucosal proteins to provide a habitat for microbial colonization, which binds to human colon cells to generate artificial mucosa or microbiome organs. FAMS are simple to design, inexpensive, and can modulate their rheological properties in reaction to environmental conditions (e.g., ionic strength and pH), ensuring that they are useful for drug screening and in vivo studies.

3.3. Supramolecular drug delivery system in the small intestine

Ionic-sensitive SDDSs have been inspired by the complex ion environment in the small intestine because of the salts in the intestinal fluid, including KCl (6.8 mM), KH_2PO_4 (0.8 mM), $NaHCO_3$ (85 mM), NaCl (38.4 mM), $MgCl_2$ (0.33 mM), and $CaCl_2$ (0.6 mM) [102]. Alginates are widely used as oral materials and have attracted the attention of researchers. Patta et al. [156] established an 8-h gastrointestinal-retention oral drug delivery system using electrostatic interaction with −14 kcal/mol Gibbs energy between ionized alginate and chitosan. A similar material was used in a study by Taymouri et al. [157], in which a series of ionic-sensitive delivery systems composed of alginate and delivered proteins were prepared and confirmed to dissociate at high physiological ionic strength and under the influence of microions in the solution, which led to charge detection effects [158,159]. Carrageenan-based supramolecular materials are used as orally administered drugs, which can cross-link with iron ions and release drugs into the intestinal environment [160–162].

Swelling SDDSs have been widely applied in the hydrogel state. Typically, swelling ability is related to factors such as shape, network structure, uniform degree of network, inner network interaction, hydrophilicity, porosity, rheology, thermal ability, and environmental ionic concentration. The carboxymethyl cellulose-based hydrogel was designed as a swelling-controlled-release cargo to deliver soybean peptides in the small intestine, and different release rates were recorded owing to complex factors including crystallinity, porosity, pH, electrostatic interaction, and movement of polymer chains [163,164]. Absorbing moisture causes SDDS to swell and form an obvious mesh-like network, which increases the volume of SDDS and prolongs the distance between the supramolecular chains. This result, in the expansion of networks owing to the weakening of the weak bond linkage, allowing drugs to be delivered smoothly via oral administration [165]. Another study on microparticles comprising of three pectins and $CaCl_2$ that formed a supramolecular gel showed different swelling abilities in SGF, SIF, and SCF. SVC gels (campion pectins) swelled in SGF and SIF, while maintaining a stable swollen state for 24 h in SCF. The LMC gel (duckweed pectins) swelled in all simulated gastrointestinal fluids and dissolved in SCF. The apple pectin gel was swollen in SGF, began to dissolve in SIF, and dissolved in SCF within 30 min [166].

Mucoadhesive SDDSs [167] were developed by considering the specific environment of the mucus layer mentioned in Section 2.2. Supramolecular interactions can help cargo penetrate the mucus layer, reach the intestinal epithelial cell layer, and adhere to the mucosa of the gastrointestinal tissue. Without penetration and resistance, the drug vehicle would probably flush down the intestinal tract, resulting in drug wastage and reduced drug efficiency [168]. For instance, *Ganoderma lucidum* spores were designed as a porous vehicle after iturin A (peptide) treatment and switched to a hydrophilic vehicle after iturin A and KOH treatment and to a hydrophobic vehicle after iturin A and HCl treatment. The retention time was approximately 120 h. The drug release profile followed first-order kinetics, and the low release constants indicated controlled and prolonged drug release ability [169]. Furthermore, sticky hydrophobic and charged substances exhibited motion in terms of adhesion in another study [170].

Oral microneedle SDDSs were developed based on their pH-responsive, temperature-responsive, swelling, and mucoadhesive abilities. Attracted by porcupine fish and their defensive status (Fig. 8a and b), Gao et al. used the swelling supramolecular material sodium carboxymethyl cellulose to ensure astonishing absorption and swelling ability, resulting in maintenance of the gastrointestinal tract for a relatively long time. The drugs were loaded into the arrow part of the oral microneedle SDDS (Fig. 8c), which was designed on a high-performance stretchable base that could stretch nearly 50 % longer (Fig. 8d), with an expansion of approximately 20-fold after swelling (Fig. 8e). A schematic of a spherical SDDS of oral microneedles is shown in Fig. 8f, showing the flexible film and absorbent gel corresponding to replicating the quills, skin, and water retention in the abdominal region of the porcupinefish. The swelling capacity of SDDS in water and ex vivo minipig intestines is shown in Fig. 8g and h. The microneedle expands and relies on natural gut motility to facilitate needle insertion, adherence to the mucosa, and discharge of medication. After enduring continuous muscular squeezing, the microneedle mechanism hit its exhaustion threshold, fragmented, and was eliminated from the body via the digestive system (Fig. 8i) [171]. A similar study was conducted by Zhang et al. [172]; however, a magnet was used to control the movement of the SDDS (Fig. 8j). As per the figure, the magnetic field-guided oral microneedle SDDS penetrates the small intestinal wall (Fig. 8k). After penetration through the wall of the small intestine, the magnetic substance would be separated owing to degradation, resulting in retention of the tips for lasting drug release (Fig. 8l).

These oral microneedle SDDSs aim to penetrate the mucus layer and deliver drugs to the epithelial cell layer. The objective of oral microneedle SDDS is to breach the mucosal barrier and facilitate drug delivery to the epithelial cells. For example, a temperature-triggered SDDS (Fig. 9a) was developed and applied for oral drug delivery. Using the temperature-sensitive material paraffin wax as hinge segments to form a structure perpendicular to the small intestinal epithelial layer and deliver insulin to the plasma in rats (Fig. 9b), the microinjector (green line) achieved a higher plasma insulin concentration than intrarectally injected insulin (blue line), achieving controlled release compared with intravenously injected insulin (red line). Testing the AUC of insulin indicated that insulin efficacy was not significantly different between IV insulin and the microinjector SDDS (Fig. 9c). Furthermore, supramolecular chitosan has been used to enhance the adhesive ability of this SDDS [173]. Another SDDS was designed as a jet-trigger (Fig. 9d) for rocket-inspired effervescent motors (RIEMs) [174]. $NaHCO_3$ and citric acid were mixed with poly(vinylpyrrolidone) (PVP) and encapsulated in enteric-soluble capsules (Fig. 9d), resulting in the generation of CO_2

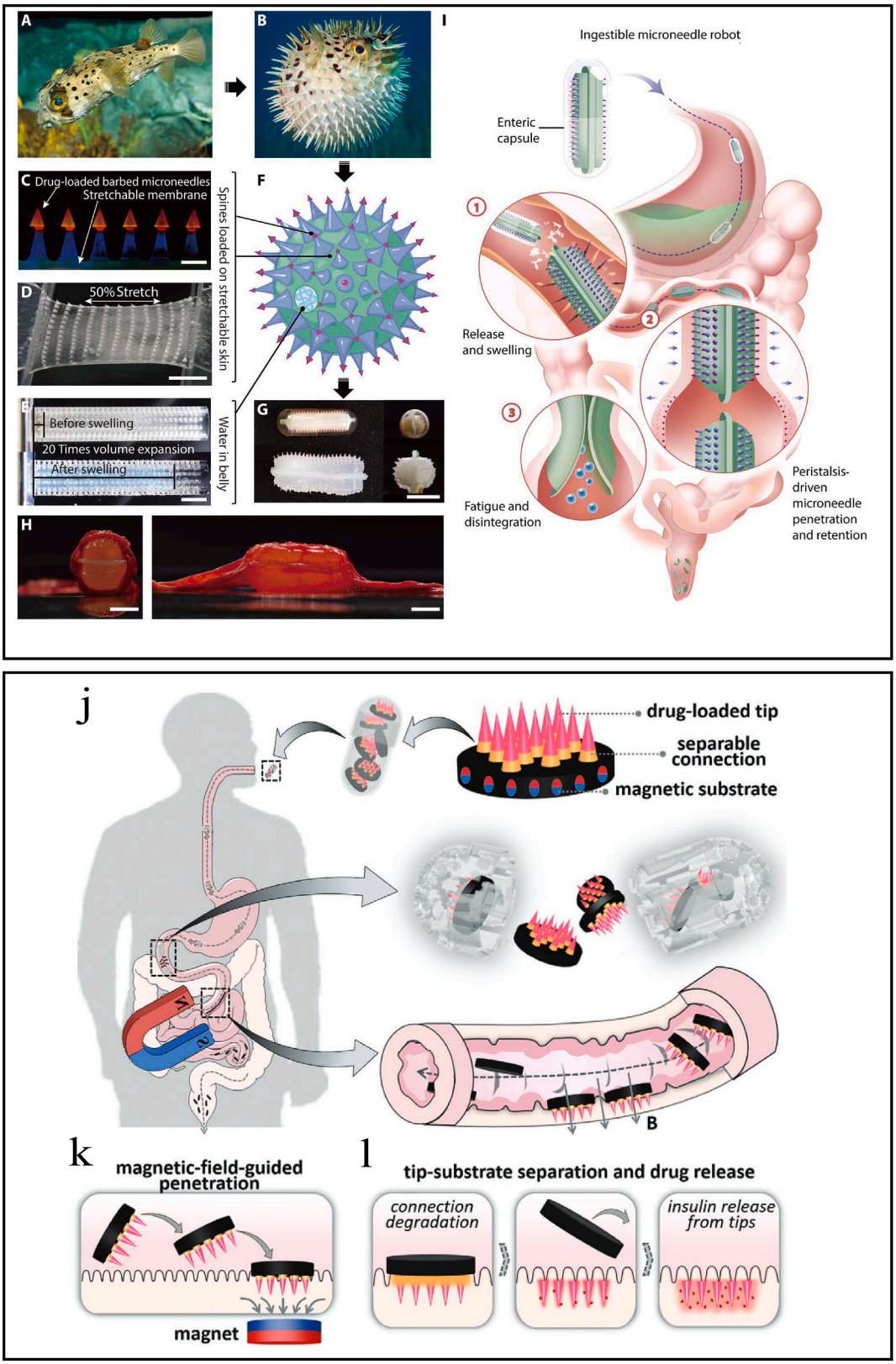

Fig. 8. Oral microneedle SDDSs. (a-i) porcupine fish inspired oral microneedle SDDS. (a-b) porcupine fish at calm and frightened status. (c) A fluorescent image showing the microneedles with 1 mm bar; (d) Photograph of the stretched microneedle patch with a 5 mm scale bar. (e) Photograph of the swelling SDDS before (top) and after swelling (bottom) with a 15 mm scale bar. (f) Schematic depiction of the bioinspired SDDS. (g) Photographs of the microneedle SDDS pre- and post-swelling with a 10 mm scale bar. (h) Images of a swollen microneedle SDDS in ex vivo minipig intestine with a 10 mm scale bar. (i) Schematic of microneedle SDDS delivery route through a digestive tract [171]. (j-l) Magenetic-filed-guide oral microneedle SDDS. (j) Schematic depiction of magnet microneedle SDDS. (k) Microneedle SDDS guided by the magnet and penetrate epthilal cell layer. (l) Degradation of SDDS and release of drugs from the inserted microneedle [172]. Reprinted and adapted from Ref [171] [172] with permission.

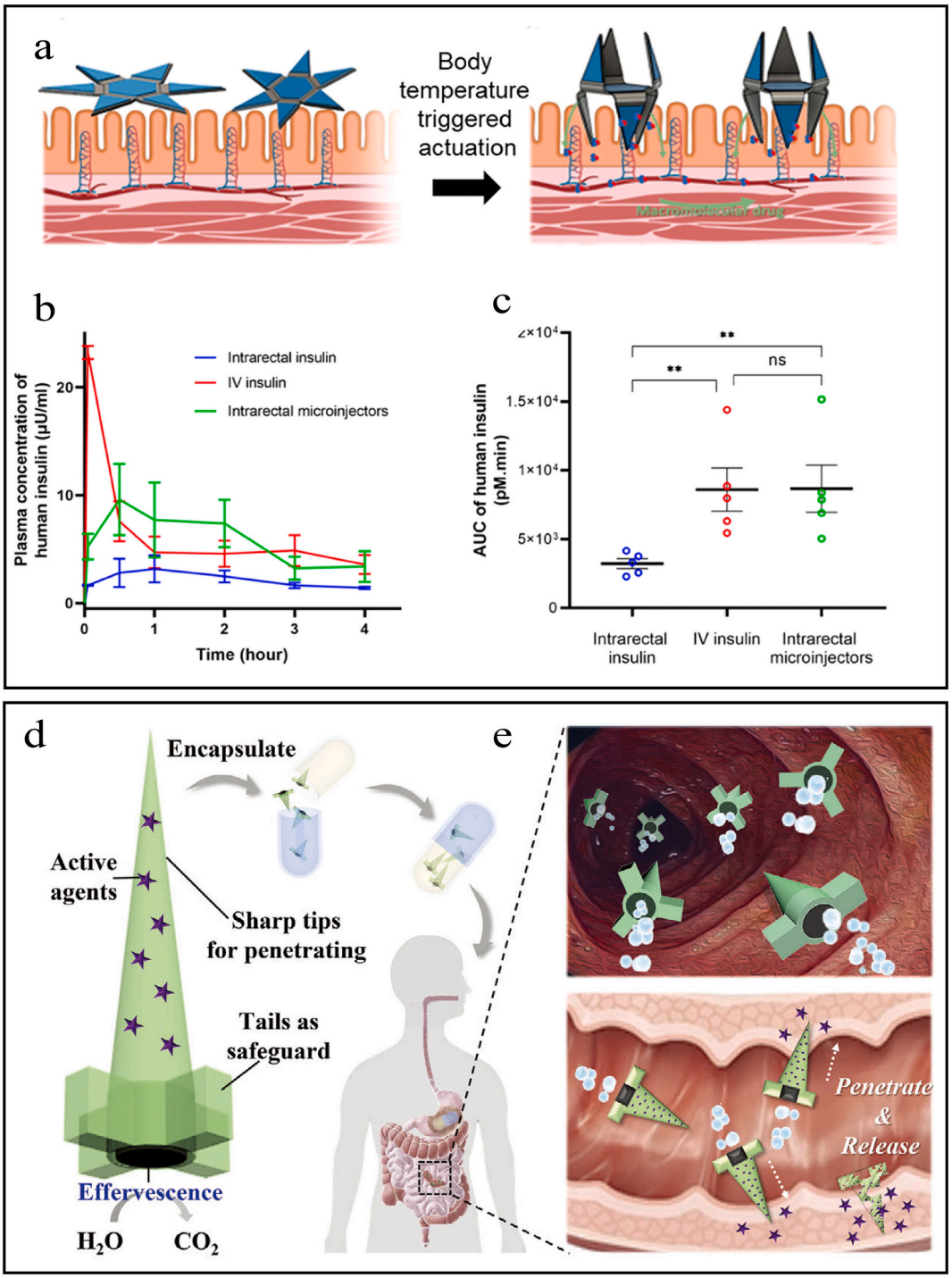

Fig. 9. Stimulation-resposive oral microneedle SDDSs. (a-c) Body temperature triggered SDDS. (a) Schematic depiction of two microinjectors, each with an injection arm that penetrates the mucosal layer after being heated to body temperature, ensuring the transport of macromolecular drugs across the mucosal epithelial barrier. (b-c) Pharmacokinetic profile and AUC of the concentration of human insulin measured in mice plasma after 4 h. Intravenously injected insulin (Red); oral microinjectors (green); intrarectally insulin (blue) [173]. (d-e) Jet-type oral microneedle SDDS. (d) Schematic illustration of the rocket-like effervescent micromotors. (e) Schematic depiction of RIEMs for orally delivering active agents in vivo [174]. Reprinted and adapted from Ref [173] [174] with permission. (For interpretation of the references to colour in this figure legend, the reader is referred to the web version of this article.)

when SDDS reached the intestinal digestion fluid (Fig. 9e).

SDDS intestinal self-assembly is an intelligent system that responds to comprehensive and complex intestinal environments, including pH, ion concentration, digestion enzymes, and temperature. To enhance the efficacy of DPP4 inhibitors, Pugliese et al. [175] established a nanogel using the RADA16 peptide to encapsulate Lup1 as a DPP4 activity inhibitor to help control blood sugar levels in humans. After spontaneous self-assembly of the RADA16 peptide, the supramolecular organization of RADA16-Lup1 was formed and DPP4 activity was impaired by 29 % in human serum compared to unencapsulated Lup1 by 18.1 %. The self-assembly trigger was determined to be an external stimulus, including the pH, temperature, or the presence of monovalent or divalent electrolyte ions. Another study demonstrated self-assembled peptides (5–15 amino acids, 605–2067 Da) derived from *Crassostrea gigas* as oral

treatment ingredients to heal wounds in mice, with significant wound healing promotion ($p < 0.05$) [176]. Self-assembly of SDDS could also deliver the β-sheet peptide KLVFF to suppres tumor cell proliferation by activating the generation of reactive oxygen species (ROS). The polymer-peptide conjugate self-assembled in vivo [177].

Insua et al. developed a supramolecular pH-responsive drug delivery system, they focused on a particular cyclic peptide (CPx) capable of forming nanotubes by one-dimensional (1D) self-assembly in an aqueous solution and then further arranging them into tubular bilayers to form giant two-dimensional (2D) nanosheets [178]. These nanosheets have remarkable dimensions at the mesoscopic scale and can be reversibly transformed by stimuli such as temperature and pH, including changes in the state of dispersion, aggregation, and assembly. Such materials are generated through a sequential one-dimensional to two-dimensional self-assembly process with hierarchical organization. Regarding supramolecular pH-responsiveness, the self-assembly behavior of CPx cyclic peptides at different pH values has attracted significant attention. At pH 7.4, nanotubes have a highly anionic character on surface because of the degree of deprotonation of glutamic acid (>99.9 %) and the neutrality of histidine residues (>96 %). This leads to the assembly of nanotubes via a hydrophobic bilayer structure, where layer-to-layer displacement produces stable π-stackingof leucine zippers and tryptophan indoles. The negatively charged surface of this structure prevents individual layers from clumping and is stabilized by hydrogen bonds between the side chains of histidine and glutamine. In addition, the morphology of the nanosheets was affected by the pH change. When the pH was adjusted to the histidine pKa value (pH 6.0), protonation of the histidine imidazole ring led to disintegration (or collapse) of the nanosheets owing to increased electrostatic forces between the cyclic peptide monomers. As the pH was further lowered to the pKa value of glutamic acid (pH 4.0), electrostatic repulsion resumed despite the formation of some electrostatic aggregates, and the nanosheet structure was maintained when the pH was decreased to where the CPx monomers acquired a full positive charge (pH 2.8). These experimental results emphasize the crucial role of glutamic acid and histidine in the two-dimensional self-assembly of CPx and confirm that dynamic remodeling of nanosheets can be achieved by modulating the pH. To offer some guidence for the proper SDDS along with the oral tract, the strength and limitation of SDDSs are demonstrated in Table 3.

Other aspects of self-assembled peptides have also been investigated. Wang et al. [179] evaluated the self-assembly of short peptides into nanoribbons, particularly the mechanism by which β-sheets interact with polar zippers to form higher-order structures. Short peptides were used based on the formula Ac-I3XGK-NH_2, where X represents different amino acid residues, including uncharged polar amino acids (glutamine Q, serine S, and asparagine N) and hydrophobic amino acids (such as glycine G, norvaline norV, and leucine L). Altering the position of X resulted in variable self-assembly behaviors and nanostructured morphologies. Transmission electron microscopy and atomic force microscopy confirmed that the wide and flat nanoribbons formed by Ac-I3QGK-NH_2 were approximately 50 nm wide and exhibited a rigid and flat morphology. The small-angle neutron scattering data indicated that the Ac-I3QGK-NH_2 nanoribbons comprised multilayered β-sheets, with each layer being approximately 3.8 nm thick. Furthermore, circular dichroism and Fourier transform infrared spectroscopy measurements confirmed that all designed peptides adopted β-sheet conformations. ^{13}C {15 N} REDOR using solid-state nuclear magnetic resonance techniques further elucidated the stacking mode of β-sheets in Ac-I3QGK-NH_2 nanoribbons, which featured an antiparallel arrangement and a one-residue shift. These findings suggest that the formation of polar zippers is mediated by hydrogen-bond interactions between the β-sheets, which promote further lateral stacking of the β-sheets to form wide nanoribbons.

Control of the structure of self-assembled peptides has also been demonstrated in other studies. Zhao et al. [180] designed several hexapeptides and used isoleucine and valine to adjust the hydrophobicity of hexapeptide, and finally found that the peptide bolaphiles would usually form long nanotubes by the single layer of peptide due to structure of molecule, β-sheet secondary structure and the shape and hydrophobicity of side-chains. Adjusting the hydrophobicity and variation in the core side chain demonstrated that the size of the peptide nanotubes could be adjusted to 100–100 nm.

Metal coordination is one of the supramolecular interaction. Liu et al. [181] described a method for the in situ polymerization of nanoscale metal-organic framework (MOF) to improve their stability under digestive environments and enable intracellular stimulus-responsive drug delivery. The team found that by wrapping the polymer around the MOF surface, the MOF could be protected from decomposition by phosphate ions or acidic environments, thus preventing the leakage of the drug carrier. In vivo positron emission tomography studies revealed that ^{64}Cu-labeled polymer-coated MOF nanoparticles had a prolonged circulation time in vivo and accumulated in tumors to a greater extent than unmodified MOF nanoparticles. This suggests that MOF nanoparticles with enhanced stability owing to in situ polymerization can serve as effective drug trucks for targeted drug delivery and controlled release into tumors.

Bao et al. [133] constructed gold-copper MOF nanosheets (AuTPyP-Cu NSs) using a ligand self-assembly strategy, which responded to both pH and sonication to synergistically trigger cuproptosis (copper death) and enhance chemotherapy. The AuTPyP-Cu NSs released Cu ions in a controlled manner in the presence of an acidic tumor microenvironment and sonication. AuTPyP-Cu NSs can control the release of Cu ions in an acidic tumor microenvironment under ultrasound, which activates iron-sulfur protein 1 (FDX1)-mediated cuproptosis through the generation of ROS by reacting with glutathione. Furthermore, the released AuTPyPs specifically bindto thioredoxin reductase and activate a redox imbalance in tumor cells. Moreover, this study elucidated the controlled assembly of multiresponsive nanotherapeutics and the application of specific ROS modulation in anticancer therapy.

Combining the advantages and disadvantages of SDDSs, we present the advantages and limitations of the applied SDDSs as follows: Time-dependent SDDS are designed to regulate drug release according to a predetermined temporal mechanism. These systems typically use materials, such as water-soluble matrices or osmotic pumps, where the drug release rate and duration are programmed in advance and remain unaffected by external environmental factors or physiological fluctuations. A significant advantage of time-dependent SDDSs are their ability to maintain a consistent drug concentration over time, minimizing fluctuations in plasma drug levels. This feature is advantageous to treat chronic conditions that require stable, long-term drug concentrations, such as hypertension and diabetes. Moreover, time-dependent systems reduce the frequency of drug administration, which can improve patient adherence to the prescribed regimens.

However, a primary drawback of time-dependent SDDSs is their lack of flexibility, as they cannot be adjusted to accommodate individual patient differences or physiological variations. Specifically, if a patient's condition changes, the drug release rate and dosage may no longer be optimal, potentially compromising the therapeutic outcome. In addition, these systems may encounter issues such as rapid drug release at the onset or slow release toward the end of the dosing period, which could cause either overdose or insufficient drug delivery. Consequently, although time-dependent SDDS are suitable for the stable, long-term treatment of chronic diseases, their applicability to personalized medicine remains limited. Future research should focus on integrating biological feedback mechanisms and intelligent control systems to enhance the adaptability and responsiveness of time-dependent SDDS.

Temperature-responsive SDDSs regulate drug release based on the thermosensitivity of the materials used. When the external or local temperature changes, the thermoresponsive polymers in the drug delivery system undergo physical or chemical transformations, such as the transition from a hydrophilic to a hydrophobic state, which leads to the release of the drug. Typical materials include poly(N-

Table 3
Strength and shortage of supramolecular drug delivery system.

Supramolecular Drug Delivery System (SDDS)	Materials with supramolecular interactions	Supramolecular mechanism	Applied site	Trigger	Strength	Limitation	Ref
Time-dependent SDDS	Pluronic P123	Hydrogen bond interaction	Colon	pH 7.4	Target release profile with 88.35 % of the dose released after an 8 h lag period	Elimination risk	[137]
Time- dependent SDDS	PEG, PLA, Elastollan®1185, Eudragit L100–55	Hydrogen bond interaction	Stomach	SGF	One week stomach retention	Low stabilization and drug loading	[142]
Time-dependent SDDS	Carboxymethyl beta-cyclodextrin	Host-guest interaction, Hydrogen bond interaction, self-assembly	Gastrointestine tract with *E. coli* and *S. aureus*	pH 7.4	Synchronously antibacterial property	Low drug loading rate	[143]
Temperature-responsive SDDS	PCL, PEG, Eudragit E PO	Hydrogen bond interaction	Esophagus or stomach	Warm water (55 °C)	Long-term retention	Too hot for esophagus, hard control, leakage risk	[141]
Temperature-responsive SDDS	PNIPAm, Pluronic F127, Silk Fibroin	Hydrogen bond interaction Hydrophobic Force	Cutaneous, mucosal or splanchnic diseases	20° to 37 °C	Excellent penetration and strong fixation	Reverse drug osmosis	[131]
Temperature-responsive SDDS	HPMC	Hydrophobic interaction	Gastrointestine tract	55 to 70 °C formed, 37 °C released	Erosion mechanism	Low biocompatibility	[130]
Temperature-responsive SDDS	Monolinolein (MLO)	Self-assembly	Colon	38 °C	Preventing leakage	Inaccurate targeting	[145]
pH-responsive SDDS	Acid-resistant Zr-based MOF	Metal Coordination, Hydrogen Bonding	intestinal tract	~pH 8.0	High encapsulation capacity (92.72 %) and encapsulation efficiency (44.08 %) in only 10 min	Elimination risk, too complex with organic solvent during preparation	[96]
pH-responsive SDDS	Liposomes, Chitooligosaccharides, phospholipids	Electrostatic Interaction, Hydrogen Bonding, Hydrophobic Force	MCF-7 tumor cells	Acidic environment	Inhibit the growth of MCF-7 cells after 72 h	Complex system	[147]
pH-responsive SDDS	DNA, acrylamide, and insulin	Electrostatic interactions, hydrogen bonding, self-assembly	Stomach and duodenum	~pH 7.2	Stable under extreme acidic conditions	Low mechanical properties	[149]
pH-responsive SDDS	Chitosan, FcRn-modified porous silicon particles, and hypromellose acetate succinate	van der Waals interaction, hydrogen bonding	Intestine	~pH 6.8	Targeted sustained and effective drug release	Short-term retention	[151]
pH-responsive SDDS	DSPE-PEG, poly (amidoamine) dendrimer	Electrostatic Interaction, self-assembly	Periodontal tissues	Lipase, low pH	Multiple functions, High loading efficiency, High biocompatibility	Systemic toxicity risk	[45]
pH-responsive SDDS	Isoguanosine-phenylboronic-guanosine	Self-assembly, hydrogen bonding, metal coordination, π-stacking	Oral squamous cell carcinoma	Acidic tumor microenvironment	Dual-functional, exceptional stability (more than one year), excellent sustained release capability	Not suitable for mouth pH	[153]
pH-responsive SDDS	Ginsenoside CK, chitin-derived homing peptide (A54 peptide)	Self-assembly,	Liver	~pH 7.4	Promote apoptosis	High risk of biotoxicity	[154]
pH-responsive SDDS	Fmoc-pentafluoro-*L*-phenylalanine	Hydrogen bonding	Colon	pH 6.5	Mimics the double layer architecture of native human colonic mucus	Short residence time	[155]
Ionic-sensitive SDDS	Chitosan-arginine, and alginate	Electrostatic interaction	Gastric mucosa and intestinal tract	pH 2.5	Easy to prepare and store, Structural changes in pH response	Inappropriate targeting	[156]
Ionic-sensitive SDDS	Alginate	Electrostatic interaction	Colon	pH 7.4 ionic strength 150 mM	Pulse transmission	Inadequate response sensitivity	[157]
Ionic-sensitive SDDS	Polypyrrole	Electrostatic interaction	Gastrointestinal tract	Current or voltage	Linear response, controlled and programmable drug delivery	13 wt% drug loading	[159]
Ionic-sensitive SDDS	κ-Carrageenan, polyacrylamide	Electrostatic Interaction, hydrogen bonding, hydrophobic interaction, Self-assembly,	Artificial diaphragm, tendon, and cartilage	External stimulus	Self-healing, excellent cytocompatibility, outstanding mechanical behaviors and biocompatibility	Unknown drug loading capacity and release rate	[160]

(*continued on next page*)

Table 3 (*continued*)

Supramolecular Drug Delivery System (SDDS)	Materials with supramolecular interactions	Supramolecular mechanism	Applied site	Trigger	Strength	Limitation	Ref
Swelling SDDS	PAM, chitosan, sodium alginate.	Electrostatic interaction, hydrogen bonding	Stomach	SGF	Reside in the stomach with intact shape for 16 days	Abdominal bloating	[136]
Swelling SDDS	Polyacrylic acid, polyvinyl alcohol	Hydrogen bonding, self- assembly	Stomach	SGF	Swell in the stomach within 60 min, and remain soft but robust in the gastric cavity for up to 29 days	Obstruction risk, abdominal bloating	[135]
Swelling SDDS	κ-carrageenan, poly(acrylic acid/dimethylaminoethyl methacrylate)	Electrostatic Interaction, hydrogen bonding	Tumor tissue	Temperature, pH, magnetic field	Triple-responsive	Unknown biosafety	[162]
Swelling SDDS	Carboxymethyl cellulose, and polyvinyl alcohol	Hydrogen bonding	small intestine	SGF	No chemical crosslinker and coating technology	Uncontrolled rate of drug release	[163]
Swelling SDDS	Pectin, isooctane and Tween 80	Hydrophobic interaction	Stomach, intestine, colon	SGF and SIF	provide the stronger satiating effect	Gastrointestinal burden, electrolyte imbalance	[166]
Mucoadhesive SDDS	Tamarind seed polysaccharide, carboxymethylcellulose, and chitosan	Hydrophobic interaction, Electrostatic Interaction, hydrogen bonding	Oral cavity	Saliva	High swelling, slower and more sustained release, 100 % release at 40 min	Low drug loading	[164]
Mucoadhesive SDDS	Mesoporous silica nanoparticles	Electrostatic Interaction, hydrogen bonding	Intestine	Intestinal mucus	Interactions are spontaneous and thermodynamically favorable	Doubtful utility in humans	[167]
Mucoadhesive SDDS	TEMPO oxidized Konjac glucomannan (sOKGM) microspheres	Self-assembly, Electrostatic Interaction,	Colon	Neutral pH at intestinal conditions	High mucoadhesive and mucus-penetrating properties	Poor oral effect	[168]
Mucoadhesive SDDS	Ganoderma lucidum spores (GLSs)	Host-guest Interaction, affinity interaction	Stomach, intestine	SGF and SIF	Long stomach retention time	Low loading rate	[169]
Mucoadhesive SDDS	mRNA, puromycin ligation, TBMB, and PK15 (amino acid sequence: fMet-ACSDRFRNCPADEALC-$(GS)_3$)	Affinity interaction, π-stacking	Stomach, gut epithelia	FGFR3c	High affinity, stability	Uncertain biotoxicy risk	[170]
Oral microneedle SDDS	PEGDA, polyvinyl alcohol and acrylamide	Hydrogen bonding	Intestine	Intestinal fluids	High bioavailability	Slow to reach action site	[171]
Oral microneedle SDDS	Gelatin methacryloyl (GelMA)	Hydrogen bonding	Intestine	external magnetic guidance	Rapidly reach target site	Slight gut damage	[172]
Oral microneedle SDDS	Chitosan, and alginate	Hydrogen bonding	Gastrointestinal tract	Physiological temperature	Small size allows for bulk use	Poor biocompatibility and security (Cr)	[173]
Oral microneedle SDDS	PVP, and GleMA	Hydrogen bonding	Gastrointestinal tract	Intestinal fluid	Direct drug absorption	Gut damage risk	[174]

isopropylacrylamide), which exhibits a transition near body temperature (37 °C), making it particularly suitable for localized treatments such as tumor therapy and site-specific drug delivery. Temperature-responsive SDDSs can be precisely controlled via external heat sources (such as radiofrequency heating and laser thermal therapy) or by endogenous temperature changes (such as localized temperature increases in tumor areas). One of the key advantages of these systems is their ability to achieve targeted drug release, which significantly reduces systemic side effects, especially in applications such as cancer treatment.

Nevertheless, the main challenge of temperature-responsive SDDSs are their dependence on temperature fluctuations. Variations in body temperature, limitations of external temperature control devices, and difficulties in maintaining localized temperature control can affect the precision of drug release. In addition, some thermoresponsive polymers may experience structural instability during repeated temperature cycles, which could compromise the long-term efficacy of the system. Therefore, the development of intelligent temperature control systems and feedback mechanisms based on biological sensors to achieve more precise temperature regulation and drug release remains a critical for future development. Furthermore, the biocompatibility and stability of thermoresponsive materials are also important research topics, particularly concerning their safety in long-term therapies.

pH-responsive SDDSs use changes in pH as a trigger to control drug release by exploiting the dissolution, swelling, or expansion properties of polymers. These systems are widely used in gastrointestinal drug delivery, in which the pH gradient between the stomach and intestinal environments can be harnessed for targeted drug release. For example, polymers such as Eudragit and chitosan remain stable in acidic environments and undergo swelling or dissolution under alkaline conditions, releasing encapsulated drugs. pH-responsive SDDSs are useful in oral drug delivery, especially for drugs that are sensitive to stomach acids, such as protein-based drugs and antibiotics. These systems effectively protect drugs from degradation by stomach acid and facilitate drug release in the neutral pH environment of the small intestine. Furthermore, pH-responsive SDDSs can modulate the hydrophilicity and hydrophobicity of polymers, enabling sustained release and targeted drug delivery within the intestine.

Conversely, the main limitation of these systems lies in their dependence on gastric pH variability. Individual differences in gastric acid secretion and gastrointestinal disorders (such as peptic ulcers and functional dyspepsia) can cause significant fluctuations in pH, leading to inconsistent drug release. Moreover, some pH-responsive polymers may suffer from biostability issues at extreme pH levels, potentially

compromising system reliability. Therefore, enhancing the flexibility and stability of such systems remains a critical challenge. In addition, personalized drug release mechanisms may improve the applicability of pH-responsive SDDSs for diverse patient populations, addressing individual physiological variations more effectively.

Ionic-responsive SDDSs trigger drug release by sensing changes in ion concentrations within the body. These systems typically rely on ion exchange reactions or ion-crosslinking properties of polymers to control drug release. The common materials used in these systems include chitosan, alginate, and similar biopolymers. Upon exposure to specific ions, such as calcium or magnesium, the polymer undergoes structural changes, which triggers the release of the encapsulated drug. Ionic-responsive SDDSs are frequently used for targeted delivery, particularly in applications related to cancer therapy, infectious diseases, and inflammatory conditions, where the system can respond to local ion concentration fluctuations, enabling precise drug release. The main advantage of ionic-responsive SDDSs are their biocompatibility. As the concentrations of ions, such as calcium and sodium are relatively stable and well-regulated in the body, these systems exhibit strong adaptability to the physiological environment. Moreover, their ability to use natural ion gradients ensures minimal interference from normal biological processes.

In contrast, ionic-responsive SDDSs also have certain limitations. First, ion concentration changes can vary significantly between individuals or under different disease states, leading to a reduced predictability of drug release. Second, the ion responsiveness of some systems can be influenced by several factors, such as diet, medication intake, and pathophysiological conditions of the patient, which can cause unpredictable drug release patterns. Enhancing the ion selectivity and improving the stability of these systems remain critical areas for future research to ensure their clinical feasibility and reliability.

Swelling SDDSs regulate drug release through the absorption of water or bodily fluids, which causes the materials to expand. These systems typically comprise hydrogels or superabsorbent materials, that absorb bodily fluids and undergo swelling, resulting in controlled, slow release of the encapsulated drug. The primary advantage of swelling SDDSs lies in their ability to provide sustained and stable drug release, making them particularly suitable to treat chronic diseases (such as hypertension, diabetes, and chronic pain management) and localized therapy. Compared with traditional drug delivery systems, swelling SDDSs reduce the frequency of administration, which enhances patient adherence to treatment regimens. Moreover, hydrogel materials exhibit excellent biocompatibility, and their drug release rate can be modulated by adjusting their crosslinking density, hydrophilicity, and other material properties.

The main limitation of swelling SDDSs is that their drug release rate can be influenced by environmental factors like, solution viscosity, temperature, and ion concentration, which may lead to uneven swelling and thus affect the consistency and controllability of drug release. In addition, as the system remains in the body over time, the degradability and stability of the materials may become limiting factors for their long-term use. Therefore, the key challenge in developing swelling SDDSs is the creation of efficient, multifunctional materials that improve the consistency of drug release. The incorporation of biodegradable technologies to ensure the safety and stability of the system during prolonged use remains a critical area for future research and development.

Mucoadhesive SDDSs are designed to adhere to mucosal surfaces (such as the oral cavity, eyes, nasal passages, and gastrointestinal tract) to prolong the residence time of the drug, enabling local or systemic drug delivery. These systems typically use biocompatible polymers with adhesive properties, such as chitosan, carbopol, and HPMC, which interact with glycosaminoglycans or glycoproteins present in the mucosal layer. Mucoadhesive SDDS are effective in localized treatments, including oral ulcers, ocular diseases, and nasal drug delivery. By enhancing the affinity between the drug and target mucosal surface, these systems significantly extend the residence time of the drug at the site of action, thus improving the bioavailability of the drug and reducing the frequency of administration, which ultimately enhances patient adherence to the treatment regimen.

Despite these advantages, mucoadhesive SDDS present certain challenges. For instance, variations in the mucosal structure between individuals may cause differences in the adhesive performance of the drug, leading to inconsistent drug release rates. Moreover, the long-term use of mucoadhesive systems may cause local discomfort or even allergic reactions, which can negatively impact patient acceptance. To overcome these issues, future research should focus on developing novel adhesive materials or the improving biocompatibility to enhance the stability and therapeutic efficacy of these systems.

Oral microneedle SDDSs are emerging technology that use tiny needle-like structures (microneedles) to penetrate the mucosal layer of the gastrointestinal tract, enabling direct drug absorption. These microneedles typically range from tens to hundreds of micrometers in diameter and are small enough to avoid pain while effectively penetrating the epithelial cell layer, facilitating the absorption of drugs across the mucosal barrier. The primary advantage of the oral microneedle SDDSs lies in their ability to enhance drug bioavailability, especially for drugs that exhibit poor oral absorption, such as macromolecular biologics (e.g., insulin, vaccines, and antibody-based drugs). These drugs are traditionally limited in oral delivery owing to degradation or poor absorption in the gastrointestinal tract. Using microneedle technology, drugs can directly enter the bloodstream, bypassing the digestive and metabolic processes of the gatrointestinal tract and significantly improving their efficacy. In addition, compared to traditional injectable drug delivery methods, microneedle delivery systems provide bioavailability similar to injections while avoiding the discomfort and pain associated with needles. Furthermore, microneedle systems can enable precise drug release through self-contained drug carriers, minimizing unnecessary side effects. The design of microneedles also allows integration with miniaturized drug storage devices, enabling long-acting drug release in the body.

Oral microneedle SDDSs technology have several challenges. First, the production cost is relatively high, particularly in large-scale manufacturing, as it requires precise equipment to fabricate and validate the microneedle size, shape, and penetration ability. Furthermore, the stability and biocompatibility of microneedle systems require further investigation, particularly in ensuring that microneedles do not cause damage or adverse reactions in the gastrointestinal tract during prolonged use. Current research is focused on optimizing microneedle materials (such as polymers, metals, and ceramics) to enhance their adhesion properties in the gastrointestinal tract and improve the controlled release of drugs. Another challenge is the drug release rate and drug stability after microneedle penetration; precisely controlling drug release and ensuring the stability of the drug remain critical issues for the future development of this technology.

3.4. Supramolecular drug delivery system in a cell

Intestinal epithelial cells are the last physical barrier to drug delivery into the serum, allowing drugs to enter circulation. There are two main pathways for achieving this goal: active cell transport and drug delivery through tight junctions.

Opening tight junctions facilitates the paracellular transport and target transcellular transport, but inevitably increases the risk of autoimmune disease, bacterial infection and inflammatory bowel diseases [43,182–185]. Subapical to the tight junction are the adherens junctions and desmosomes, which are linked to actin-based microfilaments and cytokeratin-based intermediate filaments, respectively. These cytoskeletal structures provide the tensile strength that supports tight junctions and maintains cell shape [186]. The first tight junction protein to be discovered was zonula occludens 1 (ZO-1), followed by the two related proteins ZO-2 and ZO-3 [186,187]. These discoveries were followed by the discovery of the tetraspan transmembrane tight junction proteins

occludin and the claudins [186,188–190]. Tight junctions are comprised of ZO-1, claudins, junctional adhesion molecules (JAM), coxsackievirus and adenovirus receptor (CAR), Tamps protein group, actin, and myosin (Fig. 2f). The tight junctions opening is reversible, but can also produce irreversible results when the drug is too acidic or in too high concentration. Therefore, adjusting the pH or concentration of the drug can promote drug delivery while reduce the risk of infection and inflammation. A single citric acid solution of different concentrations dramatically opened the tight junctions and the tight junctions could not recover within 24 h. Li et al. designed a core-shell structure delivering peptide nanodrugs with citric acid crosslinked carboxymethylcellulose as the shell [191]. The designed CA-NPs (pH 4.6) were weakly acidic, and when the concentration of citric acid in the drug was l less than or equal to 5 mg/ml, the tight junctions opened and finally recovered to normal at 24 h. Dong et al. utilized choline ionic liquids (choline-geranic acid, Ch-Ger; choline-citric acid, Ch-Cit) to enhance nasal delivery of glucagon, the result showed the arrangement and distribution of ZO-1 did not significantly change after co-incubation with ionic liquid at lower concentrations (5 mmol/L) compared with the control group [192]. However, after interference of high ionic liquid concentrations, it showed that the distribution of ZO-1 underwent a significant rearrangement, which resulted in partial breakage or disorganisation of boundaries. After a 24-h recovery period, the blurring boundaries of ZO-1 became distinct, except for the 80 mmol/L of Ch-Cit. Therefore, adjusting the factors such as pH or concentration of the drug can ensure efficiency and good safety. Han et al. manufactured DSPE-PCB as a drug carrier to deliver insulin without opening tight junction [43].

Active cellular transport is primarily mediated by proteins located on the cellular membrane. For example, Leu-Gln-Pro-Glu was encapsulated in liposomes and coated with *Lactobacillus acidophilus* CICC 6074 S-layer protein. With the amphiphilic structure and extraordinary adhesion ability of SLP, the liposome vehicle could self-assemble, reduce fusion, and prolong the retention time. Furthermore, cells can endocytose liposomes, and cell membranes have a similar structure; this process helps in the delivery of drugs into cells [193]. Apical sodium-dependent bile acid transporters are also crucial for cellular drug delivery [194]. SDDSs help drugs reach the target site and remain in position for a period. As the digestion process continues, drugs released from the weakened supramolecule compound are actively absorbed and transported by cells [195–197]. Oral insulin can be delivered via this pathway [198].

Xiao et al. [199] used SDDS for oral drug delivery. Novel combination therapy strategy for UC that delivers TNFα siRNA (siTNF) and IL-22 via orally targeted nanoparticles. SiTNF loaded into galactosylation-modified polymer nanoparticles (NPs). These nanoparticles successfully targeted siTNF delivery to macrophages and inhibited the production of TNFα. Moreover, together with IL-22, NPs embedded in the hydrogel demonstrated an enhanced ability to promote mucosal healing. This hydrogel showed better therapeutic efficacy in a mouse UC model than hydrogels with NPs or IL-22 alone, indicating that the supramolecular interaction in the inner part of the drug delivery system promoted the controlled release and oral drug efficacy of TNFα and IL-22. This study demonstrated the potential of targeted delivery of siRNA and IL-22 to the colon via the oral route, providing a novel strategy for combination therapy for UC. The nanoparticle-mediated co-delivery of siRNA and IL-22 improved therapeutic efficacy and, reduced side effects and thus, may be a promising pharmaceutical preparation for UC treatment.

The delivery of substances through cellular pathways using SDDS manufactured using a supramolecular mechanism has also been demonstrated in some studies. Ramesh et al. [200] reported a novel supramolecular nanoparticle (DSNs) capable of co-delivering two kinase inhibitors to simultaneously inhibit CSF1R and MAPK signaling pathways in tumor-associated macrophages. BLZ-945 (a CSF1R inhibitor) and selumetinib (a MAPK inhibitor) were synthesized as amphiphilic molecules usinga supramolecular self-assembly technique and formed DSNs in combination with auxiliary lipids. These nanoparticles had an average diameter of 98.5 ± 31 nm, and their size and potential remained stable for 6 days when stored at 4 °C. In human serum, DSNs showed good stability for up to 10 h. DSNs showed efficient endocytosis by M2-type macrophages in vitro and significantly increased the intracellular accumulation of inhibitors after 4 h. DSNs achieved longer inhibition of the CSF1R and MAPK signaling pathways in M2-type macrophages than the combinations of free inhibitors. Furthermore, M2-type macrophages treated with DSNs did not show significant cytotoxicity within 72 h, whereas the free inhibitor combination exhibited dose-dependent toxicity with an inhibitory half concentration (IC_{50}) of 66 nM. In a 4 T1 mouse model of breast cancer, DSNs accumulated significantly in tumor tissues, and at three doses (15 mg/kg each), the tumor volume was significantly reduced in DSN-treated mice compared with controls. Flow cytometric analysis revealed an increase in M1-type macrophages ($CD11b^{+}CD80^{+}$) in DSN-treated tumor tissues; in contrast, the number of M2-type macrophages decreased. In addition, a higher rate of tumor cell apoptosis was observed in DSN-treated tumor tissues, and the percentage of apoptotic cells was higher than in the other groups, as measured by TUNEL staining. These results suggest that DSNs, formed as a nanoparticle system through supramolecular self-assembly, can effectively co-deliver two kinase inhibitors to tumor-associated macrophages, achieve sustained inhibition of the CSF1R and MAPK signaling pathways, promote the transition of M2-type macrophages to M1-type macrophages, and show enhanced antitumor effects.

Yu et al. [201] studied SDDS drug delivery into cells and established a pathogen−/temperature/alternating magnetic-field-responsive drug delivery system. Specifically, the SDDS assembly comprises two heterogeneous mesoporous silica nanoparticles (MSNs) for the co-delivery of antimicrobial peptides and antibiotics to synergistically eradicate pathogenic biofilms. These supramolecular assemblies comprise macroporous MSNs with β-cyclodextrin (β-CD)-modified polyethyleneimine (MSNLP@PEICD, host MSNs, H) and magnetic MSNs adorned with adamantane (MagNP@MSNA-CB, guest MSNs, G). The host-guest interaction is an obvious characteristic of supramolecular interactions. Through the host-guest interaction between β-CD and adamantane, host MSNs and guest MSNs could spontaneously form co-assemblies. The host MSNs had an average diameter of 90–110 nm and pore size of 7–10 nm, whereas the guest MSNs had a diameter of 35–50 nm. The H + G co-assemblies, had a size distribution of 250–480 nm and possessed a higher ζ-potential than the host or guest MSNs alone. In the presence of pathogenic cells, the H + G co-assemblies couldslowly release melittin, whereas the release efficiency of melittin and ofloxacin increased significantly under heating or AMF stimulation. In in vitro experiments, the drug-loaded H + G co-assemblies exhibited a higher biofilm eradication ability to remove biofilm biomass and kill pathogen cells than MSNs or free drugs alone. In addition, the co-assemblies were significantly less toxic to mammalian cells than the free drugs because of the protection and encapsulation of the supramolecular structures. In an in vivo study, the H + G co-assembler eradicated pathogenic substances on implants and prevented inflammation and tissue damage.

Transparent proteins are important in transcellular drug delivery; for instance, subfamily B1 (hormone receptor) of Class B G protein-coupled receptors in humans is listed in Table 4. To treat and prevent diabetes and to control body weight, the GLP-1R is the crucial receptor to connect with agonists. Continued research has revealed the details of GLP-1R structure [202,203], which will help in the development of GLP-1R agonists. To date, 14 types of GLP-1R agonists have been developed, among which WB4–24 demonstrated the highest efficacy [204], and semaglutide demonstrated promising prolonged and controlled release ability [11].

The curvature of the phospholipid bilayer on the cell membranes influences drug absorption and delivery. Bao et al. [205] found that the permeability of the rod-like probing molecule D289 on the exterior of small vesicles (~100 nm, larger curvature) was reduced compared to that of large vesicles (~1000 nm, small curvature); moreover, increasing temperatures resulted in a higher permeability of the lipid films, which

Table 4
Subfamily B1 (hormone receptor) of Class B G protein-coupled receptors in humans (reformed from ref. [213], HUGO human gene nomenclature database [214] and Guide to Pharmacology database [215]).

Gene name	Gene products	Principal functions controlled by the receptor	Ligands	Value (Parameter)
CRHR1	Corticotropin releasing factor 1 (CRF_1) receptor	Secretion of ACTH [216]	Tyr^0-CRF	9.3 (pK_d) [217]
			Urocortin 1	8.6–9.5 (pK_d) [218]
			Urocortin 2	5.3–5.4 (pK_d) [218]
			Corticotrophin-releasing hormone	7.1–9.0 (pK_d) [219]
CRHR2	Corticotropin releasing factor 2 (CRF_2) receptor	Stress-related autonomic, neuroendocrine and behavioral function [216]	Urocortin 1	9.0–9.6 (pK_d) [217,218]
			Urocortin 2	9.3 (pK_d) [216,220]
			Urocortin 3	7.9–8.0 (pK_d) [218]
			Corticotrophin-releasing hormone	6.5–7.4 (pK_d) [217]
			CRF (perhaps) [216]	N. A.
PTH1R	Parathyroid hormone 1 (PTH1) receptor	Calcium homeostasis in bone and kidney; skeletal, pancreatic, epidermal, and mammary glands [221,222]	PCO371	5.4 (pEC_{50}) [223]
			PTH-related peptide (PTHLH)	4.5–8.6 (pIC_{50}) [224–226]
PTH2R	Parathyroid hormone 2 (PTH2) receptor	–	TIP39 [227]	7.6–9.2 (pIC_{50}) [228,229]
SCTR	Secretin receptor	Secretion of HCO_3^-; enzymes, and K^+ by the pancreas [230]	Secretin (SCT)	9.7 (pEC_{50}) [231]
VIPR1	$VPAC_1$ receptor	Neuromodulation, T-cell differentiation	VIP	8.5–9.8 (pK_i) [232–234]
			PACAP-27	8.9 (pK_i) [233]
			PACAP-38	8.2 (pK_i) [233]
VIPR2	$VPAC_2$ receptor	Circadian rhythms [235]	VIP	9.2 (pK_d) [236]
			PACAP-27	7.6–9.4 (pEC_{50}) [237,238]
			PACAP-38	7.7–9.3 (pEC_{50}) [237]
ADCYAP1R1	PAC_1 receptor	Glucose homeostasis, nociception, learning, and memory, circadian, rhythms [239–243]	VIP	<6.0–8.4 (pK_i) [244]
			PACAP-27	6.9–8.5 (pK_i) [244]
			PACAP-38	6.9–9.0 (pK_i) [244]
GHRHR	Growth hormone releasing hormone (GHRH) receptor	Release of pituitary growth hormone [230]	GHRH [230]	N. A.
			JMR-132	9.9 (pIC_{50}) [245]
			JI-38 [246]	N. A.
GCGR	Glucagon receptor	Hepatic glycogenolysis and gluconeogenesis, pancreatic secretion of insulin [230]	Glucagon (GCG)	9.0 (pEC_{50}) [247]
			NNC1702	7.3 (pIC_{50}) [248]
			Glucagon	6.9–7.0 (pK_i) [249]
GLP1R	Glucagon-related peptide 1 (GLP-1) receptor	Pancreatic secretion of insulin and glucagon [230]	GLP-1-(7–36)-amide	9.3 (pK_d) [249]
			GLP-1-(7–37)	N. A.
			Lixisenatide	8.9 (pK_i) [250]
			Tirzepatide	8.4 (pK_i) [74]
			Semaglutide	11.2 (pEC_{50}) [251]
			Liraglutide	10.2 (pEC_{50}) [252]
			Albiglutide	7.7 (pEC_{50}) [253]
			Peptide 5	8.5 (pEC_{50}) [254]
			WB4–24	4.9 (pA_2) [204]
			Orforglipron	8.5 (pK_i) [77]
			Danuglipron	6.4 (pK_i) [255]
			Exendin-4	8.7–9.0 (pK_i) [249]
			Exendin-3 [256]	N.A.
GLP2R	Glucagon-related peptide 2 (GLP-2) receptor	Proliferation of the intestinal mucosal villus epithelium [230]	GLP-2 (GCG)	8.5 (pIC_{50}) [257]
			GLP-2-(3−33)	7.4 (pIC_{50}) [257]
			GLP-2 analog 10	10.6 (pEC_{50}) [258]
			Apraglutide	10.5 (pEC_{50}) [259]
			Teduglutide [260]	N.A.
CALCRL	Calcitonin receptor-like receptor	Vascular tone	α-CGRP	7.68 [261]
			Adrenomedullin [262]	N.A.
CALCR	Calcitonin receptor	Calcitonin: calcium homeostasis in bone and kidney; amylin: postprandial glucagon secretion, nutrient transit through the stomach	Calcitonin	9.0–11.2 (pEC_{50}) [263,264]
			Amylin (IAPP)	8.0–9.2 (pEC_{50}) [265,266]
			KBP-088	8.4 (pEC_{50}) [267]
			Davalintide	8.3 (pEC_{50}) [267]
			Pramlintide	8.3 (pEC_{50}) [265]
			α-CGRP	6.2–8.4 (pEC_{50}) [263,268]
			β-CGRP	7.2 (pEC_{50}) [263]
			Adrenomedullin	6.7–7.7 (pEC_{50}) [263,264]
			Adrenomedullin 2/ intermedin	6.5 (pEC_{50}) [263]

proved that the phospholipid bilayer on cell membranes is temperature-responsive. Xie et al. [206] established a supramolecular antibacterial peptide delivery system using host-guest supramolecular interactions between branched cyclodextrin and cationic linear peptides appended with azobenzene side chains. This delivery system was triggered by ultraviolet light (λ = 365), and notably, P1/tri-β-CD, comprising a single peptide sample and trigeminal β-cyclodextrin through supramolecular interactions, formed an ultrathin nanosheet with a height of approximately 1.85 nm.

Permeation enhancers act without opening tight junctions. Bzik et al. [207] focused on 1-phenylpiperazine and found that it improved intestinal mucosal permeability in rats by activating 5-HT4 receptors and increasing intracellular cAMP levels. However, the pharmacological activity of 1-phenylpiperazine limits its further development as an oral formulation. Weng et al. [208] revealed that sodium N-[8-(2-hydroxybenzoyl)amino]-caprylate could form tight complexes with insulin, improving its cellular uptake through passive diffusion and improving its intestinal mucosal permeability, thus offering a new strategy for designing an insulin delivery system with high oral bioavailability. Fein et al. [209] conducted a structure-function analysis of 13 phenylpiperazine derivatives and discovered that several of these derivatives significantly increased the permeability of Caco-2 cell monolayers to the fluorescent marker calcein with low toxicity, indicating their potential as intestinal permeation enhancers rather than opening tight junctions. These studies demonstrate that through supramolecular mechanisms, such as cell membrane permeability and cytoskeletal proteins, the intestinal permeability of polypeptide-based drugs can be effectively enhanced, providing valuable routes for prospective drug delivery systems.

Permeation enhancers open tight junctions in the epithelial cell layer. Artursson et al. [108] used negatively charged nanoparticles approximately 50 nm to enhance the permeability of intestinal cells and allowed the oral delivery of polypeptide-based drugs such as insulin. These nanoparticles interact with intestinal surface receptors and activate myosin light chain kinase, resulting in cytoskeletal contraction and increased paracellular permeability to peptide drugs. Tran et al. [210] investigated sodium caprate (C10) as an enhancer of intestinal absorption of a GLP-1/GIP coagonist peptide (LY). They found that C10 increased the absorption of the LY peptide in rats and minipigs by reducing tight junction protein levels and improving membrane fluidity, that is, by opening tight junctions. Lamson et al. [211] discovered that the dozen-nanometers, negatively charged silicon nanoparticles could be used as physicochemical permeation enhancers that promote the delivery of proteins orally. These nanoparticles have been shown to attach to receptors on the intestinal surface, open tight junctions, and improve the uptake of prototype medications across Caco-2 monolayers and mouse intestinal tracts in vivo.

These studies have shown that the permeation enhancers opening of tight junctions is a feasible approach. However, safety and toxicity are critical considerations in oral delivery systems; opening tight junctions results in some drawbacks, including intestinal electrolyte disorder, tissue or muscle spasms, and risks associated with autoimmune disorders, bacterial infections, and inflammatory bowel diseases [43,183,212].

4. Outlook

Incorporating the aforementioned insights, supramolecular oral drug delivery systems have secured a niche in the domain of oral medication owing to their exceptional biocompatibility, controlled-release characteristics, and ability to be activated by various stimuli or the unique gastrointestinal microenvironment for drug release. However, it is crucial to select materials for oral SDDSs that are friendly to the human gastrointestinal tract, to ensure that neither the materials nor their metabolites cause irritation, leading to disorders or spasms in the gut.

At the chemical level, the selection should focus on materials that are inert and do not irritate the gastrointestinal lining. At the physical level, the design of SDDSs must consider strategies to protect the drug as it traverses the mucus layer, ensuring that the epithelial cell membranes remain intact and the tight junctions of the epithelial cells are preserved and restored. In addition, if the permeability of the epithelial cell membrane is modulated to facilitate drug absorption and transport, the mechanisms and substances that restore the membrane permeability must be considered.

With continuous advancements in medical technology, SDDSs are evolving. Time-dependent SDDSs aim to enhance drug bioavailability and reduce side effects, though high development costs remain a challenge. Balancing innovation with cost control is key for commercialization. Temperature-responsive SDDSs need better methods to regulate phase transition temperatures efficiently. Developing multi-stimulus responsive systems for biological lesions will be important for future research. pH-responsive SDDSs are growing in use. Future focus should be on using biodegradable materials and optimizing production processes, incorporating AI to reduce costs. Ion-sensitive SDDSs, with their applications in ocular, nasal, and oral drug delivery, need further research to address limitations in excipient types and properties like rheology. Swelling SDDSs show promise in drug delivery and biotechnology, especially for encapsulating living cells. Future work should focus on non-toxic, biocompatible materials and improving delivery stability. Mucoadhesive SDDSs have seen progress with intelligent materials like hydrogels and nanoparticles. As technology matures, they will enhance precision therapy. Oral microneedle SDDSs face challenges in drug absorption and preparation. Future efforts should focus on improving intestinal absorption and protecting drug molecules. In short, future perspectives are shown as follows:

(i) New supramolecular mechanism. A new supramolecular mechanism could pave the way for developing oral SDDSs, with approaches aligned with the principles of green chemistry and mild reaction conditions representing the future direction of oral SDDSs.
(ii) New electronic SDDS. The electrification of oral SDDSs is becoming a trend, combining traditional oral supramolecular drugs with electronic circuits and chips. This integration enables the electronicization of SDDSs, forming the core of SDDSs with “computing power and intelligence.”
(iii) New digital SDDS. Digitizing new SDDS allows for personalized drug customization based on data, reducing the burden on the kidneys and liver, and achieving truly precise and effective oral delivery of drugs.
(iv) New release type. In new SDDSs, adapting to patient needs, developing new release modes, improving patient compliance, and reducing dosing frequency are key goals. Achieving intelligent drug delivery—where a single oral administration enables automatic control and sustained release over an extended period—represents a significant advancement.

Overall, with continued development, future SDDSs are expected to exhibit properties such as high biocompatibility, accuracy, personalization, intelligence, controllability.

5. Conclusions

SDDSs have demonstrated their unique ability for easy preparation and long-lasting controlled release in oral drug delivery. The role of SDDSs in oral pharmaceuticals has been comprehensively reviewed. The intricate journey of a drug after oral administration has been described, particularly focusing on the anatomical and physiological challenges it encounters, including the oral cavity, gastrointestinal tract, and cellular barriers. Subsequently, an in-depth analysis of contemporary oral delivery systems and technologies tailored for peptide- and protein-based drugs from an anatomical standpoint is presented. Specifically, diseases

such as diabetes mellitus and the burgeoning obesity epidemic have attracted attention, and SDDSs for GLP-1R agonists show promising potential. Furthermore, a systematically cataloged agonists for subfamily B1 (hormone receptors) of Class B G protein-coupled receptors has been presented, which help modulate key physiological processes. This knowledge not only not only contributes to a deeper understanding of supramolecular technologies and the complex human milieu encountered during oral drug administration, but also underscores the significance of these systems in facilitating the active transport of therapeutic polypeptide-based drugs. These findings are expected to prompt further advances in polypeptide-based drug development, enhancing the efficacy of oral drug delivery systems. We propose that in the field of oral delivery, with the help of artificial intelligence, SDDSs can develop toward electronization and digitalization to achieve enhanced controlled release capabilities.

CRediT authorship contribution statement

Jiawen Chen: Writing – review & editing, Writing – original draft, Visualization, Validation, Resources, Methodology, Formal analysis. **Tianqi Liu:** Writing – review & editing, Writing – original draft, Validation, Resources, Methodology, Formal analysis. **Mi Wang:** Writing – review & editing, Validation, Resources. **Beibei Lu:** Writing – review & editing, Validation, Resources. **De Bai:** Writing – review & editing, Validation, Resources. **Jiaqi Shang:** Writing – review & editing, Validation, Resources. **Yingjun Chen:** Resources, Validation, Writing – review & editing. **Jiaheng Zhang:** Writing – review & editing, Supervision, Conceptualization.

Declaration of competing interest

All authors have none conflicts to declare.

Acknowledgment

This research was financially supported by the National Natural Science Foundation of China (Nos. U21A20307), the Shenzhen Science and Technology Innovation Committee (Nos. GXWD20201230155427003-20200821181245001, GXWD20201230155427003-20200821181809001, and ZX20200151), the Department of Science and Technology of Guangdong Province (No. 2020A1515110879).

Data availability

Data will be made available on request.

References

[1] V.S. Malik, F.B. Hu, The role of sugar-sweetened beverages in the global epidemics of obesity and chronic diseases, Nat. Rev. Endocrinol. 18 (2022) 205–218, https://doi.org/10.1038/s41574-021-00627-6.
[2] B.A. Swinburn, V.I. Kraak, S. Allender, V.J. Atkins, P.I. Baker, J.R. Bogard, H. Brinsden, A. Calvillo, O. De Schutter, R. Devarajan, M. Ezzati, S. Friel, S. Goenka, R.A. Hammond, G. Hastings, C. Hawkes, M. Herrero, P.S. Hovmand, M. Howden, L.M. Jaacks, A.B. Kapetanaki, M. Kasman, H.V. Kuhnlein, S. K. Kumanyika, B. Larijani, T. Lobstein, M.W. Long, V.K.R. Matsudo, S.D.H. Mills, G. Morgan, A. Morshed, P.M. Nece, A. Pan, D.W. Patterson, G. Sacks, M. Shekar, G.L. Simmons, W. Smit, A. Tootee, S. Vandevijvere, W.E. Waterlander, L. Wolfenden, W.H. Dietz, The global syndemic of obesity, undernutrition, and climate change: the lancet commission report, Lancet 393 (2019) 791–846, https://doi.org/10.1016/S0140-6736(18)32822-8.
[3] M.J. Pereira, J.W. Eriksson, Emerging role of SGLT-2 inhibitors for the treatment of obesity, Drugs 79 (2019) 219–230, https://doi.org/10.1007/s40265-019-1057-0.
[4] H. Waters, M. Graf, The Costs of Chronic Disease in the US, St, Milken Inst, Monica CA, 2018.
[5] Y.C. Chooi, C. Ding, F. Magkos, The epidemiology of obesity, Metabolis 92 (2019) 6–10, https://doi.org/10.1016/j.metabol.2018.09.005.
[6] T. Lobstein, H. Brinsden, M. Neveux. World Obesity Atlas 2022, 2022. https://www.worldobesity.org/resources/resource-library/world-obesity-atlas-2022.
[7] A. Okunogbe, R. Nugent, G. Spencer, J. Powis, J. Ralston, J. Wilding, Economic impacts of overweight and obesity: current and future estimates for 161 countries, BMJ Glob. Health 7 (2022) e009773, https://doi.org/10.1136/bmjgh-2022-009773.
[8] WHO Acceleration Plan to Stop Obesity. https://www.who.int/publications-detail-redirect/9789240075634, 2025.
[9] Z.J. Ward, S.N. Bleich, A.L. Cradock, J.L. Barrett, C.M. Giles, C. Flax, M.W. Long, S.L. Gortmaker, Projected U.S. state-level prevalence of adult obesity and severe obesity, N. Engl. J. Med. 381 (2019) 2440–2450, https://doi.org/10.1056/NEJMsa1909301.
[10] S. Hay, G.B. of D. 2015 O. Collaborators, Health effects of overweight and obesity in 195 countries over 25 years, N. Engl. J. Med. 377 (2017). https://ora.ox.ac.uk/objects/uuid:51a548b1-294d-4402-851d-1d90051a0211.
[11] C.M. Apovian, M.E. McDonnell, CagriSema and the link between obesity and type 2 diabetes, Lancet 402 (2023) 671–673, https://doi.org/10.1016/S0140-6736(23)01291-6.
[12] D.J. Cram, J.M. Cram, Host-guest chemistry, Science 183 (1974) 803–809, https://doi.org/10.1126/science.183.4127.803.
[13] J.-M. Lehn, Supramolecular chemistry: receptors, catalysts, and carriers, Science 227 (1985) 849–856, https://doi.org/10.1126/science.227.4689.849.
[14] Q. Song, Z. Cheng, M. Kariuki, S.C.L. Hall, S.K. Hill, J.Y. Rho, S. Perrier, Molecular self-assembly and supramolecular chemistry of cyclic peptides, Chem. Rev. 121 (2021) 13936–13995, https://doi.org/10.1021/acs.chemrev.0c01291.
[15] M.J. Webber, R. Langer, Drug delivery by supramolecular design, Chem. Soc. Rev. 46 (2017) 6600–6620, https://doi.org/10.1039/C7CS00391A.
[16] E.Y. Xue, W.-J. Shi, W.-P. Fong, D.K.P. Ng, Targeted delivery and site-specific activation of β-Cyclodextrin-conjugated photosensitizers for photodynamic therapy through a supramolecular bio-orthogonal approach, J. Med. Chem. 64 (2021) 15461–15476, https://doi.org/10.1021/acs.jmedchem.1c01505.
[17] H. Wang, Y. Yang, B. Yuan, X.-L. Ni, J.-F. Xu, X. Zhang, Cucurbit[10]uril-encapsulated cationic porphyrins with enhanced fluorescence emission and photostability for cell imaging, ACS Appl. Mater. Interfaces 13 (2021) 2269–2276, https://doi.org/10.1021/acsami.0c18725.
[18] C.L. Maikawa, A.A.A. Smith, L. Zou, G.A. Roth, E.C. Gale, L.M. Stapleton, S. W. Baker, J.L. Mann, A.C. Yu, S. Correa, A.K. Grosskopf, C.S. Liong, C.M. Meis, D. Chan, M. Troxell, D.M. Maahs, B.A. Buckingham, M.J. Webber, E.A. Appel, A co-formulation of supramolecularly stabilized insulin and pramlintide enhances mealtime glucagon suppression in diabetic pigs, Nat. Biomed. Eng. 4 (2020) 507–517, https://doi.org/10.1038/s41551-020-0555-4.
[19] F. Gelain, Z. Luo, S. Zhang, Self-assembling peptide EAK16 and RADA16 nanofiber scaffold hydrogel, Chem. Rev. 120 (2020) 13434–13460, https://doi.org/10.1021/acs.chemrev.0c00690.
[20] Y. Jung, J.S. Choi, J. Ryu, Z. Zhang, Y. Lim, Cooperative assembly of self-adjusting α-helical coiled coils along the length of an mRNA chain to form a thermodynamically stable nanotube carrier, J. Am. Chem. Soc. 145 (2023) 23048–23056, https://doi.org/10.1021/jacs.3c05638.
[21] Y. Li, S. Liu, M. Liang, Y. Cui, H. Zhao, Q. Gao, Glycocalixarene with luminescence for Warburg effect-mediated tumor imaging and targeted drug delivery, Chem. Commun. 57 (2021) 9728–9731, https://doi.org/10.1039/D1CC04169J.
[22] Y. Geng, L. Qiu, Y. Cheng, J. Li, Y. Ma, C. Zhao, Y. Cai, X. Zhang, J. Chen, Y. Pan, K. Wang, X. Yao, D. Guo, J. Wu, Alleviating recombinant tissue plasminogen activator-induced hemorrhagic transformation in ischemic stroke via targeted delivery of a ferroptosis inhibitor, Adv. Sci. (2024) 2309517, https://doi.org/10.1002/advs.202309517.
[23] N.K. Mishra, M. Østergaard, S.R. Midtgaard, S.S. Strindberg, S. Winkler, S. Wu, T. J. Sørensen, T. Hassenkam, J.-C.N. Poulsen, L.L. Leggio, H.M. Nielsen, L. Arleth, N.J. Christensen, P.W. Thulstrup, K.J. Jensen, Controlling the fractal dimension in self-assembly of terpyridine modified insulin by Fe^{2+} and Eu^{3+} to direct in vivo effects, Nanoscale 13 (2021) 8467–8473, https://doi.org/10.1039/D1NR00414J.
[24] G. Engudar, C. Rodríguez-Rodríguez, N.K. Mishra, M. Bergamo, G. Amouroux, K. J. Jensen, K. Saatchi, U.O. Häfeli, Metal-ion coordinated self-assembly of human insulin directs kinetics of insulin release as determined by preclinical SPECT/CT imaging, J. Control. Release 343 (2022) 347–360, https://doi.org/10.1016/j.jconrel.2022.01.032.
[25] J. Han, A.F.B. Räder, F. Reichart, B. Aikman, M.N. Wenzel, B. Woods, M. Weinmüller, B.S. Ludwig, S. Stürup, G.M.M. Groothuis, H.P. Permentier, R. Bischoff, H. Kessler, P. Horvatovich, A. Casini, Bioconjugation of supramolecular metallacages to integrin ligands for targeted delivery of cisplatin, Bioconjug. Chem. 29 (2018) 3856–3865, https://doi.org/10.1021/acs.bioconjchem.8b00682.
[26] G. Yang, W. Zheng, G. Tao, L. Wu, Q.-F. Zhou, Z. Kochovski, T. Ji, H. Chen, X. Li, Y. Lu, H. Ding, H.-B. Yang, G. Chen, M. Jiang, Diversiform and transformable glyco-nanostructures constructed from amphiphilic supramolecular metallocarbohydrates through hierarchical self-assembly: the balance between metallacycles and saccharides, ACS Nano 13 (2019) 13474–13485, https://doi.org/10.1021/acsnano.9b07134.
[27] P. Zhou, R. Xing, Q. Li, J. Li, C. Yuan, X. Yan, Steering phase-separated droplets to control fibrillar network evolution of supramolecular peptide hydrogels, Matter 6 (2023) 1945–1963, https://doi.org/10.1016/j.matt.2023.03.029.
[28] R. Chang, C. Yuan, P. Zhou, R. Xing, X. Yan, Peptide self-assembly: from ordered to disordered, Acc. Chem. Res. 57 (2024) 289–301, https://doi.org/10.1021/acs.accounts.3c00592.
[29] R. Chang, Q. Zou, L. Zhao, Y. Liu, R. Xing, X. Yan, Amino-acid-encoded supramolecular photothermal nanomedicine for enhanced cancer therapy, Adv. Mater. 34 (2022) 2200139, https://doi.org/10.1002/adma.202200139.

[30] R. Xing, C. Yuan, S. Li, J. Song, J. Li, X. Yan, Charge-induced secondary structure transformation of amyloid-derived dipeptide assemblies from β-sheet to α-helix, Angew. Chem. Int. Ed. 57 (2018) 1537–1542, https://doi.org/10.1002/anie.201710642.

[31] X. Cai, Y. Xu, L. Zhao, J. Xu, S. Li, C. Wen, X. Xia, Q. Dong, X. Hu, X. Wang, L. Chen, Z. Chen, W. Tan, In situ pepsin-assisted needle assembly of magnetic-graphitic-nanocapsules for enhanced gastric retention and mucus penetration, Nano Today 36 (2021) 101032, https://doi.org/10.1016/j.nantod.2020.101032.

[32] G. Duché, C. Heu, P. Thordarson, Development and characterization of nanoscale gel-core liposomes using a short self-assembled peptide hydrogel: implications for drug delivery, ACS Appl. Nano Mater. 6 (2023) 14745–14755, https://doi.org/10.1021/acsanm.3c02172.

[33] Z. Wang, J. Zhang, Y. Wang, J. Zhou, X. Jiao, M. Han, X. Zhang, H. Hu, R. Su, Y. Zhang, W. Qi, Overcoming endosomal escape barriers in gene drug delivery using de novo designed pH-responsive peptides, ACS Nano 18 (2024) 10324–10340, https://doi.org/10.1021/acsnano.4c02400.

[34] T.D. Brown, K.A. Whitehead, S. Mitragotri, Materials for oral delivery of proteins and peptides, Nat. Rev. Mater. 5 (2020) 127–148, https://doi.org/10.1038/s41578-019-0156-6.

[35] J.M. Riddle, J.W. Estes, Oral contraceptives in ancient and medieval times, Am. Sci. 80 (1992) 226–233. http://www.jstor.org/stable/29774642.

[36] K.L. Wolf, H. Prahm, H. Harms, Über den ordnungszustand der moleküle in flüssigkeiten, Z. Phys. Chem. 36B (1937) 237–287, https://doi.org/10.1515/zpch-1937-3618.

[37] D.E. Atkinson, Biological feedback control at the molecular level, Science 150 (1965) 851–857, https://doi.org/10.1126/science.150.3698.851.

[38] The Nobel Prize in Chemistry 1987, NobelPrize.Org, 2025. https://www.nobelprize.org/prizes/chemistry/1987/summary.

[39] Joint FAO/WHO Expert Committee on Food Additives, Alpha-cyclodextrin, Evaluations of the Joint FAO/WHO Expert Committee on Food Additives. https://apps.who.int/food-additives-contaminants-jecfa-database/Home/Chemical/1600, 2001.

[40] US Food and Drug Administration, GRN No. 678 Alpha-Cyclodextrin, Generally Recognized as Safe (GARS) Notices. https://www.cfsanappsexternal.fda.gov/scripts/fdcc/?set=GRASNotices&id=678, 2025.

[41] L.-W. Xia, R. Xie, X.-J. Ju, W. Wang, Q. Chen, L.-Y. Chu, Nano-structured smart hydrogels with rapid response and high elasticity, Nat. Commun. 4 (2013) 2226, https://doi.org/10.1038/ncomms3226.

[42] The Nobel Prize in Chemistry 2016, NobelPrize.Org, 2025. https://www.nobelprize.org/prizes/chemistry/2016/summary/.

[43] X. Han, Y. Lu, J. Xie, E. Zhang, H. Zhu, H. Du, K. Wang, B. Song, C. Yang, Y. Shi, Z. Cao, Zwitterionic micelles efficiently deliver oral insulin without opening tight junctions, Nat. Nanotechnol. 15 (2020) 605–614, https://doi.org/10.1038/s41565-020-0693-6.

[44] J.R. Jørgensen, L.H.E. Thamdrup, K. Kamguyan, L.H. Nielsen, H.M. Nielsen, A. Boisen, T. Rades, A. Müllertz, Design of a self-unfolding delivery concept for oral administration of macromolecules, J. Control. Release 329 (2021) 948–954, https://doi.org/10.1016/j.jconrel.2020.10.024.

[45] L. Wang, Y. Li, M. Ren, X. Wang, L. Li, F. Liu, Y. Lan, S. Yang, J. Song, pH and lipase-responsive nanocarrier-mediated dual drug delivery system to treat periodontitis in diabetic rats, Bioact. Mater. 18 (2022) 254–266, https://doi.org/10.1016/j.bioactmat.2022.02.008.

[46] X.-Q. Zhou, P. Wang, V. Ramu, L. Zhang, S. Jiang, X. Li, S. Abyar, P. Papadopoulou, Y. Shao, L. Bretin, M.A. Siegler, F. Buda, A. Kros, J. Fan, X. Peng, W. Sun, S. Bonnet, In vivo metallophilic self-assembly of a light-activated anticancer drug, Nat. Chem. 15 (2023) 980–987, https://doi.org/10.1038/s41557-023-01199-w.

[47] J.-S. Guo, J.-J. Li, Z.-H. Wang, Y. Liu, Y.-X. Yue, H.-B. Li, X.-H. Zhao, Y.-J. Sun, Y.-H. Ding, F. Ding, D.-S. Guo, L. Wang, Y. Chen, Dual hypoxia-responsive supramolecular complex for cancer target therapy, Nat. Commun. 14 (2023) 5634, https://doi.org/10.1038/s41467-023-41388-2.

[48] M. Dockerill, D.J. Ford, S. Angerani, I. Alwis, L.J. Dowman, J. Ripoll-Rozada, R. E. Smythe, J.S.T. Liu, P.J.B. Pereira, S.P. Jackson, R.J. Payne, N. Winssinger, Development of supramolecular anticoagulants with on-demand reversibility, Nat. Biotechnol. (2024), https://doi.org/10.1038/s41587-024-02209-z.

[49] G. Song, D. Yang, Y. Wang, C. De Graaf, Q. Zhou, S. Jiang, K. Liu, X. Cai, A. Dai, G. Lin, D. Liu, F. Wu, Y. Wu, S. Zhao, L. Ye, G.W. Han, J. Lau, B. Wu, M.A. Hanson, Z.-J. Liu, M.-W. Wang, R.C. Stevens, Human GLP-1 receptor transmembrane domain structure in complex with allosteric modulators, Nature 546 (2017) 312–315, https://doi.org/10.1038/nature22378.

[50] P.K. Lund, R.H. Goodman, P.C. Dee, J.F. Habener, Pancreatic preproglucagon cDNA contains two glucagon-related coding sequences arranged in tandem, Proc. Natl. Acad. Sci. 79 (1982) 345–349, https://doi.org/10.1073/pnas.79.2.345.

[51] H. Tager, M. Hohenboken, J. Markese, R.J. Dinerstein, Identification and localization of glucagon-related peptides in rat brain, Proc. Natl. Acad. Sci. 77 (1980) 6229–6233, https://doi.org/10.1073/pnas.77.10.6229.

[52] G.I. Bell, R.F. Santerre, G.T. Mullenbach, Hamster preproglucagon contains the sequence of glucagon and two related peptides, Nature 302 (1983) 716–718, https://doi.org/10.1038/302716a0.

[53] A.J. Moody, J.J. Holst, L. Thim, S.L. Jensen, Relationship of glicentin to proglucagon and glucagon in the porcine pancreas, Nature 289 (1981) 514–516, https://doi.org/10.1038/289514a0.

[54] L.C. Lopez, M.L. Frazier, C.J. Su, A. Kumar, G.F. Saunders, Mammalian pancreatic preproglucagon contains three glucagon-related peptides, Proc. Natl. Acad. Sci. 80 (1983) 5485–5489, https://doi.org/10.1073/pnas.80.18.5485.

[55] G.I. Bell, R. Sanchez-Pescador, P.J. Laybourn, R.C. Najarian, Exon duplication and divergence in the human preproglucagon gene, Nature 304 (1983) 368–371, https://doi.org/10.1038/304368a0.

[56] J.J. Holst, C. Ørskov, O. Vagn Nielsen, T.W. Schwartz, Truncated glucagon-like peptide I, an insulin-releasing hormone from the distal gut, FEBS Lett. 211 (1987) 169–174, https://doi.org/10.1016/0014-5793(87)81430-8.

[57] S. Mojsov, G.C. Weir, J.F. Habener, Insulinotropin: glucagon-like peptide I (7-37) co-encoded in the glucagon gene is a potent stimulator of insulin release in the perfused rat pancreas, J. Clin. Invest. 79 (1987) 616–619, https://doi.org/10.1172/JCI112855.

[58] D.J. Drucker, J. Philippe, S. Mojsov, W.L. Chick, J.F. Habener, Glucagon-like peptide I stimulates insulin gene expression and increases cyclic AMP levels in a rat islet cell line, Proc. Natl. Acad. Sci. 84 (1987) 3434–3438, https://doi.org/10.1073/pnas.84.10.3434.

[59] W.T. Garvey, J.P. Frias, A.M. Jastreboff, C.W. Le Roux, N. Sattar, D. Aizenberg, H. Mao, S. Zhang, N.N. Ahmad, M.C. Bunck, I. Benabbad, X.M. Zhang, F. H. Abalos, F.C.P. Manghi, C.J. Zaidman, M.L. Vico, D. Aizenberg, P.R. Costanzo, L.P. Serra, I.J. MacKinnon, M.N. Hissa, M.H. Vidotti, J.F. Kerr Saraiva, B.B. Alves, D.R. Franco, O. Moratto, S. Murthy, G. Goyal, Y. Yamasaki, N. Sato, S. Inoue, T. Asakura, M. Shestakova, E. Khaykina, E. Troshina, N. Vorokhobina, A. Ametov, S.-T. Tu, C.-Y. Yang, I.-T. Lee, C.-N. Huang, H.-Y. Ou, G. Freeman, S. Machineni, K. Klein, S. Sultan, A. Parsa, J. Otero-Martinez, A. Gonzalez, A. Bhargava, S. Brian, C. Ince, S. Plantholt, J. Cole, A. Lacour, D. Vega, J. De Souza, J.L. Rohlf, R.C. St. John, B. Horowitz, H. Audish, R. Galindo, G. Umpierrez, J. Ard, B. Curtis, W.T. Garvey, N.J. Fraser, J. Mandry, R. Mohseni, R. Mayfield, T. Powell, C. Vance, S. Ong, A.L. Lewy-Alterbaum, A. Murray, A. Al-Karadsheh, T. Yacoub, K. Roberts, D.L. Fried, J. Rosenstock, B. Pulla, B. Bode, J. Frias, L. Klaff, R. Brazg, J. Van, A. Tan, T. Briskin, M. Rhee, T. Chaicha-Brom, P.A. Hartley, L. Nunez, G. Cortes-Maisonet, G. Soucie, S. Hsia, T. Jones, Tirzepatide once weekly for the treatment of obesity in people with type 2 diabetes (SURMOUNT-2): a double-blind, randomised, multicentre, placebo-controlled, phase 3 trial, Lancet 402 (2023) 613–626, https://doi.org/10.1016/S0140-6736(23)01200-X.

[60] S.E. Inzucchi, D.K. McGuire, New drugs for the treatment of diabetes: Part II: incretin-based therapy and beyond, Circulation 117 (2008) 574–584, https://doi.org/10.1161/CIRCULATIONAHA.107.735795.

[61] J.J. Meier, GLP-1 receptor agonists for individualized treatment of type 2 diabetes mellitus, Nat. Rev. Endocrinol. 8 (2012) 728–742, https://doi.org/10.1038/nrendo.2012.140.

[62] J. Kolic, P.E. MacDonald, cAMP-independent effects of GLP-1 on β cells, J. Clin. Invest. 125 (2015) 4327–4330, https://doi.org/10.1172/JCI85004.

[63] M.R. Hayes, K.P. Skibicka, H.J. Grill, Caudal brainstem processing is sufficient for behavioral, sympathetic, and parasympathetic responses driven by peripheral and hindbrain glucagon-like-peptide-1 receptor stimulation, Endocrinology 149 (2008) 4059–4068, https://doi.org/10.1210/en.2007-1743.

[64] A.R. Saxena, D.N. Gorman, R.M. Esquejo, A. Bergman, K. Chidsey, C. Buckeridge, D.A. Griffith, A.M. Kim, Danuglipron (PF-06882961) in type 2 diabetes: a randomized, placebo-controlled, multiple ascending-dose phase 1 trial, Nat. Med. 27 (2021) 1079–1087, https://doi.org/10.1038/s41591-021-01391-w.

[65] A. Flint, A. Raben, A. Astrup, J.J. Holst, Glucagon-like peptide 1 promotes satiety and suppresses energy intake in humans, J. Clin. Invest. 101 (1998) 515–520, https://doi.org/10.1172/JCI990.

[66] M. Tang-Christensen, P.J. Larsen, R. Goke, A. Fink-Jensen, D.S. Jessop, M. Moller, S.P. Sheikh, Central administration of GLP-1-(7-36) amide inhibits food and water intake in rats, Am. J. Physiol. Regul. Integr. Comp. Physiol. 271 (1996) R848–R856, https://doi.org/10.1152/ajpregu.1996.271.4.R848.

[67] A.P. Davenport, C.C.G. Scully, C. De Graaf, A.J.H. Brown, J.J. Maguire, Advances in therapeutic peptides targeting G protein-coupled receptors, Nat. Rev. Drug Discov. 19 (2020) 389–413, https://doi.org/10.1038/s41573-020-0062-z.

[68] R.A. DeFronzo, R.E. Ratner, J. Han, D.D. Kim, M.S. Fineman, A.D. Baron, Effects of exenatide (exendin-4) on glycemic control and weight over 30 weeks in metformin-treated patients with type 2 diabetes, Diabetes Care 28 (2005) 1092–1100, https://doi.org/10.2337/diacare.28.5.1092.

[69] F. Fehse, M. Trautmann, J.J. Holst, A.E. Halseth, N. Nanayakkara, L.L. Nielsen, M. S. Fineman, D.D. Kim, M.A. Nauck, Exenatide augments first- and second-phase insulin secretion in response to intravenous glucose in subjects with type 2 diabetes, J. Clin. Endocrinol. Metab. 90 (2005) 5991–5997, https://doi.org/10.1210/jc.2005-1093.

[70] D.J. Drucker, A. Dritselis, P. Kirkpatrick, Liraglutide, Nat. Rev. Drug Discov. 9 (2010) 267–268, https://doi.org/10.1038/nrd3148.

[71] M. Christensen, F.K. Knop, J.J. Holst, T. Vilsboll, Lixisenatide, a novel GLP-1 receptor agonist for the treatment of type 2 diabetes mellitus, Idrugs 12 (2009) 503–513.

[72] S.P. Marso, S.C. Bain, A. Consoli, F.G. Eliaschewitz, E. Jódar, L.A. Leiter, I. Lingvay, J. Rosenstock, J. Seufert, M.L. Warren, V. Woo, O. Hansen, A.G. Holst, J. Pettersson, T. Vilsbøll, Semaglutide and cardiovascular outcomes in patients with type 2 diabetes, N. Engl. J. Med. 375 (2016) 1834–1844, https://doi.org/10.1056/NEJMoa1607141.

[73] L.J. Scott, Dulaglutide: a review in type 2 diabetes, Drugs 80 (2020) 197–208, https://doi.org/10.1007/s40265-020-01260-9.

[74] T. Coskun, K.W. Sloop, C. Loghin, J. Alsina-Fernandez, S. Urva, K.B. Bokvist, X. Cui, D.A. Briere, O. Cabrera, W.C. Roell, U. Kuchibhotla, J.S. Moyers, C. T. Benson, R.E. Gimeno, D.A. D'Alessio, A. Haupt, LY3298176, a novel dual GIP and GLP-1 receptor agonist for the treatment of type 2 diabetes mellitus: from discovery to clinical proof of concept, Mol. Metab. 18 (2018) 3–14, https://doi.org/10.1016/j.molmet.2018.09.009.

[75] L.B. Knudsen, D. Kiel, M. Teng, C. Behrens, D. Bhumralkar, J.T. Kodra, J.J. Holst, C.B. Jeppesen, M.D. Johnson, J.C. De Jong, A.S. Jorgensen, T. Kercher, J. Kostrowicki, P. Madsen, P.H. Olesen, J.S. Petersen, F. Poulsen, U.G. Sidelmann, J. Sturis, L. Truesdale, J. May, J. Lau, Small-molecule agonists for the glucagon-like peptide 1 receptor, Proc. Natl. Acad. Sci. 104 (2007) 937–942, https://doi.org/10.1073/pnas.0605701104.

[76] K.G. Harikumar, D. Wootten, D.I. Pinon, C. Koole, A.M. Ball, S.G.B. Furness, B. Graham, M. Dong, A. Christopoulos, L.J. Miller, P.M. Sexton, Glucagon-like peptide-1 receptor dimerization differentially regulates agonist signaling but does not affect small molecule allostery, Proc. Natl. Acad. Sci. 109 (2012) 18607–18612, https://doi.org/10.1073/pnas.1205227109.

[77] T. Kawai, B. Sun, H. Yoshino, D. Feng, Y. Suzuki, M. Fukazawa, S. Nagao, D. B. Wainscott, A.D. Showalter, B.A. Droz, T.S. Kobilka, M.P. Coghlan, F.S. Willard, Y. Kawabe, B.K. Kobilka, K.W. Sloop, Structural basis for GLP-1 receptor activation by LY3502970, an orally active nonpeptide agonist, Proc. Natl. Acad. Sci. 117 (2020) 29959–29967, https://doi.org/10.1073/pnas.2014879117.

[78] B.P. Cary, X. Zhang, J. Cao, R.M. Johnson, S.J. Piper, E.J. Gerrard, D. Wootten, P. M. Sexton, New insights into the structure and function of class b1 GPCRs, Endocr. Rev. 44 (2023) 492–517, https://doi.org/10.1210/endrev/bnac033.

[79] P. Zhao, Y.-L. Liang, M.J. Belousoff, G. Deganutti, M.M. Fletcher, F.S. Willard, M. G. Bell, M.E. Christe, K.W. Sloop, A. Inoue, T.T. Truong, L. Clydesdale, S.G. B. Furness, A. Christopoulos, M.-W. Wang, L.J. Miller, C.A. Reynolds, R. Danev, P. M. Sexton, D. Wootten, Activation of the GLP-1 receptor by a non-peptidic agonist, Nature 577 (2020) 432–436, https://doi.org/10.1038/s41586-019-1902-z.

[80] D. Chen, J. Liao, N. Li, C. Zhou, Q. Liu, G. Wang, R. Zhang, S. Zhang, L. Lin, K. Chen, X. Xie, F. Nan, A.A. Young, M.-W. Wang, A nonpeptidic agonist of glucagon-like peptide 1 receptors with efficacy in diabetic *db / db* mice, Proc. Natl. Acad. Sci. 104 (2007) 943–948, https://doi.org/10.1073/pnas.0610173104.

[81] M. He, N. Guan, W. Gao, Q. Liu, X. Wu, D. Ma, D. Zhong, G. Ge, C. Li, X. Chen, L. Yang, J. Liao, M. Wang, A continued saga of boc5, the first non-peptidic glucagon-like peptide-1 receptor agonist with in vivo activities, Acta Pharmacol. Sin. 33 (2012) 148–154, https://doi.org/10.1038/aps.2011.169.

[82] W. Wan, Q. Qin, L. Xie, H. Zhang, F. Wu, R.C. Stevens, Y. Liu, GLP-1R signaling and functional molecules in incretin therapy, Molecules 28 (2023) 751, https://doi.org/10.3390/molecules28020751.

[83] B. Eshaghi, A. Schudel, I. Sadeghi, Z. Chen, A.H. Lee, M. Kanelli, F. Tierney, J. Han, B. Ingalls, D.M. Francis, G. Li, U. von Andrian, R. Langer, A. Jaklenec, The role of engineered materials in mucosal vaccination strategies, Nat. Rev. Mater. 9 (2024) 29–45, https://doi.org/10.1038/s41578-023-00625-2.

[84] P.K.P. Burnell, L. Asking, L. Borgström, S.C. Nichols, B. Olsson, D. Prime, I. Shrubb, Studies of the human oropharyngeal airspaces using magnetic resonance imaging IV—the oropharyngeal retention effect for four inhalation delivery systems, J. Aerosol. Med. 20 (2007) 269–281, https://doi.org/10.1089/jam.2007.0566.

[85] S.P. Newman, H.-K. Chan, In vitro-in vivo correlations (IVIVCs) of deposition for drugs given by oral inhalation, Adv. Drug Deliv. Rev. 167 (2020) 135–147, https://doi.org/10.1016/j.addr.2020.06.023.

[86] L.M. Hernández, M.K. Taylor, Salivary gland anatomy and physiology, in: D. A. Granger, M.K. Taylor (Eds.), Salivary Bioscience: Foundations of Interdisciplinary Saliva Research and Applications, Springer International Publishing, Cham, 2020, pp. 11–20, https://doi.org/10.1007/978-3-030-35784-9_2.

[87] T. Nagai, R. Konishi, Buccal/gingival drug delivery systems, J. Control. Release 6 (1987) 353–360, https://doi.org/10.1016/0168-3659(87)90088-5.

[88] S. Şenel, M.J. Rathbone, M. Cansız, I. Pather, Recent developments in buccal and sublingual delivery systems, Expert Opin. Drug Deliv. 9 (2012) 615–628, https://doi.org/10.1517/17425247.2012.676040.

[89] G.J. Tortora, B. Derrickson, Anatomy & Physiology, 2025.

[90] Y. Inamoto, E. Saitoh, S. Okada, H. Kagaya, S. Shibata, M. Baba, K. Onogi, S. Hashimoto, K. Katada, P. Wattanapan, J.B. Palmer, Anatomy of the larynx and pharynx: effects of age, gender and height revealed by multidetector computed tomography, J. Oral Rehabil. 42 (2015) 670–677, https://doi.org/10.1111/joor.12298.

[91] J.E. Hutchison, Greener nanoscience: a proactive approach to advancing applications and reducing implications of nanotechnology, ACS Nano 2 (2008) 395–402, https://doi.org/10.1021/nn800131j.

[92] Y. Zhou, J. Sun, Y.-S. Cheng, Comparison of deposition in the USP and physical mouth–throat models with solid and liquid particles, J. Aerosol Med. Pulm. Drug Deliv. 24 (2011) 277–284, https://doi.org/10.1089/jamp.2011.0882.

[93] U. Pharmacopeia, Aerosols, nasal sprays, metered-dose inhalers, and dry powder inhalers, US Pharmacopeia (2009) 32.

[94] K.W. Stapleton, E. Guentsch, M.K. Hoskinson, W.H. Finlay, On the suitability of k–ε turbulence modeling for aerosol deposition in the mouth and throat: a comparison with experiment, J. Aerosol Sci. 31 (2000) 739–749, https://doi.org/10.1016/S0021-8502(99)00547-9.

[95] K.-H. Cheng, Y.-S. Cheng, H.-C. Yeh, D.L. Swift, Deposition of ultrafine aerosols in the head airways during natural breathing and during simulated breath holding using replicate human upper airway casts, Aerosol Sci. Technol. 23 (1995) 465–474, https://doi.org/10.1080/02786829508965329.

[96] W. Liu, R. Ma, S. Lu, Y. Wen, H. Li, J. Wang, B. Sun, Acid-resistant mesoporous metal–organic frameworks as carriers for targeted hypoglycemic peptide delivery: peptide encapsulation, release, and bioactivity, ACS Appl. Mater. Interfaces 14 (2022) 55447–55457, https://doi.org/10.1021/acsami.2c18452.

[97] J.P. Wilson, Surface area of the small intestine in man, Gut 8 (1967) 618–621, https://doi.org/10.1136/gut.8.6.618.

[98] P. Lundquist, G. Khodus, Z. Niu, L.N. Thwala, F. McCartney, I. Simoff, E. Andersson, A. Beloqui, A. Mabondzo, S. Robla, D.-L. Webb, P.M. Hellström, Å. V. Keita, E. Sima, N. Csaba, M. Sundbom, V. Preat, D.J. Brayden, M.J. Alonso, P. Artursson, Barriers to the intestinal absorption of four insulin-loaded arginine-rich nanoparticles in human and rat, ACS Nano 16 (2022) 14210–14229, https://doi.org/10.1021/acsnano.2c04330.

[99] D.P. Lima, D.G. Diniz, S.A.S. Moimaz, D.H. Sumida, A.C. Okamoto, Saliva: reflection of the body, Int. J. Infect. Dis. 14 (2010) e184–e188, https://doi.org/10.1016/j.ijid.2009.04.022.

[100] Y. Zhou, Z. Liu, Saliva biomarkers in oral disease, Clin. Chim. Acta 548 (2023) 117503, https://doi.org/10.1016/j.cca.2023.117503.

[101] M. Song, H. Bai, P. Zhang, X. Zhou, B. Ying, Promising applications of human-derived saliva biomarker testing in clinical diagnostics, Int. J. Oral Sci. 15 (2023) 1–17, https://doi.org/10.1038/s41368-022-00209-w.

[102] A. Brodkorb, L. Egger, M. Alminger, P. Alvito, R. Assunção, S. Ballance, T. Bohn, C. Bourlieu-Lacanal, R. Boutrou, F. Carrière, A. Clemente, M. Corredig, D. Dupont, C. Dufour, C. Edwards, M. Golding, S. Karakaya, B. Kirkhus, S. Le Feunteun, U. Lesmes, A. Macierzanka, A.R. Mackie, C. Martins, S. Marze, D.J. McClements, O. Ménard, M. Minekus, R. Portmann, C.N. Santos, I. Souchon, R.P. Singh, G. E. Vegarud, M.S.J. Wickham, W. Weitschies, I. Recio, INFOGEST static in vitro simulation of gastrointestinal food digestion, Nat. Protoc. 14 (2019) 991–1014, https://doi.org/10.1038/s41596-018-0119-1.

[103] D.J. Brayden, Evolving peptides for oral intake, Nat. Biomed. Eng. 4 (2020) 487–488, https://doi.org/10.1038/s41551-020-0559-0.

[104] C. Rundfeldt, P. Klein, D. Boison, A. Rotenberg, R. D'Ambrosio, C. Eastman, B. Purnell, M. Murugan, H.P. Goodkin, W. Löscher, Preclinical pharmacokinetics and tolerability of a novel meglumine-based parenteral solution of topiramate and topiramate combinations for treatment of status epilepticus, Epilepsia 64 (2023) 888–899, https://doi.org/10.1111/epi.17520.

[105] H.-H. Frey, W. Löscher, Anticonvulsant potency of unmetabolized diazepam, Pharmacology 25 (2008) 154–159, https://doi.org/10.1159/000137737.

[106] X. Song, E. Tsakiridis, G.R. Steinberg, Y. Pei, Targeting AMP-activated protein kinase (AMPK) for treatment of autosomal dominant polycystic kidney disease, Cell. Signal. 73 (2020) 109704, https://doi.org/10.1016/j.cellsig.2020.109704.

[107] F. Wu, L. Yang, K. Hang, M. Laursen, L. Wu, G.W. Han, Q. Ren, N.K. Roed, G. Lin, M.A. Hanson, H. Jiang, M.-W. Wang, S. Reedtz-Runge, G. Song, R.C. Stevens, Full-length human GLP-1 receptor structure without orthosteric ligands, Nat. Commun. 11 (2020) 1272, https://doi.org/10.1038/s41467-020-14934-5.

[108] P. Artursson, P. Lundquist, A new opening for orally taken peptide drugs, Nat. Biomed. Eng. 4 (2020) 12–13, https://doi.org/10.1038/s41551-019-0513-1.

[109] Q. Xin, Y. Zhang, P. Yu, Y. Zhao, F. Sun, H. Zhang, Z. Ma, S. Sun, X. Yang, S. Tao, X. Xu, C. Ding, J. Li, Oral environment-adaptive peptide–polymer conjugate for caries prevention with targeting, antibacterial, and antifouling abilities, Chem. Mater. 36 (2024) 1691–1706, https://doi.org/10.1021/acs.chemmater.3c03027.

[110] Q. Xin, Z. Ma, S. Sun, H. Zhang, Y. Zhang, L. Zuo, Y. Yang, J. Xie, C. Ding, J. Li, Supramolecular self-healing antifouling coating for dental materials, ACS Appl. Mater. Interfaces 15 (2023) 41403–41416, https://doi.org/10.1021/acsami.3c09628.

[111] X. Jing, S. Wang, H. Tang, D. Li, F. Zhou, L. Xin, Q. He, S. Hu, T. Zhang, T. Chen, J. Song, Dynamically bioresponsive DNA hydrogel incorporated with dual-functional stem cells from apical papilla-derived exosomes promotes diabetic bone regeneration, ACS Appl. Mater. Interfaces 14 (2022) 16082–16099, https://doi.org/10.1021/acsami.2c02278.

[112] E. Caffarel-Salvador, S. Kim, V. Soares, R.Y. Tian, S.R. Stern, D. Minahan, R. Yona, X. Lu, F.R. Zakaria, J. Collins, J. Wainer, J. Wong, R. McManus, S. Tamang, S. McDonnell, K. Ishida, A. Hayward, X. Liu, F. Hubálek, J. Fels, A. Vegge, M. R. Frederiksen, U. Rahbek, T. Yoshitake, J. Fujimoto, N. Roxhed, R. Langer, G. Traverso, A microneedle platform for buccal macromolecule delivery, Sci. Adv. 7 (2021) eabe2620, https://doi.org/10.1126/sciadv.abe2620.

[113] D. Shen, H. Yu, L. Wang, Y. Wang, Y. Hong, C. Li, Molecular docking-guided design on glucose-responsive nanoparticles for microneedle fabrication and "three-meal-per-day" blood-glucose regulation, ACS Appl. Mater. Interfaces 15 (2023) 31330–31343, https://doi.org/10.1021/acsami.3c06483.

[114] S.H. Kelly, E.E. Opolot, Y. Wu, B. Cossette, A.K. Varadhan, J.H. Collier, Tabletized supramolecular assemblies for sublingual peptide immunization, Adv. Healthc. Mater. 10 (2021) 2001614, https://doi.org/10.1002/adhm.202001614.

[115] S.H. Kelly, Y. Wu, A.K. Varadhan, E.J. Curvino, A.S. Chong, J.H. Collier, Enabling sublingual peptide immunization with molecular self-assemblies, Biomaterials 241 (2020) 119903, https://doi.org/10.1016/j.biomaterials.2020.119903.

[116] S.H. Kelly, N.L. Votaw, B.J. Cossette, Y. Wu, S. Shetty, L.S. Shores, L.A. Issah, J. H. Collier, A sublingual nanofiber vaccine to prevent urinary tract infections, Sci. Adv. 8 (2022) eabq4120, https://doi.org/10.1126/sciadv.abq4120.

[117] H. Jia, Y. Shang, H. Cao, Y. Gao, J. Liu, L. Yang, C. Yang, C. Ren, Z. Wang, J. Liu, A minimalist supramolecular nanovaccine forcefully propels the tfh cell and GC B cell responses, Chem. Eng. J. 435 (2022) 134782, https://doi.org/10.1016/j.cej.2022.134782.

[118] S. Jia, S. Ji, J. Zhao, Y. Lv, J. Wang, D. Sun, D. Ding, A fluorinated supramolecular self-assembled peptide as nanovaccine adjuvant for enhanced cancer vaccine therapy, Small Methods 7 (2023) 2201409, https://doi.org/10.1002/smtd.202201409.

[119] S.H. Kelly, B.J. Cossette, A.K. Varadhan, Y. Wu, J.H. Collier, Titrating polyarginine into nanofibers enhances cyclic-dinucleotide adjuvanticity *in vitro* and after sublingual immunization, ACS Biomater. Sci. Eng. 7 (2021) 1876–1888, https://doi.org/10.1021/acsbiomaterials.0c01429.

[120] J.T. Chung, M. Rafiei, Y. Chau, Self-adjuvanted L -arginine-modified dextran-based nanogels for sustained local antigenic protein delivery to antigen-presenting cells and enhanced cellular and humoral immune responses, Biomater. Sci. 12 (2024) 1771–1787, https://doi.org/10.1039/D3BM01150J.
[121] X. Chen, H. Li, W. Xu, K. Huang, B. Zhai, X. He, Self-assembling cyclodextrin-based nanoparticles enhance the cellular delivery of hydrophobic allicin, J. Agric. Food Chem. 68 (2020) 11144–11150, https://doi.org/10.1021/acs.jafc.0c01900.
[122] F. Topuz, M.E. Kilic, E. Durgun, G. Szekely, Fast-dissolving antibacterial nanofibers of cyclodextrin/antibiotic inclusion complexes for oral drug delivery, J. Colloid Interface Sci. 585 (2021) 184–194, https://doi.org/10.1016/j.jcis.2020.11.072.
[123] S. Li, R. Ma, X. Hu, H. Li, W. Geng, X. Kong, C. Zhang, D. Guo, Drug in drug: a host–guest formulation of azocalixarene with hydroxychloroquine for synergistic anti-inflammation, Adv. Mater. 34 (2022) 2203765, https://doi.org/10.1002/adma.202203765.
[124] L. Xu, J. Chai, Y. Wang, X. Zhao, D.-S. Guo, L. Shi, Z. Zhang, Y. Liu, Calixarene-integrated nano-drug delivery system for tumor-targeted delivery and tracking of anti-cancer drugs in vivo, Nano Res. 15 (2022) 7295–7303, https://doi.org/10.1007/s12274-022-4332-4.
[125] Y.I. Aleksandrova, D.N. Shurpik, V.A. Nazmutdinova, P.V. Zelenikhin, E. V. Subakaeva, E.A. Sokolova, Y.O. Leonteva, A.V. Mironova, A.R. Kayumov, V. S. Petrovskii, I.I. Potemkin, I.I. Stoikov, Antibacterial activity of various morphologies of films based on guanidine derivatives of pillar[5]arene: influence of the nature of one substitute on self-assembly, ACS Appl. Mater. Interfaces 16 (2024) 17163–17181, https://doi.org/10.1021/acsami.3c18610.
[126] H. Wang, Y.-Q. Yan, Y. Yi, Z.-Y. Wei, H. Chen, J.-F. Xu, H. Wang, Y. Zhao, X. Zhang, Supramolecular Peptide Therapeutics: Host–Guest Interaction-Assisted Systemic Delivery of Anticancer Peptides, 2020.
[127] F. Bröseler, C. Tietmann, C. Bommer, T. Drechsel, M. Heinzel-Gutenbrunner, S. Jepsen, Randomised clinical trial investigating self-assembling peptide P11-4 in the treatment of early caries, Clin. Oral Investig. 24 (2020) 123–132, https://doi.org/10.1007/s00784-019-02901-4.
[128] F. Gelain, Self-assembling peptide scaffolds in the clinic, Npj Regener, Med. 6(9) (2021), https://doi.org/10.1038/s41536-020-00116-w.
[129] R. Freeman, M. Han, Z. Álvarez, J.A. Lewis, J.R. Wester, N. Stephanopoulos, M. T. McClendon, C. Lynsky, J.M. Godbe, H. Sangji, E. Luijten, S.I. Stupp, Reversible self-assembly of superstructured networks, Science 362 (2018) 808–813, https://doi.org/10.1126/science.aat6141.
[130] L.-H. Chen, P.S. Doyle, Thermogelling hydroxypropyl methylcellulose nanoemulsions as templates to formulate poorly water-soluble drugs into oral thin films containing drug nanoparticles, Chem. Mater. 34 (2022) 5194–5205, https://doi.org/10.1021/acs.chemmater.2c00801.
[131] Z. Zhu, J. Wang, X. Pei, J. Chen, X. Wei, Y. Liu, P. Xia, Q. Wan, Z. Gu, Y. He, Blue-ringed octopus-inspired microneedle patch for robust tissue surface adhesion and active injection drug delivery, Sci. Adv. 9 (2023) eadh2213, https://doi.org/10.1126/sciadv.adh2213.
[132] S.S. Lee, T. Fyrner, F. Chen, Z. Álvarez, E. Sleep, D.S. Chun, J.A. Weiner, R. W. Cook, R.D. Freshman, M.S. Schallmo, K.M. Katchko, A.D. Schneider, J. T. Smith, C. Yun, G. Singh, S.Z. Hashmi, M.T. McClendon, Z. Yu, S.R. Stock, W. K. Hsu, E.L. Hsu, S.I. Stupp, Sulfated glycopeptide nanostructures for multipotent protein activation, Nat. Nanotechnol. 12 (2017) 821–829, https://doi.org/10.1038/nnano.2017.109.
[133] J. Bao, J. Wang, S. Chen, S. Liu, Z. Wang, W. Zhang, C. Zhao, Y. Sha, X. Yang, Y. Li, Y. Zhong, F. Bai, Coordination self-assembled AuTPyP-cu metal–organic framework nanosheets with pH/ultrasound dual-responsiveness for synergistically triggering cuproptosis-augmented chemotherapy, ACS Nano 18 (2024) 9100–9113, https://doi.org/10.1021/acsnano.3c13225.
[134] Z. Chen, Y. Wang, H. Chen, J. Law, H. Pu, S. Xie, F. Duan, Y. Sun, N. Liu, J. Yu, A magnetic multi-layer soft robot for on-demand targeted adhesion, Nat. Commun. 15 (2024) 644, https://doi.org/10.1038/s41467-024-44995-9.
[135] X. Liu, C. Steiger, S. Lin, G.A. Parada, J. Liu, H.F. Chan, H. Yuk, N.V. Phan, J. Collins, S. Tamang, G. Traverso, X. Zhao, Ingestible hydrogel device, Nat. Commun. 10 (2019) 493, https://doi.org/10.1038/s41467-019-08355-2.
[136] X. Jin, C. Wei, C. Wu, W. Zhang, Gastric fluid-induced double network hydrogel with high swelling ratio and long-term mechanical stability, Compos. Part B Eng. 236 (2022) 109816, https://doi.org/10.1016/j.compositesb.2022.109816.
[137] S.M. El-Hady, M.H.H. AbouGhaly, M.M. El-Ashmoony, H.S. Helmy, O.N. El-Gazayerly, Colon targeting of celecoxib nanomixed micelles using pulsatile drug delivery systems for the prevention of inflammatory bowel disease, Int. J. Pharm. 576 (2020) 118982, https://doi.org/10.1016/j.ijpharm.2019.118982.
[138] B. Leung, P. Dharmaratne, W. Yan, B.C.L. Chan, C.B.S. Lau, K.-P. Fung, M. Ip, S.S. Y. Leung, Development of thermosensitive hydrogel containing methylene blue for topical antimicrobial photodynamic therapy, J. Photochem. Photobiol. B 203 (2020) 111776, https://doi.org/10.1016/j.jphotobiol.2020.111776.
[139] A.M. Bellinger, M. Jafari, T.M. Grant, S. Zhang, H.C. Slater, E.A. Wenger, S. Mo, Y.-A.L. Lee, H. Mazdiyasni, L. Kogan, R. Barman, C. Cleveland, L. Booth, T. Bensel, D. Minahan, H.M. Hurowitz, T. Tai, J. Daily, B. Nikolic, L. Wood, P. A. Eckhoff, R. Langer, G. Traverso, Oral, ultra–long-lasting drug delivery: application toward malaria elimination goals, Sci. Transl. Med. 8 (2016), https://doi.org/10.1126/scitranslmed.aag2374.
[140] N. Salessiotis, Measurement of the diameter of the pylorus in man: Part I. Experimental project for clinical application, Am. J. Surg. 124 (1972) 331–333, https://doi.org/10.1016/0002-9610(72)90036-0.
[141] S. Babaee, S. Pajovic, A.R. Kirtane, J. Shi, E. Caffarel-Salvador, K. Hess, J. E. Collins, S. Tamang, A.V. Wahane, A.M. Hayward, H. Mazdiyasni, R. Langer, G. Traverso, Temperature-responsive biometamaterials for gastrointestinal applications, Sci. Transl. Med. 11 (2019) eaau8581, https://doi.org/10.1126/scitranslmed.aau8581.
[142] A.R. Kirtane, O. Abouzid, D. Minahan, T. Bensel, A.L. Hill, C. Selinger, A. Bershteyn, M. Craig, S.S. Mo, H. Mazdiyasni, C. Cleveland, J. Rogner, Y.-A. L. Lee, L. Booth, F. Javid, S.J. Wu, T. Grant, A.M. Bellinger, B. Nikolic, A. Hayward, L. Wood, P.A. Eckhoff, M.A. Nowak, R. Langer, G. Traverso, Development of an oral once-weekly drug delivery system for HIV antiretroviral therapy, Nat. Commun. 9 (2018) 2, https://doi.org/10.1038/s41467-017-02294-6.
[143] S. Wang, Y. Hou, S. Zhang, J. Li, Q. Chen, M. Yu, W. Li, Sustained antibacterial activity of berberine hydrochloride loaded supramolecular organoclay networks with hydrogen-bonding junctions, J. Mater. Chem. B 6 (2018) 4972–4984, https://doi.org/10.1039/C8TB01018H.
[144] M.T. Cook, P. Haddow, S.B. Kirton, W.J. McAuley, Polymers exhibiting lower critical solution temperatures as a route to thermoreversible gelators for healthcare, Adv. Funct. Mater. 31 (2021) 2008123, https://doi.org/10.1002/adfm.202008123.
[145] M. Carone, M.R. Spalinger, R.A. Gaultney, R. Mezzenga, K. Hlavačková, A. Mookhoek, P. Krebs, G. Rogler, P. Luciani, S. Aleandri, Temperature-triggered in situ forming lipid mesophase gel for local treatment of ulcerative colitis, Nat. Commun. 14 (2023) 3489, https://doi.org/10.1038/s41467-023-39013-3.
[146] R. Wang, X. Yao, T. Li, X. Li, M. Jin, Y. Ni, W. Yuan, X. Xie, L. Lu, M. Li, Reversible Thermoresponsive hydrogel fabricated from natural biopolymer for the improvement of critical limb ischemia by controlling release of stem cells, Adv. Healthcare Mater. 8 (2019) 1900967, https://doi.org/10.1002/adhm.201900967.
[147] R. Li, Y. Lyu, S. Luo, H. Wang, X. Zheng, L. Li, N. Ao, Z. Zha, Fabrication of a multi-level drug release platform with liposomes, chitooligosaccharides, phospholipids and injectable chitosan hydrogel to enhance anti-tumor effectiveness, Carbohydr. Polym. 269 (2021) 118322, https://doi.org/10.1016/j.carbpol.2021.118322.
[148] A.M. Piras, Y. Zambito, S. Burgalassi, D. Monti, S. Tampucci, E. Terreni, A. Fabiano, F. Balzano, G. Uccello-Barretta, P. Chetoni, A water-soluble, mucoadhesive quaternary ammonium chitosan-methyl-β-cyclodextrin conjugate forming inclusion complexes with dexamethasone, J. Mater. Sci. Mater. Med. 29 (2018) 42, https://doi.org/10.1007/s10856-018-6048-2.
[149] Y. Hu, S. Gao, H. Lu, J.Y. Ying, Acid-resistant and physiological pH-responsive DNA hydrogel composed of a-motif and i-motif toward oral insulin delivery, J. Am. Chem. Soc. 144 (2022) 5461–5470, https://doi.org/10.1021/jacs.1c13426.
[150] T. Koga, Y. Oatari, H. Motoda, S. Nishimura, Y. Sasaki, Y. Okamoto, D. Yamamoto, A. Shioi, N. Higashi, Star-shaped peptide–polymer hybrids as fast pH-responsive supramolecular hydrogels, 2022.
[151] J.P. Martins, D. Liu, F. Fontana, M.P.A. Ferreira, A. Correia, S. Valentino, M. Kemell, K. Moslova, E. Mäkilä, J. Salonen, J. Hirvonen, B. Sarmento, H. A. Santos, Microfluidic nanoassembly of bioengineered chitosan-modified FcRn-targeted porous silicon nanoparticles @ hypromellose acetate succinate for oral delivery of antidiabetic peptides, ACS Appl. Mater. Interfaces 10 (2018) 44354–44367, https://doi.org/10.1021/acsami.8b20821.
[152] Y. Xiang, H. Mao, S. Tong, C. Liu, R. Yan, L. Zhao, L. Zhu, C. Bao, A facile and versatile approach to construct photoactivated peptide hydrogels by regulating electrostatic repulsion, ACS Nano 17 (2023) 5536–5547, https://doi.org/10.1021/acsnano.2c10896.
[153] T. Liu, Y. Du, Y. Yan, S. Song, J. Qi, X. Xia, X. Hu, Q. Chen, J. Liu, X. Zeng, H. Zhao, pH-responsive dual-functional hydrogel integrating localized delivery and anti-cancer activities for highly effective therapy in PDX of OSCC, Mater. Today 62 (2023) 71–97, https://doi.org/10.1016/j.mattod.2022.12.009.
[154] J. Zhang, Y. Jiang, Y. Li, W. Li, J. Zhou, J. Chen, Z. Shang, Q. Gu, W. Wang, T. Shen, W. Hu, Micelles modified with a chitosan-derived homing peptide for targeted intracellular delivery of ginsenoside compound K to liver cancer cells, Carbohydr. Polym. 230 (2020) 115576, https://doi.org/10.1016/j.carbpol.2019.115576.
[155] M.A. Miller, S. Medina, Synthetic colonic mucus enables the development of modular microbiome organoids, Adv. Funct. Mater. 34 (2024) 2402514, https://doi.org/10.1002/adfm.202402514.
[156] A.C.M. Fernandes Patta, P.D. Mathews, R.R.M. Madrid, V.L.S. Rigoni, E.R. Silva, O. Mertins, Polyionic complexes of chitosan-N-arginine with alginate as pH responsive and mucoadhesive particles for oral drug delivery applications, Int. J. Biol. Macromol. 148 (2020) 550–564, https://doi.org/10.1016/j.ijbiomac.2020.01.160.
[157] V. Rahmani, Protein-alginate complexes as pH-/ion-sensitive carriers of proteins, Int. J. Pharm. (2018) 452–461, https://doi.org/10.1016/j.ijpharm.2017.11.039.
[158] F. Weinbreck, R. De Vries, P. Schrooyen, C.G. De Kruif, Complex coacervation of whey proteins and gum arabic, Biomacromolecules 4 (2003) 293–303, https://doi.org/10.1021/bm025667n.
[159] D. Samanta, N. Hosseini-Nassab, R.N. Zare, Electroresponsive nanoparticles for drug delivery on demand, Nanoscale 8 (2016) 9310–9317, https://doi.org/10.1039/C6NR01884J.
[160] Y. Deng, M. Huang, D. Sun, Y. Hou, Y. Li, T. Dong, X. Wang, L. Zhang, W. Yang, Dual physically cross-linked κ-carrageenan-based double network hydrogels with superior self-healing performance for biomedical application, ACS Appl. Mater. Interfaces 10 (2018) 37544–37554, https://doi.org/10.1021/acsami.8b15385.
[161] M.C. García, Ionic-strength-responsive polymers for drug delivery applications, 2019, pp. 393–409, https://doi.org/10.1016/B978-0-08-101995-5.00014-3.
[162] G. Geyik, N. Işıklan, Design and fabrication of hybrid triple-responsive κ-carrageenan-based nanospheres for controlled drug delivery, Int. J. Biol.

Macromol. 192 (2021) 701–715, https://doi.org/10.1016/j.ijbiomac.2021.10.007.
[163] J. Ye, L. Liu, W. Lan, J. Xiong, Targeted release of soybean peptide from CMC/PVA hydrogels in simulated intestinal fluid and their pharmacokinetics, Carbohydr. Polym. 310 (2023) 120713, https://doi.org/10.1016/j.carbpol.2023.120713.
[164] S. Ji, R. Sun, W. Wang, Q. Xia, Preparation, characterization, and evaluation of tamarind seed polysaccharide-carboxymethylcellulose buccal films loaded with soybean peptides-chitosan nanoparticles, Food Hydrocoll. 141 (2023) 108684, https://doi.org/10.1016/j.foodhyd.2023.108684.
[165] L. Chen, L. Gruzinskyte, S.L. Jørgensen, A. Boisen, S.K. Srivastava, An ingestible self-polymerizing system for targeted sampling of gut microbiota and biomarkers, ACS Nano 14 (2020) 12072–12081, https://doi.org/10.1021/acsnano.0c05426.
[166] E.A. Günter, D.S. Khramova, P.A. Markov, O.V. Popeyko, A.K. Melekhin, V. S. Beloserov, E.A. Martinson, S.G. Litvinets, S.V. Popov, Swelling behavior and satiating effect of the gel microparticles obtained from callus cultures pectins, Int. J. Biol. Macromol. 123 (2019) 300–307, https://doi.org/10.1016/j.ijbiomac.2018.11.081.
[167] M. Tollemeto, Z. Huang, J.B. Christensen, H. Mørck Nielsen, S. Rønholt, Mucoadhesive dendrons conjugated to mesoporous silica nanoparticles as a drug delivery approach for orally administered biopharmaceuticals, ACS Appl. Mater. Interfaces 15 (2023) 8798–8810, https://doi.org/10.1021/acsami.2c16502.
[168] R. Zhao, S. Du, Y. Liu, C. Lv, Y. Song, X. Chen, B. Zhang, D. Li, S. Gao, W. Cui, M. V. Plikus, X. Hou, K. Wu, Z. Liu, Z. Liu, Y. Cong, Y. Li, Z. Yu, Mucoadhesive-to-penetrating controllable peptosomes-in-microspheres co-loaded with anti-miR-31 oligonucleotide and curcumin for targeted colorectal cancer therapy, Theranostics 10 (2020) 3594–3611, https://doi.org/10.7150/thno.40318.
[169] N. Liao, B. Pang, H. Jin, X. Zhao, D. Shao, C. Jiang, J. Shi, Modifications of *ganoderma lucidum* spores into digestive-tissue highly adherent porous carriers with selective affinity to hydrophilic or hydrophobic drugs, Biomaterials 299 (2023) 122177, https://doi.org/10.1016/j.biomaterials.2023.122177.
[170] C. Villequey, S.S. Zurmühl, C.N. Cramer, B. Bhusan, B. Andersen, Q. Ren, H. Liu, X. Qu, Y. Yang, J. Pan, Q. Chen, M. Münzel, An efficient mRNA display protocol yields potent bicyclic peptide inhibitors for FGFR3c: outperforming linear and monocyclic formats in affinity and stability, Chem. Sci. 15 (2024) 6122–6129, https://doi.org/10.1039/D3SC04763F.
[171] X. Gao, J. Li, J. Li, M. Zhang, J. Xu, Pain-free oral delivery of biologic drugs using intestinal peristalsis–actuated microneedle robots, Sci. Adv. 10 (2024) eadj7067, https://doi.org/10.1126/sciadv.adj7067.
[172] X. Zhang, G. Chen, X. Fu, Y. Wang, Y. Zhao, Magneto-responsive microneedle robots for intestinal macromolecule delivery, Adv. Mater. 33 (2021) 2104932, https://doi.org/10.1002/adma.202104932.
[173] A. Ghosh, W. Liu, L. Li, G.J. Pahapale, S.Y. Choi, L. Xu, Q. Huang, R. Zhang, Z. Zhong, F.M. Selaru, D.H. Gracias, Autonomous untethered microinjectors for gastrointestinal delivery of insulin, ACS Nano 16 (2022) 16211–16220, https://doi.org/10.1021/acsnano.2c05098.
[174] L. Cai, G. Chen, L. Sun, S. Miao, L. Shang, Y. Zhao, L. Sun, Rocket-inspired effervescent motors for oral macromolecule delivery, Adv. Mater. 35 (2023) 2210679, https://doi.org/10.1002/adma.202210679.
[175] R. Pugliese, C. Bollati, F. Gelain, A. Arnoldi, C. Lammi, A supramolecular approach to develop new soybean and lupin peptide nanogels with enhanced dipeptidyl peptidase IV (DPP-IV) inhibitory activity, J. Agric. Food Chem. 67 (2019) 3615–3623, https://doi.org/10.1021/acs.jafc.8b07264.
[176] F. Yang, Z. Wang, D. Zhao, L. Hu, S. Cui, L. Chen, T. Guo, P. Pan, J. Chen, Food-derived *Crassostrea gigas* peptides self-assembled supramolecules for scarless healing, Compos. Part B 246 (2022) 110265, https://doi.org/10.1016/j.compositesb.2022.110265.
[177] D.-B. Cheng, X.-H. Zhang, Y.-J. Gao, L. Ji, D. Hou, Z. Wang, W. Xu, Z.-Y. Qiao, H. Wang, Endogenous reactive oxygen species-triggered morphology transformation for enhanced cooperative interaction with mitochondria, J. Am. Chem. Soc. 141 (2019) 7235–7239, https://doi.org/10.1021/jacs.8b07727.
[178] I. Insua, J. Montenegro, 1D to 2D self assembly of cyclic peptides, J. Am. Chem. Soc. 142 (2020) 300–307, https://doi.org/10.1021/jacs.9b10582.
[179] M. Wang, J. Wang, P. Zhou, J. Deng, Y. Zhao, Y. Sun, W. Yang, D. Wang, Z. Li, X. Hu, S.M. King, S.E. Rogers, H. Cox, T.A. Waigh, J. Yang, J.R. Lu, H. Xu, Nanoribbons self-assembled from short peptides demonstrate the formation of polar zippers between β-sheets, Nat. Commun. 9 (2018) 5118, https://doi.org/10.1038/s41467-018-07583-2.
[180] Y. Zhao, W. Yang, D. Wang, J. Wang, Z. Li, X. Hu, S. King, S. Rogers, J.R. Lu, H. Xu, Controlling the diameters of nanotubes self-assembled from designed peptide bolaphiles, Small 14 (2018) 1703216, https://doi.org/10.1002/smll.201703216.
[181] Y. Liu, C.S. Gong, Y. Dai, Z. Yang, G. Yu, Y. Liu, M. Zhang, L. Lin, W. Tang, Z. Zhou, G. Zhu, J. Chen, O. Jacobson, D.O. Kiesewetter, Z. Wang, X. Chen, In situ polymerization on nanoscale metal-organic frameworks for enhanced physiological stability and stimulus-responsive intracellular drug delivery, Biomaterials 218 (2019) 119365, https://doi.org/10.1016/j.biomaterials.2019.119365.
[182] H. Iyer, A. Khedkar, M. Verma, Oral insulin – a review of current status, diabetes, Obes. Metab. 12 (2010) 179–185, https://doi.org/10.1111/j.1463-1326.2009.01150.x.
[183] A. Lerner, T. Matthias, Changes in intestinal tight junction permeability associated with industrial food additives explain the rising incidence of autoimmune disease, Autoimmun. Rev. 14 (2015) 479–489, https://doi.org/10.1016/j.autrev.2015.01.009.
[184] S. Maher, R.J. Mrsny, D.J. Brayden, Intestinal permeation enhancers for oral peptide delivery, Adv. Drug Deliv. Rev. 106 (2016) 277–319, https://doi.org/10.1016/j.addr.2016.06.005.
[185] F. McCartney, J.P. Gleeson, D.J. Brayden, Safety concerns over the use of intestinal permeation enhancers: a mini-review, Tissue Barriers 4 (2016) e1176822, https://doi.org/10.1080/21688370.2016.1176822.
[186] A. Horowitz, S.D. Chanez-Paredes, X. Haest, J.R. Turner, Paracellular permeability and tight junction regulation in gut health and disease, Nat. Rev. Gastroenterol. Hepatol. 20 (2023) 417–432, https://doi.org/10.1038/s41575-023-00766-3.
[187] B.R. Stevenson, J.D. Siliciano, M.S. Mooseker, D.A. Goodenough, Identification of ZO-1: a high molecular weight polypeptide associated with the tight junction (zonula occludens) in a variety of epithelia, J. Cell Biol. 103 (1986) 755–766, https://doi.org/10.1083/jcb.103.3.755.
[188] M. Furuse, K. Fujita, T. Hiiragi, K. Fujimoto, S. Tsukita, Claudin-1 and -2: novel integral membrane proteins localizing at tight junctions with no sequence similarity to occludin, J. Cell Biol. 141 (1998) 1539–1550, https://doi.org/10.1083/jcb.141.7.1539.
[189] M. Furuse, T. Hirase, M. Itoh, A. Nagafuchi, S. Yonemura, S. Tsukita, S. Tsukita, Occludin: a novel integral membrane protein localizing at tight junctions, J. Cell Biol. 123 (1993) 1777–1788, https://doi.org/10.1083/jcb.123.6.1777.
[190] K. Mineta, Y. Yamamoto, Y. Yamazaki, H. Tanaka, Y. Tada, K. Saito, A. Tamura, M. Igarashi, T. Endo, K. Takeuchi, S. Tsukita, Predicted expansion of the claudin multigene family, FEBS Lett. 585 (2011) 606–612, https://doi.org/10.1016/j.febslet.2011.01.028.
[191] C. Li, L. Yuan, X. Zhang, A. Zhang, Y. Pan, Y. Wang, W. Qu, H. Hao, S.A. Algharib, D. Chen, S. Xie, Core-shell nanosystems designed for effective oral delivery of polypeptide drugs, J. Control. Release 352 (2022) 540–555, https://doi.org/10.1016/j.jconrel.2022.10.031.
[192] Z. Dong, L. Zhang, G. Li, Y. Li, H. He, Y. Lu, W. Wu, J. Qi, Mechanism and performance of choline-based ionic liquids in enhancing nasal delivery of glucagon, J. Control. Release 375 (2024) 812–828, https://doi.org/10.1016/j.jconrel.2024.09.035.
[193] X. Jiang, D. Pan, M. Tao, T. Zhang, X. Zeng, Z. Wu, Y. Guo, New nanocarrier system for liposomes coated with *lactobacillus acidophilus* S-layer protein to improve leu–gln–pro–glu absorption through the intestinal epithelium, J. Agric. Food Chem. 69 (2021) 7593–7602, https://doi.org/10.1021/acs.jafc.1c01498.
[194] L. Wang, Q. Liu, X. Hu, C. Zhou, Y. Ma, X. Wang, Y. Tang, K. Chen, X. Wang, Y. Liu, Enhanced oral absorption and liver distribution of polymeric nanoparticles through traveling the enterohepatic circulation pathways of bile acid, ACS Appl. Mater. Interfaces 14 (2022) 41712–41725, https://doi.org/10.1021/acsami.2c10322.
[195] X. Bao, K. Qian, M. Xu, Y. Chen, H. Wang, T. Pan, Z. Wang, P. Yao, L. Lin, Intestinal epithelium penetration of liraglutide via cholic acid pre-complexation and zein/rhamnolipids nanocomposite delivery, J. Nanobiotechnol. 21 (2023) 16, https://doi.org/10.1186/s12951-022-01743-9.
[196] A.S. Chowdhury, R.G. Bai, T. Islam, M. Abir, M. Narayan, Z. Khatun, M. Nurunnabi, Bile acid linked β-glucan nanoparticles for liver specific oral delivery of biologics, Biomater. Sci. 10 (2022) 2929–2939. https://pubs.rsc.org/en/content/articlehtml/2022/bm/d2bm00316c (accessed April 25, 2024).
[197] S.M.S. Shahriar, J.M. An, M.N. Hasan, S.S. Surwase, Y.-C. Kim, D.Y. Lee, S. Cho, Y. Lee, Plasmid DNA nanoparticles for nonviral oral gene therapy, Nano Lett. 21 (2021) 4666–4675, https://doi.org/10.1021/acs.nanolett.1c00832.
[198] W. Fan, D. Xia, Q. Zhu, X. Li, S. He, C. Zhu, S. Guo, L. Hovgaard, M. Yang, Y. Gan, Functional nanoparticles exploit the bile acid pathway to overcome multiple barriers of the intestinal epithelium for oral insulin delivery, Biomaterials 151 (2018) 13–23, https://doi.org/10.1016/j.biomaterials.2017.10.022.
[199] B. Xiao, Q. Chen, Z. Zhang, L. Wang, Y. Kang, T. Denning, D. Merlin, TNFα gene silencing mediated by orally targeted nanoparticles combined with interleukin-22 for synergistic combination therapy of ulcerative colitis, J. Control. Release 287 (2018) 235–246, https://doi.org/10.1016/j.jconrel.2018.08.021.
[200] A. Ramesh, A. Brouillard, S. Kumar, D. Nandi, A. Kulkarni, Dual inhibition of CSF1R and MAPK pathways using supramolecular nanoparticles enhances macrophage immunotherapy, Biomaterials 227 (2020) 119559, https://doi.org/10.1016/j.biomaterials.2019.119559.
[201] Q. Yu, T. Deng, F.-C. Lin, B. Zhang, J.I. Zink, Supramolecular assemblies of heterogeneous mesoporous silica nanoparticles to co-deliver antimicrobial peptides and antibiotics for synergistic eradication of pathogenic biofilms, ACS Nano 14 (2020) 5926–5937, https://doi.org/10.1021/acsnano.0c01336.
[202] Y.-L. Liang, M. Khoshouei, A. Glukhova, S.G.B. Furness, P. Zhao, L. Clydesdale, C. Koole, T.T. Truong, D.M. Thal, S. Lei, M. Radjainia, R. Danev, W. Baumeister, M.-W. Wang, L.J. Miller, A. Christopoulos, P.M. Sexton, D. Wootten, Phase-plate cryo-EM structure of a biased agonist-bound human GLP-1 receptor–gs complex, Nature 555 (2018) 121–125, https://doi.org/10.1038/nature25773.
[203] B.P. Cary, G. Deganutti, P. Zhao, T.T. Truong, S.J. Piper, X. Liu, M.J. Belousoff, R. Danev, P.M. Sexton, D. Wootten, S.H. Gellman, Structural and functional diversity among agonist-bound states of the GLP-1 receptor, Nat. Chem. Biol. 18 (2022) 256–263, https://doi.org/10.1038/s41589-021-00945-w.
[204] H. Fan, N. Gong, T.-F. Li, A.-N. Ma, X.-Y. Wu, M.-W. Wang, Y.-X. Wang, The non-peptide GLP-1 receptor agonist WB4-24 blocks inflammatory nociception by stimulating β-endorphin release from spinal microglia, Br. J. Pharmacol. 172 (2015) 64–79, https://doi.org/10.1111/bph.12895.
[205] B. Xu, S.-L. Chen, Y. Zhang, B. Li, Q. Yuan, W. Gan, Evaluating the cross-membrane dynamics of a charged molecule on lipid films with different surface curvature, J. Colloid Interface Sci. 610 (2022) 376–384, https://doi.org/10.1016/j.jcis.2021.12.015.

[206] X. Xie, B. Gao, Z. Ma, J. Liu, J. Zhang, J. Liang, Z. Chen, L. Wu, W. Li, Host–guest interaction driven peptide assembly into photoresponsive two-dimensional nanosheets with switchable antibacterial activity, CCS Chem. 3 (2021) 1949–1962, https://doi.org/10.31635/ccschem.020.202000312.
[207] V.A. Bzik, D.J. Brayden, An assessment of the permeation enhancer, 1-phenylpiperazine (PPZ), on paracellular flux across rat intestinal mucosae in ussing chambers, Pharm. Res. 33 (2016) 2506–2516, https://doi.org/10.1007/s11095-016-1975-4.
[208] H. Weng, L. Hu, L. Hu, Y. Zhou, A. Wang, N. Wang, W. Li, C. Zhu, S. Guo, M. Yu, Y. Gan, The complexation of insulin with sodium *N*-[8-(2-hydroxybenzoyl) amino]-caprylate for enhanced oral delivery: effects of concentration, ratio, and pH, Chin. Chem. Lett. 33 (2022) 1889–1894, https://doi.org/10.1016/j.cclet.2021.10.023.
[209] K.C. Fein, N.G. Lamson, K.A. Whitehead, Structure-function analysis of phenylpiperazine derivatives as intestinal permeation enhancers, Pharm. Res. 34 (2017) 1320–1329, https://doi.org/10.1007/s11095-017-2149-8.
[210] H. Tran, E. Aihara, F.A. Mohammed, H. Qu, A. Riley, Y. Su, X. Lai, S. Huang, A. Aburub, J.J.H. Chen, O.H. Vitale, Y. Lao, S. Estwick, Z. Qi, M.E.H. ElSayed, In vivo mechanism of action of sodium caprate for improving the intestinal absorption of a GLP1/GIP coagonist peptide, Mol. Pharm. 20 (2023) 929–941, https://doi.org/10.1021/acs.molpharmaceut.2c00443.
[211] N.G. Lamson, A. Berger, K.C. Fein, K.A. Whitehead, Anionic nanoparticles enable the oral delivery of proteins by enhancing intestinal permeability, Nat. Biomed. Eng. 4 (2019) 84–96, https://doi.org/10.1038/s41551-019-0465-5.
[212] R.R. Marchelletta, M. Krishnan, M.R. Spalinger, T.W. Placone, R. Alvarez, A. Sayoc-Becerra, V. Canale, A. Shawki, Y.S. Park, L.H.P. Bernts, S. Myers, M. L. Tremblay, K.E. Barrett, E. Krystofiak, B. Kachar, D.P.B. McGovern, C.R. Weber, E.M. Hanson, L. Eckmann, D.F. McCole, T cell protein tyrosine phosphatase protects intestinal barrier function by restricting epithelial tight junction remodeling, J. Clin. Invest. 131 (2021), https://doi.org/10.1172/JCI138230.
[213] A.J. Harmar, Family-B G-protein-coupled receptors, Genome Biol. 2 (2001), https://doi.org/10.1186/gb-2001-2-12-reviews3013. REVIEWS3013.
[214] HUGO Gene Nomenclature Committee. https://www.genenames.org/, 2025 (accessed March 12, 2024).
[215] S.P. Alexander, A. Christopoulos, A.P. Davenport, E. Kelly, N.V. Marrion, J. A. Peters, E. Faccenda, S.D. Harding, A.J. Pawson, J.L. Sharman, C. Southan, J. A. Davies, C. Collaborators, THE CONCISE GUIDE TO PHARMACOLOGY 2017/18: G protein-coupled receptors, Br. J. Pharmacol. 174 (2017) S17–S129, https://doi.org/10.1111/bph.13878.
[216] K. Lewis, C. Li, M.H. Perrin, A. Blount, K. Kunitake, C. Donaldson, J. Vaughan, T. M. Reyes, J. Gulyas, W. Fischer, L. Bilezikjian, J. Rivier, P.E. Sawchenko, W. W. Vale, Identification of urocortin III, an additional member of the corticotropin-releasing factor (CRF) family with high affinity for the CRF2 receptor, Proc. Natl. Acad. Sci. 98 (2001) 7570–7575, https://doi.org/10.1073/pnas.121165198.
[217] F.M. Dautzenberg, G. Py-Lang, J. Higelin, C. Fischer, M.B. Wright, G. Huber, Different binding modes of amphibian and human corticotropin-releasing factor type 1 and type 2 receptors: evidence for evolutionary differences, J. Pharmacol. Exp. Ther. 296 (2001) 113–120.
[218] F.M. Dautzenberg, E. Gutknecht, I. Van der Linden, J.A. Olivares-Reyes, F. Dürrenberger, R.L. Hauger, Cell-type specific calcium signaling by corticotropin-releasing factor type 1 (CRF1) and 2a (CRF2(a)) receptors: phospholipase C-mediated responses in human embryonic kidney 293 but not SK-N-MC neuroblastoma cells, Biochem. Pharmacol. 68 (2004) 1833–1844, https://doi.org/10.1016/j.bcp.2004.07.013.
[219] R. Chen, K.A. Lewis, M.H. Perrin, W.W. Vale, Expression cloning of a human corticotropin-releasing-factor receptor, Proc. Natl. Acad. Sci. USA 90 (1993) 8967–8971, https://doi.org/10.1073/pnas.90.19.8967.
[220] T.M. Reyes, K. Lewis, M.H. Perrin, K.S. Kunitake, J. Vaughan, C.A. Arias, J. B. Hogenesch, J. Gulyas, J. Rivier, W.W. Vale, P.E. Sawchenko, Urocortin II: a member of the corticotropin-releasing factor (CRF) neuropeptide family that is selectively bound by type 2 CRF receptors, Proc. Natl. Acad. Sci. USA 98 (2001) 2843–2848, https://doi.org/10.1073/pnas.051626398.
[221] M.E. Dunbar, P.R. Dann, G.W. Robinson, L. Hennighausen, J.-P. Zhang, J. J. Wysolmerski, Parathyroid hormone-related protein signaling is necessary for sexual dimorphism during embryonic mammary development, Development 126 (1999) 3485–3493, https://doi.org/10.1242/dev.126.16.3485.
[222] J.J. Wysolmerski, W.M. Philbrick, M.E. Dunbar, B. Lanske, H. Kronenberg, A. Karaplis, A.E. Broadus, Rescue of the parathyroid hormone-related protein knockout mouse demonstrates that parathyroid hormone-related protein is essential for mammary gland development, Development 125 (1998) 1285–1294, https://doi.org/10.1242/dev.125.7.1285.
[223] Y. Nishimura, T. Esaki, Y. Isshiki, Y. Furuta, A. Mizutani, T. Kotake, T. Emura, Y. Watanabe, M. Ohta, T. Nakagawa, K. Ogawa, S. Arai, H. Noda, H. Kitamura, M. Shimizu, T. Tamura, H. Sato, Lead optimization and avoidance of reactive metabolite leading to PCO371, a potent, selective, and orally available human parathyroid hormone receptor 1 (hPTHR1) agonist, J. Med. Chem. 63 (2020) 5089–5099, https://doi.org/10.1021/acs.jmedchem.9b01743.
[224] M. Okazaki, S. Ferrandon, J.-P. Vilardaga, M.L. Bouxsein, J.T. Potts, T.J. Gardella, Prolonged signaling at the parathyroid hormone receptor by peptide ligands targeted to a specific receptor conformation, Proc. Natl. Acad. Sci. USA 105 (2008) 16525–16530, https://doi.org/10.1073/pnas.0808750105.
[225] T.J. Gardella, M.D. Luck, A.K. Wilson, H.T. Keutmann, S.R. Nussbaum, J.T. Potts, H.M. Kronenberg, Parathyroid hormone (PTH)-PTH-related peptide hybrid peptides reveal functional interactions between the 1-14 and 15-34 domains of the ligand, J. Biol. Chem. 270 (1995) 6584–6588, https://doi.org/10.1074/jbc.270.12.6584.
[226] K.B. Jonsson, M.R. John, R.C. Gensure, T.J. Gardella, H. Jüppner, Tuberoinfundibular peptide 39 binds to the parathyroid hormone (PTH)/PTH-related peptide receptor, but functions as an antagonist, Endocrinology 142 (2001) 704–709, https://doi.org/10.1210/endo.142.2.7945.
[227] T.B. Usdin, T. Wang, S.R.J. Hoare, É. Mezey, M. Palkovits, New members of the parathyroid hormone/parathyroid hormone receptor family: the parathyroid hormone 2 receptor and tuberoinfundibular peptide of 39 residues, Front. Neuroendocrinol. 21 (2000) 349–383, https://doi.org/10.1006/frne.2000.0203.
[228] C.P. Goold, T.B. Usdin, S.R. Hoare, Regions in rat and human parathyroid hormone (PTH) 2 receptors controlling receptor interaction with PTH and with antagonist ligands, J. Pharmacol. Exp. Ther. 299 (2001) 678–690.
[229] S.R. Hoare, J.A. Clark, T.B. Usdin, Molecular determinants of tuberoinfundibular peptide of 39 residues (TIP39) selectivity for the parathyroid hormone-2 (PTH2) receptor. N-terminal truncation of TIP39 reverses PTH2 receptor/PTH1 receptor binding selectivity, J. Biol. Chem. 275 (2000) 27274–27283, https://doi.org/10.1074/jbc.M003910200.
[230] D.J. Drucker, D. Bastille, B. Goke, K.E. Mayo, L.J. Miller, B. Thorens, The glucagon receptor family, in: The IUPHAR Receptor Compendium of Receptor Characterization and Classification, Nightingale Press, London, 2000, pp. 209–226.
[231] B.K. Chow, Molecular cloning and functional characterization of a human secretin receptor, Biochem. Biophys. Res. Commun. 212 (1995) 204–211, https://doi.org/10.1006/bbrc.1995.1957.
[232] M. Xia, S.P. Sreedharan, D.R. Bolin, G.O. Gaufo, E.J. Goetzl, Novel cyclic peptide agonist of high potency and selectivity for the type II vasoactive intestinal peptide receptor, J. Pharmacol. Exp. Ther. 281 (1997) 629–633.
[233] P. Gaudin, A. Couvineau, J.J. Maoret, C. Rouyer-Fessard, M. Laburthe, Stable expression of the recombinant human VIP1 receptor in clonal Chinese hamster ovary cells: pharmacological, functional and molecular properties, Eur. J. Pharmacol. 302 (1996) 207–214, https://doi.org/10.1016/0014-2999(96)00096-9.
[234] S.P. Sreedharan, D.R. Patel, M. Xia, S. Ichikawa, E.J. Goetzl, Human vasoactive intestinal peptide1 receptors expressed by stable transfectants couple to two distinct signaling pathways, Biochem. Biophys. Res. Commun. 203 (1994) 141–148, https://doi.org/10.1006/bbrc.1994.2160.
[235] S. Shen, C. Spratt, W.J. Sheward, I. Kallo, K. West, C.F. Morrison, C.W. Coen, H. M. Marston, A.J. Harmar, Overexpression of the human VPAC2 receptor in the suprachiasmatic nucleus alters the circadian phenotype of mice, Proc. Natl. Acad. Sci. 97 (2000) 11575–11580, https://doi.org/10.1073/pnas.97.21.11575.
[236] P. Nicole, L. Lins, C. Rouyer-Fessard, C. Drouot, P. Fulcrand, A. Thomas, A. Couvineau, J. Martinez, R. Brasseur, M. Laburthe, Identification of key residues for interaction of vasoactive intestinal peptide with human VPAC1 and VPAC2 receptors and development of a highly selective VPAC1 receptor agonist. Alanine scanning and molecular modeling of the peptide, J. Biol. Chem. 275 (2000) 24003–24012, https://doi.org/10.1074/jbc.M002325200.
[237] L. Dickson, I. Aramori, J. McCulloch, J. Sharkey, K. Finlayson, A systematic comparison of intracellular cyclic AMP and calcium signalling highlights complexities in human VPAC/PAC receptor pharmacology, Neuropharmacology 51 (2006) 1086–1098, https://doi.org/10.1016/j.neuropharm.2006.07.017.
[238] T.W. Moody, R.T. Jensen, M. Fridkin, I. Gozes, (N-stearyl, norleucine17) VIPhybrid is a broad spectrum vasoactive intestinal peptide receptor antagonist, J. Mol. Neurosci.: MN 18 (2002) 29–35, https://doi.org/10.1385/JMN:18:1-2:29.
[239] C. Otto, Y. Kovalchuk, D.P. Wolfer, P. Gass, M. Martin, W. Zuschratter, H. J. Gröne, C. Kellendonk, F. Tronche, R. Maldonado, H.-P. Lipp, A. Konnerth, G. Schütz, Impairment of mossy fiber long-term potentiation and associative learning in pituitary adenylate cyclase activating polypeptide type I receptor-deficient mice, J. Neurosci. 21 (2001) 5520–5527, https://doi.org/10.1523/JNEUROSCI.21-15-05520.2001.
[240] C. Otto, M. Martin, D. Paul Wolfer, H.-P. Lipp, R. Maldonado, G. Schütz, Altered emotional behavior in PACAP-type-I-receptor-deficient mice, Mol. Brain Res. 92 (2001) 78–84, https://doi.org/10.1016/S0169-328X(01)00153-X.
[241] J. Hannibal, F. Jamen, H.S. Nielsen, L. Journot, P. Brabet, J. Fahrenkrug, Dissociation between light-induced phase shift of the circadian rhythm and clock gene expression in mice lacking the pituitary adenylate cyclase activating polypeptide type 1 receptor, J. Neurosci. 21 (2001) 4883–4890, https://doi.org/10.1523/JNEUROSCI.21-13-04883.2001.
[242] H. Jongsma, L.M.E. Pettersson, Y. Zhang, M.K. Reimer, M. Kanje, A. Waldenström, F. Sundler, N. Danielsen, Markedly reduced chronic nociceptive response in mice lacking the PAC1 receptor, Neuroreport 12 (2001) 2215–2219.
[243] F. Jamen, K. Persson, G. Bertrand, N. Rodriguez-Henche, R. Puech, J. Bockaert, B. Ahrén, P. Brabet, PAC1 receptor–deficient mice display impaired insulinotropic response to glucose and reduced glucose tolerance, J. Clin. Invest. 105 (2000) 1307–1315, https://doi.org/10.1172/JCI9387.
[244] F.M. Dautzenberg, G. Mevenkamp, S. Wille, R.L. Hauger, N-terminal splice variants of the type I PACAP receptor: isolation, characterization and ligand binding/selectivity determinants, J. Neuroendocrinol. 11 (1999) 941–949, https://doi.org/10.1046/j.1365-2826.1999.00411.x.
[245] S. Buchholz, A.V. Schally, J.B. Engel, F. Hohla, E. Heinrich, F. Koester, J.L. Varga, G. Halmos, Potentiation of mammary cancer inhibition by combination of antagonists of growth hormone-releasing hormone with docetaxel, Proc. Natl. Acad. Sci. USA 104 (2007) 1943–1946, https://doi.org/10.1073/pnas.0610860104.
[246] R. Cai, A.V. Schally, T. Cui, L. Szalontay, G. Halmos, W. Sha, M. Kovacs, M. Jaszberenyi, J. He, F.G. Rick, P. Popovics, R. Kanashiro-Takeuchi, J.M. Hare, N.L. Block, M. Zarandi, Synthesis of new potent agonistic analogs of growth hormone-releasing hormone (GHRH) and evaluation of their endocrine and

cardiac activities, Peptides 52 (2014) 104–112, https://doi.org/10.1016/j.peptides.2013.12.010.
[247] S.L. Pohl, L. Birnbaumer, M. Rodbell, Glucagon-sensitive adenyl cylase in plasma membrane of hepatic parenchymal cells, Sci. (N.Y.) 164 (1969) 566–567, https://doi.org/10.1126/science.164.3879.566.
[248] H. Zhang, A. Qiao, L. Yang, N. Van Eps, K.S. Frederiksen, D. Yang, A. Dai, X. Cai, H. Zhang, C. Yi, C. Cao, L. He, H. Yang, J. Lau, O.P. Ernst, M.A. Hanson, R. C. Stevens, M.-W. Wang, S. Reedtz-Runge, H. Jiang, Q. Zhao, B. Wu, Structure of the glucagon receptor in complex with a glucagon analogue, Nature 553 (2018) 106–110, https://doi.org/10.1038/nature25153.
[249] R. Jorgensen, L. Martini, T.W. Schwartz, C.E. Elling, Characterization of glucagon-like peptide-1 receptor beta-arrestin 2 interaction: a high-affinity receptor phenotype, Mol. Endocrinol. (Baltim. Md,) 19 (2005) 812–823, https://doi.org/10.1210/me.2004-0312.
[250] U. Werner, G. Haschke, A.W. Herling, W. Kramer, Pharmacological profile of lixisenatide: a new GLP-1 receptor agonist for the treatment of type 2 diabetes, Regul. Pept. 164 (2010) 58–64, https://doi.org/10.1016/j.regpep.2010.05.008.
[251] J. Lau, P. Bloch, L. Schäffer, I. Pettersson, J. Spetzler, J. Kofoed, K. Madsen, L. B. Knudsen, J. McGuire, D.B. Steensgaard, H.M. Strauss, D.X. Gram, S. M. Knudsen, F.S. Nielsen, P. Thygesen, S. Reedtz-Runge, T. Kruse, Discovery of the once-weekly glucagon-like peptide-1 (GLP-1) analogue semaglutide, J. Med. Chem. 58 (2015) 7370–7380, https://doi.org/10.1021/acs.jmedchem.5b00726.
[252] L.B. Knudsen, P.F. Nielsen, P.O. Huusfeldt, N.L. Johansen, K. Madsen, F. Z. Pedersen, H. Thøgersen, M. Wilken, H. Agersø, Potent derivatives of glucagon-like peptide-1 with pharmacokinetic properties suitable for once daily administration, J. Med. Chem. 43 (2000) 1664–1669, https://doi.org/10.1021/jm9909645.
[253] L.L. Baggio, Q. Huang, T.J. Brown, D.J. Drucker, A recombinant human glucagon-like peptide (GLP)-1-albumin protein (albugon) mimics peptidergic activation of GLP-1 receptor-dependent pathways coupled with satiety, gastrointestinal motility, and glucose homeostasis, Diabetes 53 (2004) 2492–2500, https://doi.org/10.2337/diabetes.53.9.2492.
[254] A. Jazayeri, M. Rappas, A.J.H. Brown, J. Kean, J.C. Errey, N.J. Robertson, C. Fiez-Vandal, S.P. Andrews, M. Congreve, A. Bortolato, J.S. Mason, A.H. Baig, I. Teobald, A.S. Doré, M. Weir, R.M. Cooke, F.H. Marshall, Crystal structure of the GLP-1 receptor bound to a peptide agonist, Nature 546 (2017) 254–258, https://doi.org/10.1038/nature22800.
[255] D.A. Griffith, D.J. Edmonds, J.-P. Fortin, A.S. Kalgutkar, J.B. Kuzmiski, P. M. Loria, A.R. Saxena, S.W. Bagley, C. Buckeridge, J.M. Curto, D.R. Derksen, J. M. Dias, M.C. Griffor, S. Han, V.M. Jackson, M.S. Landis, D. Lettiere, C. Limberakis, Y. Liu, A.M. Mathiowetz, J.C. Patel, D.W. Piotrowski, D.A. Price, R. B. Ruggeri, D.A. Tess, A small-molecule oral agonist of the human glucagon-like peptide-1 receptor, J. Med. Chem. 65 (2022) 8208–8226, https://doi.org/10.1021/acs.jmedchem.1c01856.
[256] J.P. Raufman, L. Singh, J. Eng, Exendin-3, a novel peptide from *heloderma horridum* venom, interacts with vasoactive intestinal peptide receptors and a newly described receptor on dispersed acini from guinea pig pancreas. Description of exendin-3(9-39) amide, a specific exendin receptor antagonist, J. Biol. Chem. 266 (1991) 2897–2902.
[257] J. Thulesen, L.B. Knudsen, B. Hartmann, S. Hastrup, H. Kissow, P.B. Jeppesen, C. Ørskov, J.J. Holst, S.S. Poulsen, The truncated metabolite GLP-2 (3−33) interacts with the GLP-2 receptor as a partial agonist, Regul. Pept. 103 (2002) 9–15, https://doi.org/10.1016/s0167-0115(01)00316-0.
[258] P.-Y. Yang, H. Zou, C. Lee, A. Muppidi, E. Chao, Q. Fu, X. Luo, D. Wang, P. G. Schultz, W. Shen, Stapled, long-acting glucagon-like peptide 2 analog with efficacy in dextran sodium sulfate induced mouse colitis models, J. Med. Chem. 61 (2018) 3218–3223, https://doi.org/10.1021/acs.jmedchem.7b00768.
[259] D.M. Hargrove, S. Alagarsamy, G. Croston, R. Laporte, S. Qi, K. Srinivasan, J. Sueiras-Diaz, K. Wiśniewski, J. Hartwig, M. Lu, A.P. Posch, H. Wiśniewska, C. D. Schteingart, P.J.-M. Rivière, V. Dimitriadou, Pharmacological characterization of apraglutide, a novel long-acting peptidic glucagon-like peptide-2 agonist, for the treatment of short bowel syndrome, J. Pharmacol. Exp. Ther. 373 (2020) 193–203, https://doi.org/10.1124/jpet.119.262238.
[260] K. McKeage, Teduglutide: a guide to its use in short bowel syndrome, Clin. Drug Investig. 35 (2015) 335–340, https://doi.org/10.1007/s40261-015-0286-6.
[261] G. Christopoulos, K.J. Perry, M. Morfis, N. Tilakaratne, Y. Gao, N.J. Fraser, M. J. Main, S.M. Foord, P.M. Sexton, Multiple amylin receptors arise from receptor activity-modifying protein interaction with the calcitonin receptor gene product, Mol. Pharmacol. 56 (1999) 235–242, https://doi.org/10.1124/mol.56.1.235.
[262] S. Hilairet, S.M. Foord, F.H. Marshall, M. Bouvier, Protein-protein interaction and not glycosylation determines the binding selectivity of heterodimers between the calcitonin receptor-like receptor and the receptor activity-modifying proteins *, J. Biol. Chem. 276 (2001) 29575–29581, https://doi.org/10.1074/jbc.M102722200.
[263] D.L. Hay, G. Christopoulos, A. Christopoulos, D.R. Poyner, P.M. Sexton, Pharmacological discrimination of calcitonin receptor: receptor activity-modifying protein complexes, Mol. Pharmacol. 67 (2005) 1655–1665, https://doi.org/10.1124/mol.104.008615.
[264] K. Kuwasako, K. Kitamura, Y. Nagoshi, T. Eto, Novel calcitonin-(8-32)-sensitive adrenomedullin receptors derived from co-expression of calcitonin receptor with receptor activity-modifying proteins, Biochem. Biophys. Res. Commun. 301 (2003) 460–464, https://doi.org/10.1016/s0006-291x(02)03072-3.
[265] J.J. Gingell, E.R. Burns, D.L. Hay, Activity of pramlintide, rat and human amylin but not Aβ1-42 at human amylin receptors, Endocrinology 155 (2014) 21–26, https://doi.org/10.1210/en.2013-1658.
[266] V. Pham, J.D. Wade, B.W. Purdue, P.M. Sexton, Spatial proximity between a photolabile residue in position 19 of salmon calcitonin and the amino terminus of the human calcitonin receptor, J. Biol. Chem. 279 (2004) 6720–6729, https://doi.org/10.1074/jbc.M307214200.
[267] S. Gydesen, K.V. Andreassen, S.T. Hjuler, J.M. Christensen, M.A. Karsdal, K. Henriksen, KBP-088, a novel DACRA with prolonged receptor activation, is superior to davalintide in terms of efficacy on body weight, Am. J. Physiol. Endocrinol. Metab. 310 (2016) E821–E827, https://doi.org/10.1152/ajpendo.00514.2015.
[268] K. Kuwasako, Y.-N. Cao, Y. Nagoshi, T. Tsuruda, K. Kitamura, T. Eto, Characterization of the human calcitonin gene-related peptide receptor subtypes associated with receptor activity-modifying proteins, Mol. Pharmacol. 65 (2004) 207–213, https://doi.org/10.1124/mol.65.1.207.